R-05-31

Thermal modelling

Preliminary site description Forsmark area – version 1.2

Jan Sundberg, Pär-Erik Back,
Anna Bengtsson, Märta Ländell
Geo Innova AB

August 2005

Svensk Kärnbränslehantering AB
Swedish Nuclear Fuel
and Waste Management Co
Box 5864
SE-102 40 Stockholm Sweden
Tel 08-459 84 00
+46 8 459 84 00
Fax 08-661 57 19
+46 8 661 57 19

ISSN 1402-3091
SKB Rapport R-05-31

Thermal modelling

Preliminary site description
Forsmark area – version 1.2

Jan Sundberg, Pär-Erik Back,
Anna Bengtsson, Märta Ländell
Geo Innova AB

August 2005

Summary

This report presents the thermal site descriptive model for the Forsmark area, version 1.2. The main objective of this report is to present the thermal modelling work where data has been identified, quality controlled, evaluated and summarised in order to make an upscaling to lithological domain level possible.

The thermal conductivity at canister scale has been modelled for two different lithological domains (RFM029 and RFM012, both dominated by granite to granodiorite (101057)). A main modelling approach has been used to determine the mean value of the thermal conductivity. Two alternative/complementary approaches have been used to evaluate the spatial variability of the thermal conductivity at domain level. The thermal modelling approaches are based on the lithological model for the Forsmark area, version 1.2 together with rock type models constituted from measured and calculated (from mineral composition) thermal conductivities.

Results indicate that the mean of thermal conductivity is expected to exhibit a small variation between the different domains, 3.46 W/(m·K) for RFM012 to 3.55 W/(m·K) for RFM029. The spatial distribution of the thermal conductivity does not follow a simple model. Lower and upper 95% confidence limits are based on the modelling results, but have been rounded of to only two significant figures. Consequently, the lower limit is 2.9 W/(m·K), while the upper is 3.8 W/(m·K). This is applicable to both the investigated domains. The temperature dependence is rather small with a decrease in thermal conductivity of 10.0% per 100°C increase in temperature for the dominating rock type.

There are a number of important uncertainties associated with these results. One of the uncertainties considers the representative scale for the canister. Another important uncertainty is the methodological uncertainties associated with the upscaling of thermal conductivity from cm-scale to canister scale. In addition, the representativeness of rock samples is uncertain and it is not known how large the bias, introduced by judgmental sample selection is.

The thermal conductivity was also investigated for RFM029 in Forsmark site description model version 1.1. The thermal conductivity is estimated to be higher in the Forsmark site description model version 1.2 than in the earlier version, for this domain. In version 1.1 it was estimated to be 3.33 W/(m·K), while in version 1.2, it is estimated to be 3.55 W/(m·K).

Mean value of heat capacity for the dominating rock types was 2.17 MJ/(m^3·K). The standard deviation was 0.17 MJ/(m^3·K), but the number of samples is relatively small. There is also a question of the representativeness of the samples. Modelling on domain level of the two lithological domains according to a Monte Carlo simulation gave the mean value 2.17 MJ/(m^3·K) of the heat capacity for both domains and standard deviations 0.16 and 0.15 MJ/(m^3K). The heat capacity exhibits large temperature dependence, about 25% increase per 100°C temperature increase for rock type granite to granodiorite (101057).

The coefficient of thermal expansion was determined to 7.2–8.0·10^{-6} m/(m·K) for the three investigated rock types. In situ temperature has been measured in five boreholes. The mean of four of the temperature loggings is 11.7°C at 500 m depth, (one deviant and short borehole excluded). Temperature vs. depth is presented in both tables and figures for each borehole. There is a variation in temperature between the boreholes at a specified depth.

Sammanfattning

Föreliggande rapport presenterar den termiska platsbeskrivningsmodellen för Forsmarksområdet version 1.2. Syftet med denna rapport är att presentera det termiska modelleringsarbetet där data har identifierats, kvalitetssäkrats, utvärderats och sammanfattats för att möjliggöra en uppskalning till litologisk domännivå.

Den termiska konduktiviteten i kapselskala har modellerats för två olika litologiska domäner (RFM029 och RFM012, båda domineras av granit till granodiorit (101057)). Det huvudsakliga angreppssättet för den termiska modelleringen har använts för bestämning av den termiska konduktivitetens medelvärde. Två alternativa/kompletterande angreppssätt har använts för att utvärdera den termiska konduktivitetens spatiala variation på domän nivå. Den termiska modelleringens olika angreppssätt baseras på den litologiska modellen för Forsmarksområdet version 1.2 tillsammans med bergartsmodeller upprättade med utgångspunkt ifrån mätningar och beräkningar (utifrån mineralsammansättning) av den termiska konduktiviteten.

Resultat indikerar att medelvärdet för den termiska konduktiviteten förväntas uppvisa endast en liten variation mellan de olika domänerna, 3,45 W/(m·K) för RFM012 till 3,55 W/(m·K). Den spatiella fördelningen för den termiska konduktiviteten följer inte någon enkel modell. Undre och övre gräns för 95 % konfidensintervall baseras på modelleringarna, men har avrundats till endast två gällande siffror. Undre gränsen är därmed 2,9 W/(m·K), medan den övre är 3,8 W/(m·K). Detta gäller för båda de undersökta domänerna. Temperaturberoendet är relativt litet med en minskning i termisk konduktivitet på 10,0 % per 100 °C temperaturökning för den dominerande bergarten.

Det finns ett antal viktiga osäkerheter associerade med dessa resultat. En av osäkerheterna tar hänsyn till den representativa skalan för kapseln. Ytterligare en viktig osäkerhet är de metodrelaterade osäkerheterna i samband med uppskalningen av den termiska konduktiviteten från cm- till kapselskala. Till detta skall även läggas osäkerheten i representativitet för bergartsproverna där det ännu inte är klargjort hur stor avvikelsen är på grund av metodiken för provernas urval.

Den termiska konduktiviteten för RFM029 undersöktes också i den termiska platsbeskrivn ingsmodellen för Forsmarksområdet version 1.1. Den termiska konduktiviteten uppskattas vara högre i den platsbeskrivande modellen för Forsmarksområdet, version 1.2, än i den tidigare versionen, för denna domän. I version 1.1. uppskattades den till 3,33 W/(m·K), medan den i version 1.2 uppskattas till 3,55 W/(m·K).

Medelvärdet för värmekapaciteten för den dominerande bergarten var 2,17 MJ/(m³·K). Standardavvikelsen var 0,17 MJ/(m³·K), men antalet prov är relativt litet. Representativiteten för proven kan ifrågasättas. Modelleringen på domännivå för de två litologiska domänerna genomfördes enligt en Monte Carlo simulering och gav medelvärdet 2,17 MJ/(m³·K) för värmekapaciteten för båda domänerna och standardavvikelserna 0,16 och 0,15 MJ/(m³·K). Värmekapaciteten uppvisar stort temperaturberoende, ungefär 25 % ökning per 100 °C temperaturökning för bergarten granit till granodiorite (101057).

Längdutvidgningskoefficienten bestämdes till 7,2–8,0·10^{-6} m/(m·K) för de tre undersökta bergarterna.

In situ temperaturer har uppmätts i fem borrhål. Medelvärdet för fyra temperaturloggningar är 11,7 °C vid 500 m djup, (ett avvikande och kort borrhål exkluderat). Temperatur relativt djup presenteras både i tabellform samt i figurer för respektive borrhål. Det finns en variation i temperatur mellan de olika borrhålen för ett specifikt djup.

Contents

1 Introduction 7

2 Objective and scope 9

3 State of knowledge at previous model version 11

4 Evaluation of primary data 13
4.1 Summary of used data 13
4.2 Geological introduction 14
4.3 Thermal conductivity from measurements 16
4.3.1 Method 16
4.3.2 Results 16
4.3.3 Temperature dependence 18
4.3.4 Compared TPS tests 19
4.3.5 Anisotropy 21
4.4 Thermal conductivity from mineral composition 21
4.4.1 Method 21
4.4.2 Result 23
4.4.3 Comparison with measurements 25
4.5 Thermal conductivity from density 28
4.6 Rock type models (PDF) of thermal conductivity 29
4.6.1 Method 29
4.6.2 Granite to granodiorite, metamorphic, medium-grained (101057) 30
4.6.3 Granodiorite, metamorphic (101056) 32
4.6.4 Tonalite to granodiorite, metamorphic (101054) 33
4.6.5 Granite, granodiorite and tonalite, metamorphic, fine- to medium-grained (101051) 35
4.6.6 Other rock types 37
4.7 Spatial variability 38
4.8 Heat capacity 39
4.8.1 Measurement method 39
4.8.2 Measurement result 39
4.8.3 Temperature dependence 40
4.8.4 Rock type models 41
4.9 Coefficient of thermal expansion 43
4.10 In situ temperature 43
4.10.1 Method 43
4.10.2 Results 44

5 Thermal model 53
5.1 Modelling assumptions and input from other disciplines 53
5.1.1 Geological model 53
5.1.2 Borehole data 54
5.2 Conceptual model 54
5.3 Modelling approach for domain properties 55
5.3.1 Introduction 55
5.3.2 Approach 1: Main approach 56
5.3.3 Alternatives to main approach 58

5.3.4 Approach 2: Addition of "within rock type" variance from the Simpevarp area 58
5.3.5 Approach 3: Addition of "between rock type" and "within rock type" variance from TPS measurements 59
5.3.6 Modelling appoach: Heat capacity 59
5.4 Domain modelling results 59
5.4.1 Approach 1: Main approach 59
5.4.2 Approach 2: Addition of "within rock type" variance from the Simpevarp area 68
5.4.3 Approach 3: Addition of "between rock type" and "within rock type" variance from TPS measurements 68
5.4.4 Modelling results: Heat capacity 69
5.5 Conclusion – modelling results 70
5.5.1 Thermal conductivity 70
5.5.2 Heat capacity 72
5.5.3 Coefficient of thermal expansion 73
5.5.4 In situ temperature 73

6 Evaluation of uncertainties 75
6.1 Thermal conductivity 75
6.1.1 Data level 75
6.1.2 Rock type level 76
6.1.3 Domain level 76
6.2 Heat capacity 78
6.3 In situ temperature 78
6.4 Thermal expansion 78

7 Feedback to other disciplines 79

8 Abbreviation list 80

References 81

Appendix A Probability plots of thermal conductivity per rock type 85

Appendix B Probability plots of domain modelling results 87

1 Introduction

The Swedish Nuclear Fuel and Waste Management Co (SKB) is responsible for the handling and final disposal of the nuclear waste produced in Sweden. Site investigations have started during 2002. The site investigations are carried out in different stages and shall provide the knowledge required to evaluate the suitability of investigated sites for a deep repository.

The interpretation of the measured data is made in terms of a site descriptive model covering geology, rock mechanics, thermal properties, hydrogeology, hydrogeochemistry, transport properties of the rock and surface ecosystems. The site descriptive model is the foundation for the understanding of investigated data and a base for planning of the repository design and for studies of constructability, environmental impact and safety assessment. A strategy for the thermal modelling is presented in /Sundberg, 2003a/.

This report presents the thermal site descriptive model for Forsmark, version 1.2, parallel to this modelling, a study on uncertainties and scale factors is ongoing for the prototype repository at the Äspö HRL /Sundberg et al. 2005a/. The experiences from this parallel study are not fully implemented in the present modelling report.

2 Objective and scope

The purpose of this document is to present the thermal modelling work for the Forsmark Site Descriptive Model version 1.2. Primary data originate from the work in connection to the Forsmark Site Descriptive Model version 1.1 which has partly been re-evaluated together with measured data in connection to the work with Forsmark Site Descriptive Model version 1.2. Data has been identified, quality controlled, evaluated and summarised in order to make the upscaling possible to domain level.

The thermal model of the bedrock describes thermal properties on lithological domain level which is of importance since the thermal properties of the rock mass affects the possible distance, both between canisters and deposition tunnels, and therefore puts requirements on the necessary repository volume. Of main interest is the thermal conductivity since it directly influences the design of a repository. Measurements of thermal properties are performed in cm scale but values are requested in the canister scale and therefore the spatial variability is required to be considered. Due to this, the thermal modelling includes elements of upscaling of thermal properties which is further described in /Sundberg et al. 2005a/. The work has been performed according to a strategy presented in /Sundberg, 2003a/.

3 State of knowledge at previous model version

In model version 1.1 of the Forsmark area the thermal properties of samples were evaluated on both rock unit and rock domain level together with a Monte Carlo simulation of borehole KFM01A.

Thermal conductivity properties were given separately for each rock unit with the lowest values for felsic to intermediate volcanic rock (103076), 2.79 W/(m·K) and the highest for granite to granodiorite (101057), 3.33 W/(m·K). The dominating rock domains (RFM029 and RFM017) had conductivities with mean values 3.41 W/(m·K) and 2.73 W/(m·K) respectively. Comparison between measured and calculated thermal conductivities showed differences of 1.9–8.8% in both directions. The in situ temperature of the Forsmark area increased from 7°C at 100 m to about 13°C at 600 m.

The main uncertainties of the thermal model in version 1.1 concerned:

- Temperature logging was only available for one borehole and the gradient with depth could not fully be explained.
- Few measurements of thermal properties with weak statistical basis and uncertainties in representativeness of calculated thermal conductivities.
- Upscaling from core samples to rock domains.
- Lack of data concerning properties at elevated temperatures and the anisotropy of thermal properties.

4 Evaluation of primary data

The evaluation of primary data includes measurements of thermal conductivity, heat capacity, temperature dependence of thermal transport properties, anisotropy for thermal conductivity, coefficient of thermal expansion and in situ temperatures. It also includes calculations of thermal conductivity from mineral composition and establishment of rock type models (PDF:s) of thermal conductivity. The spatial variation in thermal conductivity is also investigated.

4.1 Summary of used data

In Table 4-1 a summary is given of the data used in the evaluation.

Table 4-1. Summary of data used in evaluation of data.

Data specification	Ref.	Rock code	Number of samples/ measurements	Borehole (depth)
Cored borehole data				
Laboratory test of thermal properties	P-04-159 P-04-161 P-04-162 P-04-199	101057	47	KFM01A (226–235 m, 389–390 m, 492–495 m, 692–698 m), KFM02A (330–336 m, 528–536 m, 704–719 m), KFM03A (527–683 m)
		101054	3	KFM03A (262.2–262.5 m)
		101051	3	KFM03A (305.6–305.8 m)
		101056	5	KFM04A (108.8–109.8 m)
Modal analyses	P-04-103	101057	38	KFM01A, KFM02A, KFM03A
	P-04-159	101051	7	KFM01A, KFM02A, KFM03A
	P-04-161	101054	2	KFM03A
	P-04-162	101061	1	KFM03B
	SICADA			
Temperature and gradient logging	Results P-03-103 P-04-97 P-04-144 P-04-145	Interpret P-04-80 P-04-98 P-04-143		KFM01A, KFM01B, KFM02A, KFM03A, KFM04A
Boremap logging	Dominating rock type Sicada 04-158 date 04-07-07 Subordinate rock type Sicada 04-158 date 04-07-07			KFM01A, KFM01B, KFM02A, KFM03A, KFM04A
Anisotropy	Report under prep		5	KFM04A (531.0–531.4 m)
Comparing TPS measurements	P-04-186	101057	10	KFM01A (492.4–492.9 m)
Laboratory test of thermal expansion	P-04-163	101057	44	KFM01A, KFM02A, KFM03A
	P-04-164	101054	3	KFM03A
	P-04-165	101051	3	KFM03A

Data specification	Ref.	Rock code	Number of samples/ measurements	Borehole (depth)
Surfaced based data				
Laboratory test of thermal properties	P-03-08	101057	2	
		101054	2	
		101033	1	
Modal analyses	P-03-75	101057	18	
		101051	14	
		101054	15	
		101061	3	
		101033	2	
		101004	1	
		101056	3	
		101058	2	
		102017	1	
		103076	10	
		111058	2	

4.2 Geological introduction

The bedrock area, for which the thermal site descriptive model version 1.2 has been conducted, is predominated by three rock types, namely:

- Granite to granodiorite.
- Granodiorite, metamorphic.
- Tonalite to granodiorite.

Besides the three dominating rock types several subordinate rock types occur within the bedrock area for the thermal model. For illustration of the geological rock type classification of the bedrock, see Figure 4-1. The rock types that are domination for the area is not always dominating for the individual boreholes.

Further on in this report all rock types will mainly be identified and described by the rock code. Therefore, a translation table is introduced between rock codes and rock names in Table 4-2.

Table 4-2. Translation between rock codes and names of different rock types.

Rock code	Rock name
101057	Granite to granodiorite, metamorphic, medium grained
101056	Granodiorite, metamorphic
101054	Tonalite to granodiorite, metamorphic
101051	Granite, granodiorite and tonalite, metamorphic, fine- to mediumgrained
101061	Pegmatite, pegmatitic granite
103076	Felsic to intermediate volcanic rock, metamorphic
101058	Granite, metamorphic, aplitic
111058	Granite, fine- to medium-grained
101033	Diorite, quartz diorite and gabbro, metamorphic
101004	Ultramaphic rock, metamorphic
102017	Amphibolite
108019	Calc-silicate rock (skarn)

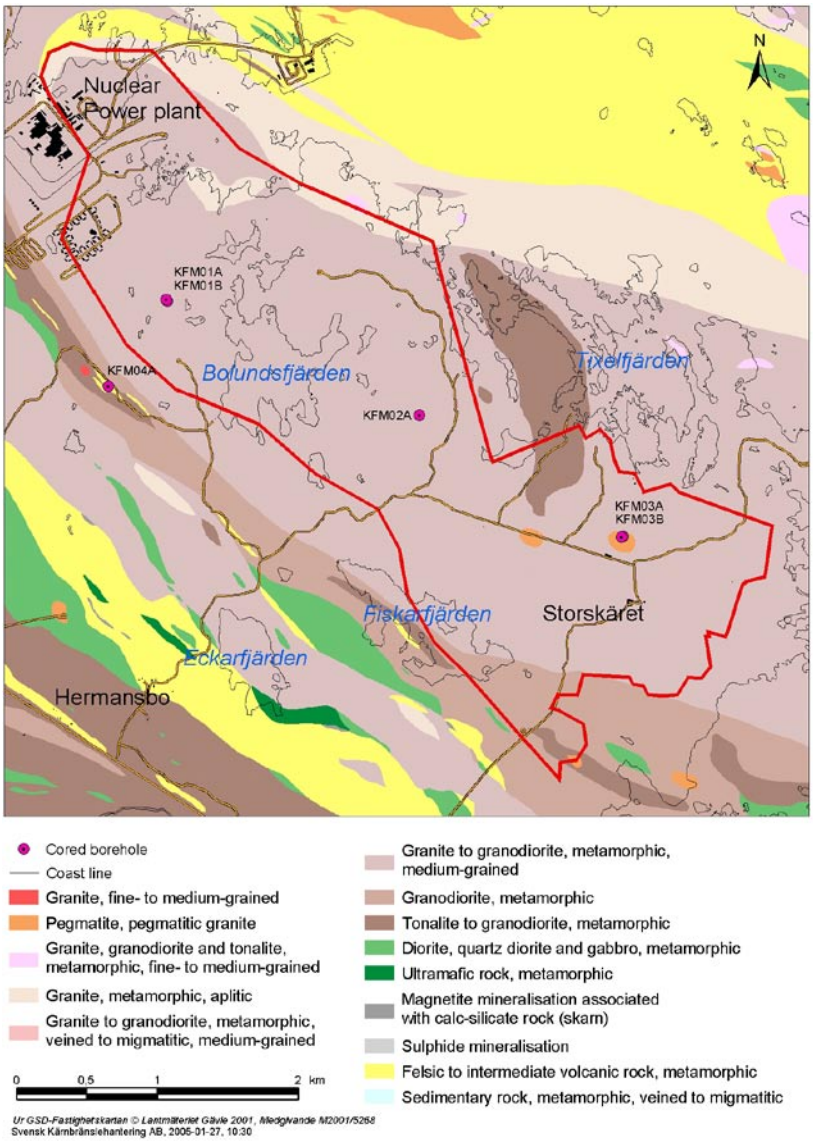

Figure 4-1. *Location of boreholes used in this report within the Forsmark area, overlaid the bedrock classification.*

Data from five different boreholes, within the Forsmark area, have been used and are evaluated in this report. Figure 4-1 illustrates the location of the boreholes.

Thermal properties of two rock domains within the Forsmark area will be calculated and suggested within this report; domain RFM029 and RFM012. The classification of rock volumes in different domains is a way of handling and simplifying large rock volumes with, relatively seen, the same properties. The dominating rock type in both domain RFM029 and RFM012 is granite to granodiorite (101057). For a more detailed description of the rock type composition in the different domains, see Table 5-1.

4.3 Thermal conductivity from measurements

4.3.1 Method

Laboratory measurements of the properties thermal conductivity and thermal diffusivity have been conducted using the TPS (Transient Plane Source) method /Gustafsson, 1991/. The TPS method can be used for measurements of thermal diffusivity and thermal conductivity of both fluids and solids, from cryogenic temperatures to about 250°C (if the sensor insulation is made of kapton). Measurements of thermal properties using the TPS method have been used before by SKB /Sundberg and Gabrielsson, 1999; Sundberg, 2002; Sundberg et al. 2005a/ and also within the thermal programme of the site investigations.

Prior to the measurements, the rock samples from the drill core are cut in two halves, each with a thickness of about 50 mm. The two intersection surfaces need to be relatively smooth in order to limit the contact resistance between the probe and the sample surface.

The principle of the TPS instrument is to place a circular probe consisting of a Ni-spiral covered by an insulating material (Mica or Kapton) between the two sample pieces. The sensor generates a heat pulse while simultaneously the heating of the specimen is recorded. The heat pulse is selected to achieve a heat increase of 1K at the sample surfaces facing the sensor. The output power and the duration of the pulse are dependent on sample size, material properties and sensor diameter. The thermal properties can be evaluated by using the fact that the resistance for the thin Ni-spiral at any time is a function of its initial resistance, the temperature increase and the temperature coefficient of the resistivity of Nickel. The measured temperatures is stored in the software and by comparing these values to a theoretical solution based on assumptions regarding a plane sensor and an infinite sample in perfect contact with the sensor surface, the thermal diffusivity and thermal conductivity can be determined. The volumetric heat capacity can thereafter be calculated.

Measurements carried out by Hot Disk has, according to the manufacturer, an accuracy of the thermal conductivity measurements of ± 2%, thermal diffusivity ± 5% and specific heat ± 7% /Hot Disk, 2004/. This is accomplished if the sample size, sensor diameter, output of power and total time of the temperature measurement is properly selected together with letting the sample reach temperature equilibrium before starting the measuring.

4.3.2 Results

In Table 4-3 the results from all conducted measurements of thermal conductivity is summarised /Adl-Zarrabi, 2003, 2004a,b,c,d/. The variability in the results is probably higher, due to the small scale, compared to determinations at larger scales. The calculations in Table 4-3 are based on the total number of TPS measurements, Table 4-4 is based on TPS measurements made in connection with modal analyses and Table 4-5 of surface samples from work in connection to version 1.1. Note that the three samples in rock types tonalite to granodiorite (101054) and granite, granodiorite and tonalite (101051) originate from two, only 0.2 m long intervals of the borehole KFM03A. The five samples from rock type granodiorite (101056) originate from a 1 m interval. Samples from rock type granite to granodiorite (101057) have a larger spatial distribution along the borehole, but the distribution is not uniform but grouped with approximately 3–5 samples in each group. The distribution for the samples from different rock types in the boreholes is shown in Figure 4-2.

Table 4-3. Measured thermal conductivity (W/(m·K)) of samples (all TPS measurements) with different rock types, using the TPS method. Samples are from boreholes KFM01A, KFM02A, KFM03A and KFM04A together with 5 surface samples.

Rock code	Rock name	Sample location	Mean	St. dev.	Max	Min	Number of samples
101057	Granite to granodiorite	Borehole KFM01A, KFM02A, KFM03A and sample PFM001159 and PFM001164	3.71	0.16	4.01	3.42	49
101054	Tonalite to granodiorite	Borehole KFM03A, PFM001157 and PFM001162	2.73	0.19	2.94	2.45	5
101051	Granite, granodiorite and tonalite	Borehole KFM03A	2.51	0.08	2.60	2.46	3
101056	Granodiorite	Borehole KFM04A	3.04	0.09	3.20	2.98	5
101033	Diorite, quartz diorite and gabbro	PFM001158	2.28		2.28	2.28	1

Table 4-4. Measured thermal conductivity (W/(m·K)) of samples in connection to modal analyses with different rock types, using the TPS method. Samples are from boreholes KFM01A, KFM02A and KFM03A together with 3 surface samples.

Rock code	Rock name	Sample location	Mean	St. dev.	Max	Min	Number of samples
101057	Granite to granodiorite	Borehole KFM01A, KFM02A, KFM03A and sample PFM001159 and PFM001164	3.70	0.17	4.01	3.47	19
101054	Tonalite to granodiorite	Borehole KFM03A and sample PFM001162	2.63	0.25	2.81	2.45	2
101051	Granite, granodiorite and tonalite	Borehole KFM03A	2.47		2.47	2.47	1

Table 4-5. Measured thermal conductivity (W/(m·K)) of surface samples taken in connection to version 1.1 with different rock types, using the TPS method.

Rock code	Rock name	Sample	Mean	St. dev.	Max	Min	Number of samples
101057	Granite to granodiorite	PFM001159 and PFM001164	3.49	0.03	3.51	3.47	2
101054	Tonalite to granodiorite	PFM001157 and PFM001162	2.70	0.35	2.94	2.45	2
101033	Diorite, quartz diorite and gabbro	PFM001158	2.28		2.28	2.28	1

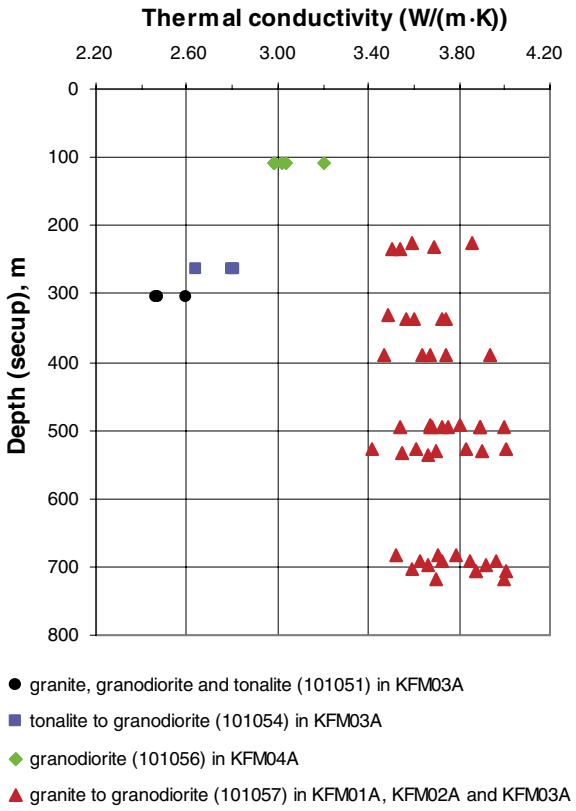

Figure 4-2. *Location in boreholes for samples used for measurements with the TPS method, divided into rock types.*

4.3.3 Temperature dependence

The temperature dependence of the thermal conductivity has been investigated by measuring 18 samples within rock type 101057, granite to granodiorite, at three different temperatures (20, 50 and 80°C) /Adl-Zarrabi, 2004c/. Figure 4-3 illustrates the measuring results for each sample while Table 4-6 summarises the temperature dependence of the thermal conductivity for rock type 101057. With increasing temperature the thermal conductivity of rock type 101057 decreases by 10.0%/100°C temperature increase, calculated mean value of 18 samples. However, the decrease of thermal conductivity varies from 6.2% to 12.3% for the individual samples.

Table 4-6. Measured temperature dependence of thermal conductivity (per 100°C temperature increase) on samples from boreholes KFM01A, KFM02A and KFM03A.

Rock code	Rock name	Sample location	Mean	St. dev.	Number of samples
101057	Granite to granodiorite	Boreholes KFM01A, KFM02A and KFM03A	–10.0%	1.9%	18

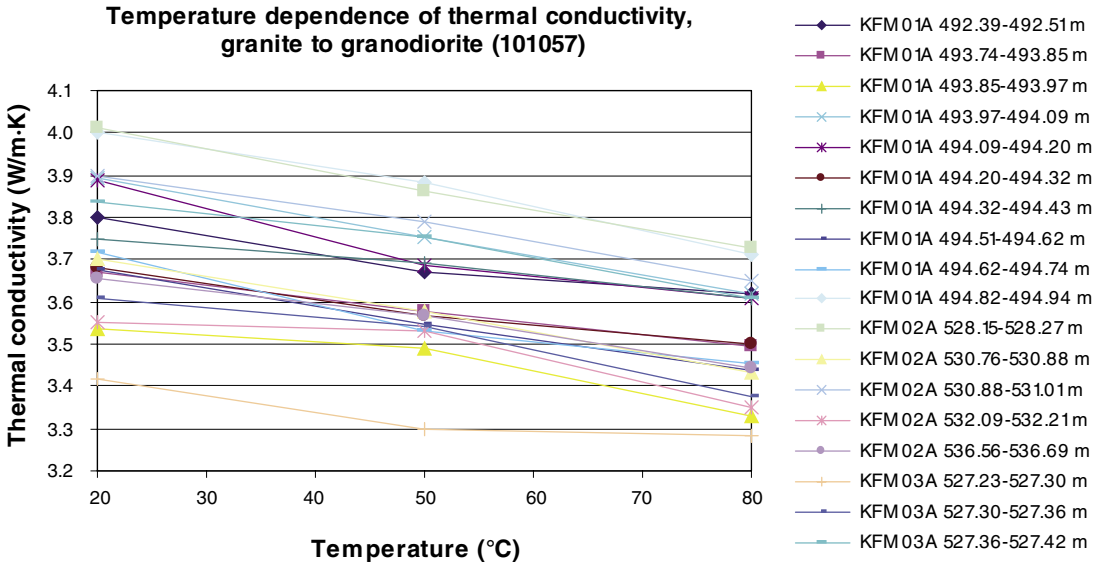

Figure 4-3. *Temperature dependence of thermal conductivity, rock type granite to granodiorite (101057).*

4.3.4 Compared TPS tests

As a step in the quality assuring of thermal data, 10 samples from KFM01A within rock type granite to granodiorite (101057) have been selected for compared TPS measurements at two different laboratories, Hot Disk AB and SP (Swedish National Testing and Research Institute). The samples have been measured at three different temperatures and the results are presented in Table 4-7 and Table 4-8. In Table 4-7 the results at all three temperatures are included, while in Table 4-8 only the results at 20°C are used. A comparison of the results from the two different laboratories is shown in Figure 4-4 and Table 4-7.

For thermal conductivity the measured difference on the same sample varies between –6.6% to 4.8% which in thermal conductivity means –0.24 W/(m·K) to 0.17 W/(m·K). The difference in heat capacity measured for the same sample varies between –12.4% to 9.7% which in heat capacity means –0.35 MJ/(m³·K) to 0.23 MJ/(m³·K).

This is further discussed in section 6.1.1.

Table 4-7. Results of TPS measurements for 10 samples from borehole KFM01A within rock type granite to granodiorite (101057). Data are based on 30 measurements (10 samples, investigated at 20°C, 50°C and 80°C). Measurements performed on the same samples by two laboratories, Hot Disk and SP. Comparison of results from TPS measurements performed by the two different laboratories on the same samples at three different temperatures, calculated as difference (%).

	Thermal conductivity (W/(m·K))		Heat capacity (MJ/(m³·K))		Thermal diffusivity (mm²/s)	
	SP	Hot Disk	SP	Hot Disk	SP	Hot Disk
Arithmetic mean	3.65	3.63	2.41	2.34	1.53	1.56
St. dev.	0.15	0.17	0.22	0.16	0.16	0.16
Min	3.33	3.37	1.96	1.97	1.28	1.30
Max	4.00	3.98	2.82	2.59	1.88	1.90
Diff. (Hot Disk-SP)/SP	–0.5%		–2.6%			–2.0%

Table 4-8. Results of TPS measurements for 10 samples from borehole KFM01A within rock type granite to granodiorite (101057). Data are based on 10 measurements (10 samples, investigated at 20°C) Measurements performed by two laboratories, Hot Disk and SP.

	Thermal conductivity (W/(m·K))		Heat capacity (MJ/(m³·K))		Thermal diffusivity (mm²/s)	
	SP	Hot Disk	SP	Hot Disk	SP	Hot Disk
Arithmetic mean	3.76	3.80	2.24	2.19	1.69	1.74
St. dev.	0.14	0.10	0.15	0.13	0.09	0.08
Min	3.54	3.64	1.96	1.97	1.59	1.65
Max	4.00	3.98	2.43	2.34	1.88	1.90

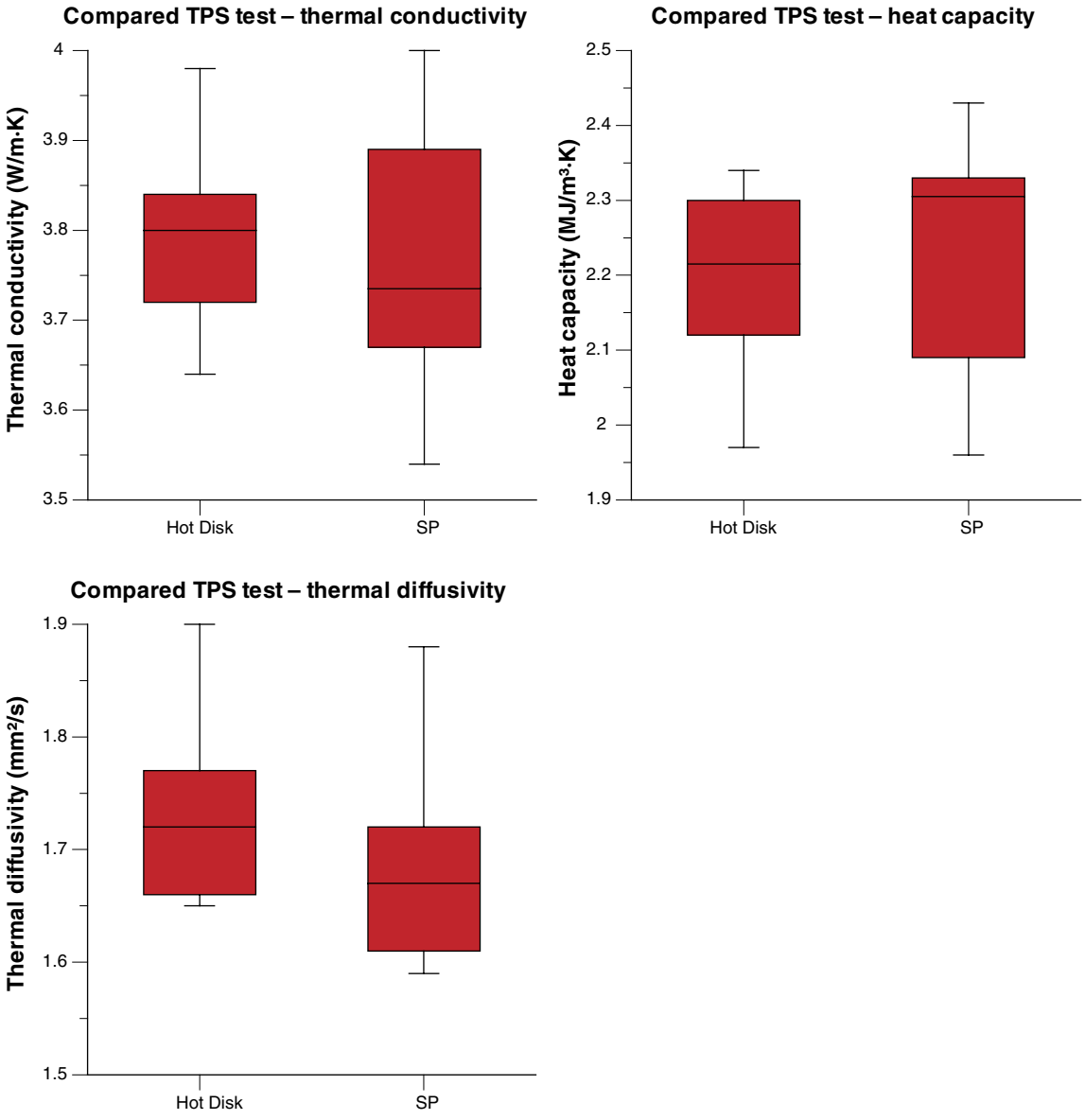

Figure 4-4. *Comparison of results for thermal conductivity, heat capacity and thermal diffusivity measured according to the TPS method. Measurements were made by both Hot Disk AB and SP (Swedish National Testing and Research Insitute). The line in the boxes represents the median, while the ends of the boxes are defined by the upper and lower quartiles. The ends of the vertical lines correspond to the maximum and minimum values.*

4.3.5 Anisotropy

Anisotropic measurements of thermal conductivity and diffusivity have been carried out by Hot Disk for five samples in borehole KFM04A /Dinges, 2004a/. The measurements were made by the TPS-method and evaluated with a special routine that makes determination of heat conductivity in the two fundamental directions possible.

The summary of the preliminary results from the measurements is presented in Table 4-9. Samples showing a clear lineation/foliation were selected for the measurements. The two directions, in which measurements were done, were axial and radial. Axial was perpendicular, and radial was parallel to the foliation. The samples were taken in the dominating granite in domain RFM029 but rather close to the border of domain RFM012. This may imply that the samples have a higher degree of anisotropy compared to the rock in the central parts of domain RFM029.

Table 4-9. Results of the anisotropic thermal conductivity measurements. The measurements were made in the two principle directions; perpendicular to foliation (λ_{axial}) and parallel to the foliation (λ_{radial}). The estimated specific heat capacity of 2.271 MJ/m^{3}K was used for the measurements.

Borehole, sampling depth (Sec Low)	λ_{axial} (W/(m·K))	Std-λ_{axial} (W/(m·K))	λ_{radial} (W/(m·K))	Std-λ_{radial} (W/(m·K))	$\lambda_{radial}/\lambda_{axial}$
KFM04A, 530.95–531.03	2.13	0.17	5.18	0.22	2.43
KFM04A, 531.03–531.12	2.84	0.15	4.04	0.18	1.42
KFM04A, 531.12–531.20	2.98	0.02	4.01	0.04	1.35
KFM04A, 531.20–531.29	3.06	0.07	4.39	0.08	1.43
KFM04A, 531.29–531.37	0.98	0.02	6.34	0.15	6.47

However, the evaluation of the measurements uses the heat capacity as input. Results of the heat capacity were not available for the current model version. Instead a fixed value for all samples of 2.271 MJ/m^3·K was used. By increasing the specific heat by 10%, λ_{axial} is decreased by roughly 10% and λ_{radial} is increased by 10% (and vice versa). The values in Table 4-9 may be both over- and underestimated.

4.4 Thermal conductivity from mineral composition

4.4.1 Method

Thermal conductivity of rock samples can be calculated with the SCA method (Self Consistent Approximation) using mineral compositions from modal analyses and reference values of the thermal conductivity of different minerals /Sundberg, 1988; Sundberg, 2003a/. Calculated values has proved to be in good agreement with the measured values /Sundberg, 1988; Sundberg, 2002/.

The following data has been available for calculations with the SCA-method.

- Modal analyses from surface samples included in Forsmark site descriptive model version 1.1, reclassified rock types by geologist Michael Stephens (Geological Survey of Sweden) /Stephens et al. 2003/.

- New modal analyses from boreholes KFM01A, KFM02A, KFM03A and KFM03B, where some are in connection with samples for measurements of thermal properties /Petersson et al. 2004; Adl-Zarrabi, 2004a,b,c/.

Samples were excluded if the sum of minerals from the modal analyse had a large divergence from 100% (2 samples). For samples with a small divergence the volume fraction of the present minerals were corrected to reach a sum of minerals of 100%. This was done by splitting the lacking or extra percent on the present minerals by a weighting factor dependent on the minerals original volume fraction. This had to be done for 24 out of 119 samples.

Reference values of thermal conductivity for different minerals have been taken from /Horai, 1971; Horai and Baldridge, 1972/. In Table 4-10 the thermal conductivities of minerals used in Forsmark site descriptive model version 1.1 together with the values used in version 1.2 are presented. The thermal conductivity of plagioclase, olivine and pyroxene depends on the chemical composition and may therefore vary within certain interval. Because of this, these minerals are marked with red in Table 4-10. For minerals marked in yellow no reference values of the thermal conductivity have been found and an estimated value of 3.00 W/m·K have been used.

Table 4-10. Summary of used thermal conductivities (W/(m·K)) of minerals /Horai, 1971; Horai and Baldridge, 1972/.

Mineral	Forsmark 1.1	Forsmark 1.2
Allanite	–	3.00
Amphibole	–	3.39
Apatite	–	1.38
Biotite	2.00	2.02
Calcite	–	3.59
Chlorite	5.10	5.15
Clinopyroxene	4.00	3.20
Epidote	2.80	2.83
Hornblend	2.80	2.81
K-feldspar	2.51	2.29
Magnetite	5.10	5.10
Muscovite	2.30	2.32
Olivine	4.50	4.57
Opaque	3.00	3.00
Orthopyroxene	4.00	3.20
Plagioclase	1.60	1.93
Prehnite	–	3.58
Quartz	7.70	7.69
Serpentine	3.50	3.53
Titanite	3.00	2.34
Zircon	–	4.54

Yellow: data missing, estimated values.

Red: unknown chemical composition of the mineral.

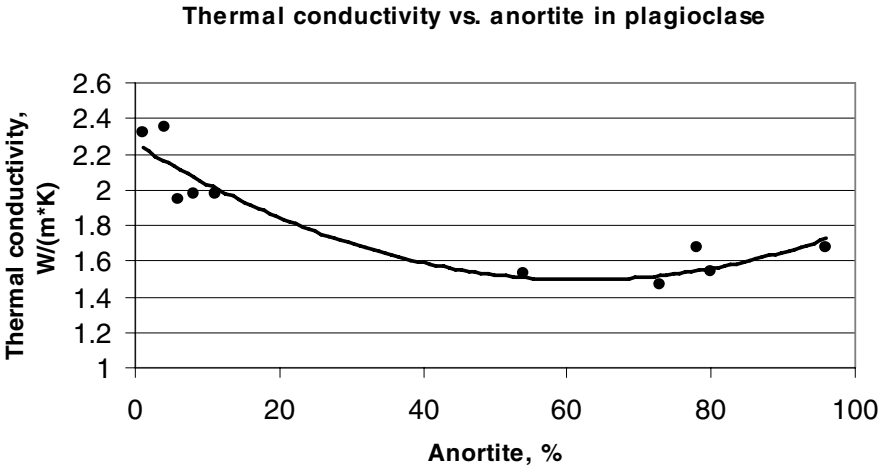

Figure 4-5. *Variation in thermal conductivity for plagioclase dependent on anortite content. Polynomial regression with equation $y=0.0002x^2–0.0246x+2.2563$ and $R^2=0.8845$.*

The thermal conductivity of the plagioclase mineral is dependent on the anortite content. This has been taken under consideration when calculating the thermal conductivity of rock samples. In Figure 4-5 the relationship is presented with a polynomial regression line. For the Forsmark area the anortite content of dominating rock types has been assumed as 15% /Stephens, 2004/. When this anortite content is applied to the regression ($y=0.0002x^2–0.0246x+2.2563$) the thermal conductivity of plagioclase within the Forsmark area is set to 1.93 W/m·K.

4.4.2 Result

The results of the SCA calculations from mineral composition are presented in Table 4-14, Table 4-12 and Table 4-13, divided on rock types. The calculations in Table 4-11 are based on all modal analyses, Table 4-12 on modal analyses from boreholes taken within the geological programme, Table 4-13 on modal analyses in connection to measurements of thermal properties in boreholes and Table 4-14 surface samples from model version 1.1.

Table 4-11. Thermal conductivity (W/(m·K)) of samples (all samples) with different rock types, calculated from the mineralogical composition with the SCA method.

Rock code	Rock name	Arithmetic mean	St. dev.	Max	Min	Number of samples
101057	Granite to granodiorite	3.56	0.24	4.04	3.07	56
101051	Granite, granodiorite and tonalite	3.10	0.24	3.42	2.61	21
101054	Tonalite to granodiorite	3.03	0.42	3.97	2.28	17
101061	Pegmatite, pegmatitic granite	3.54	0.12	3.65	3.41	4
101033	Diorite, quartz diorite and gabbro	2.36	0.21	2.51	2.20	2
101004	Ultramaphic rock	3.50				1
101056	Granodiorite	3.20	0.19	3.39	3.02	3
101058	Granite	3.47	0.12	3.55	3.38	2
102017	Amphibolite	2.43				1
103076	Felsic to intermediate volcanic rock	3.01	0.37	3.55	2.44	10
111058	Granite	3.35	0.05	3.39	3.32	2

Table 4-12. Thermal conductivity (W/(m·K)) of samples taken within the geological programme (boreholes Forsmark 1.2) with different rock types, calculated from the mineralogical composition with the SCA method.

Rock code	Rock name	Arithmetic mean	St. dev.	Max	Min	Number of samples
101057	Granite to granodiorite	3.54	0.26	4.05	3.09	20
101051	Granite, granodiorite and tonalite	3.07	0.31	3.36	2.61	6
101054	Tonalite to granodiorite	2.78				1
101061	Pegmatite, pegmatitic granite	3.47				1

Table 4-13. Thermal conductivity (W/(m·K)) of samples taken within the thermal programme (in connection to TPS measurements Forsmark 1.2) with different rock types, calculated from the mineralogical composition with the SCA method.

Rock code	Rock name	Arithmetic mean	St. dev.	Max	Min	Number of samples
101057	Granite to granodiorite	3.65	0.23	3.96	3.16	18
101051	Granite, granodiorite and tonalite	3.15				1
101054	Tonalite to granodiorite	3.18				1

Table 4-14. Thermal conductivity (W/(m·K)) of samples (surface samples Forsmark 1.1) with different rock types, calculated from the mineralogical composition with the SCA method.

Rock code	Rock name	Arithmetic mean	St. dev.	Max	Min	Number of samples
101057	Granite to granodiorite	3.50	0.20	3.86	3.24	18
101051	Granite, granodiorite and tonalite	3.11	0.23	3.42	2.66	14
101054	Tonalite to granodiorite	3.04	0.44	3.97	2.28	15
101061	Pegmatite, pegmatitic granite	3.60	0.14	3.65	3.41	3
101033	Diorite quartz diorite and gabbro	2.36	0.21	2.51	2.20	2
101004	Ultramafic rock	3.50				1
101056	Granodiorite	3.20	0.19	3.39	3.02	3
101058	Granite	3.47	0.12	3.55	3.38	2
102017	Amphibolite	2.43				1
103076	Felsic to intermediate volcanic rock	3.01	0.37	3.55	2.44	10
111058	Granite	3.35	0.05	3.39	3.32	2

Thermal conductivities calculated with the SCA method in the site descriptive model version 1.1 gave mainly lower mean values and higher standard deviations compared to the calculations in this site descriptive model version 1.2. The thermal conductivities were between 0.39 W/(m·K) higher to 0.46 W/(m·K) lower in the previous model version. The increase might depend on the fact that the thermal conductivities of minerals have been chosen slightly different and that the number of samples have increased and better represents the rock mass. This is also indicated with the reduced standard deviation.

4.4.3 Comparison with measurements

For several of the areas where thermal conductivity has been measured with the TPS method, sampling for determination of mineral composition have also been carried out. This has been performed within the thermal programme with the objective to correlate measurements of thermal properties to calculated values from the mineral composition (SCA), produced within the geological programme. In Table 4-15 the comparison of TPS and SCA data is presented. Table 4-16 and Figure 4-6 specifies the samples included in the comparison.

For the comparison the closest SCA and TPS samples, respectively, have been used. The distance between compared samples has been limited to 0.45 m, which has implied that one sample has been excluded. Yet, most of the samples are considerable closer to each other.

For rock type granite to granodiorite 20 samples have been used for the comparison, while for tonalite to granodiorite and for granite, granodiorite and tonalite only two and one samples, respectively, have been used.

Four surface samples from thermal model version 1.1 have been used in the comparison between TPS and SCA data. The rock types of these samples have been reclassified relatively model version 1.1 /Stephens, 2004/.

Statistical tests were performed to compare the mean and variance for measured (TPS) and calculated (SCA) values of thermal conductivity. Tests were performed on samples coming from the same locations for rock type granite to granodiorite (101057). Similar tests were also performed on all TPS and SCA data from the Forsmark area for rock types tonalite to granodiorite (101054) and granite, granodiorite and tonalite (101051).

Tests on samples where TPS and SCA data represent the same rock gave the following result: For 101057 no significant differences in the mean and the variance were noted (5% significance level). The paired t-test was applied to test for difference in the mean between TPS and SCA data.

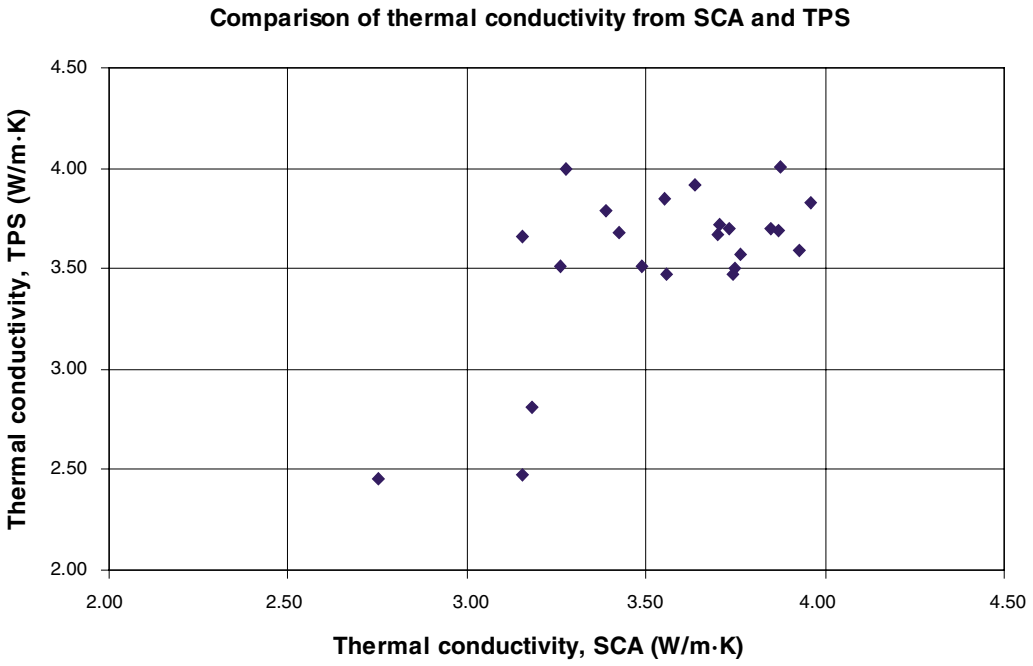

Figure 4-6. *Comparison between thermal conductivity calculated from SCA and measured according to the TPS-method.*

Table 4-15. Thermal conductivity (W/(m·K)) on samples with different rock types, calculated from the mineralogical compositions with the SCA method (samples from thermal programme), and measured with the TPS method. Samples are from boreholes KFM01A, KFM02A and KFM03A together with 4 surface samples. Mean refers to arithmetic mean.

Method		Granite to granodiorite (101057)	Tonalite to granodiorite (101054)	Granite, granodiorite and tonalite (101051)
		20 samples	2 samples	1 sample
Calculated (SCA)	Mean	3.63	2.97	3.15
	St. dev.	0.23	0.30	–
Measured (TPS)	Mean	3.69	2.63	2.47
	St. dev.	0.17	0.25	–
Diff. (SCA-TPS)/TPS		–1.5%	12.8%	27.6%

Table 4-16. Specification of samples included in the comparison of thermal conductivity (W/(m·K)) calculated from mineral composition (SCA) and measured with TPS method. The samples are taken from the rock types granite to granodiorite (101057), granite, granodiorite and tonalite (101051) and tonalite to granodiorite (101054).

Borehole/sample ID	Secup (m)	Rock code	SCA	TPS	Diff. (SCA-TPS)/TPS (%)
KFM01A	235.23	101057	3.75	3.50	7.1
KFM01A	231.28	101057	3.87	3.69	4.9
KFM01A	389.27	101057	3.70	3.67	0.9
KFM01A	389.68	101057	3.56	3.47	2.5
KFM01A	494.32	101057	3.42	3.68	–6.9
KFM01A	494.82	101057	3.28	4.00	–18.0
KFM01A	692.02	101057	3.55	3.85	–7.7
KFM01A	698.35	101057	3.64	3.92	–7.2
KFM02A	336.11	101057	3.70	3.72	–0.5
KFM02A	337.12	101057	3.77	3.57	5.5
KFM02A	530.69	101057	3.85	3.70	4.0
KFM02A	536.51	101057	3.16	3.66	–13.8
KFM02A	704.56	101057	3.93	3.59	9.4
KFM02A	719.24	101057	3.73	3.70	0.9
KFM03A	262.56	101054	3.18	2.81	13.3
KFM03A	305.87	101051	3.15	2.47	27.6
KFM03A	527.51	101057	3.96	3.83	3.4
KFM03A	527.70	101057	3.87	4.01	–3.4
KFM03A	684.21	101057	3.39	3.79	–10.7
PFM001159A		101057	3.49	3.51	–0.6
PFM001159B		101057	3.26	3.51	–7.0
PFM001162		101054	2.75	2.45	12.3
PFM001164		101057	3.74	3.47	7.8

Tests performed on all TPS and SCA data indicate that there is a significant difference in the variance for rock type 101057, which is illustrated in Figure 4-7. No significant difference in the mean could be detected by a two-sample t-test (overlapping data sets in Figure 4-7. The lower box plot in the figure illustrates the sample distribution where the middle line of the box corresponds to the median, the start and end of the box the first and third quartile and the horizontal lines from the box are upper and lower whisker, where the upper whisker extends to the highest data value within the upper limit (upper limit is estimated as Q3+1.5(Q3-Q1) where Q1 and Q3 are the first and third quartiles). For tonalite to granodiorite (101054) and granite, granodiorite and tonalite (101051) there is a significant difference in the mean values but no significant difference in variances. There are relatively few TPS measurements for these rock types (5 and 3 samples respectively) resulting is this type of comparison being relatively insecure when applying the results for the whole rock mass. For rock type tonalite to granodiorite (101054) and granite, granodiorite and tonalite (101051) the mean value of TPS measurements is smaller than the mean value of SCA calculations meaning the SCA method is overestimating the thermal conductivity. The variance of TPS measurements is smaller than the variance of SCA calculations meaning the values are distributed within a smaller interval. The situation is however different for rock type 101057, where the mean value of TPS measurements is larger than the mean value of SCA calculations meaning the SCA method is underestimating the thermal conductivity. The variance of TPS measurements is smaller than the variance of SCA calculations.

As illustrated, SCA calculations may overestimate or underestimate the thermal conductivity depending on rock type. One explanation is the uncertainty of thermal conductivity of different minerals, see section 6.1.1.

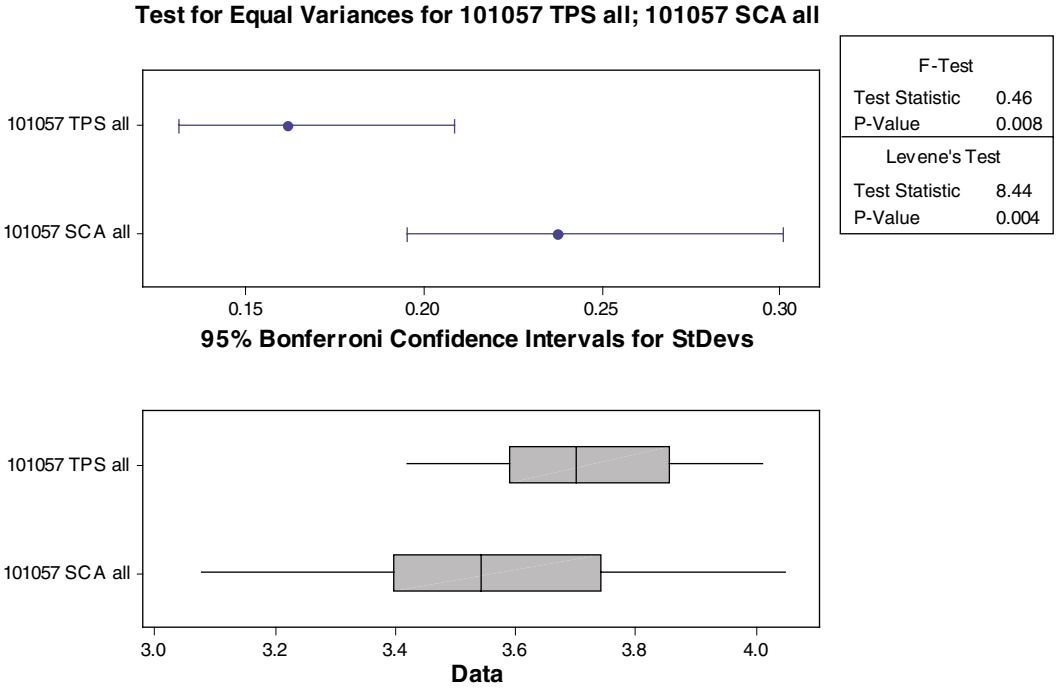

Figure 4-7. *Result of test for equal variances between all TPS measurements and SCA calculations of thermal conductivity for rock type granite to granodiorite (101057; F-test and Levene's test). There is a significant difference in variance, as indicated by the low p-values.*

For samples were both SCA- and TPS-results are available there is a difference. It should be emphasised that the samples are not exactly the same but with only a few centimetres-decimetres separation distance. Therefore, some part of the difference is probably a result of sampling.

4.5 Thermal conductivity from density

For the Simpevarp site investigation area a relationship between density and thermal conductivity for Ävrö granite has been found and is presented in /Sundberg, 2003b/. The methodology is further developed in /Sundberg et al. 2005a/. A corresponding relationship has however not been possible to apply for any of the rock types within the Forsmark site investigation area. Figure 4-8 illustrates samples where both density and thermal conductivity has been measured and shows that there is no valid relationship for any of the measured rock types. However, an obvious relationship exists between investigated rock types.

Results from density logging and geological mapping are shown in Figure 4-9.

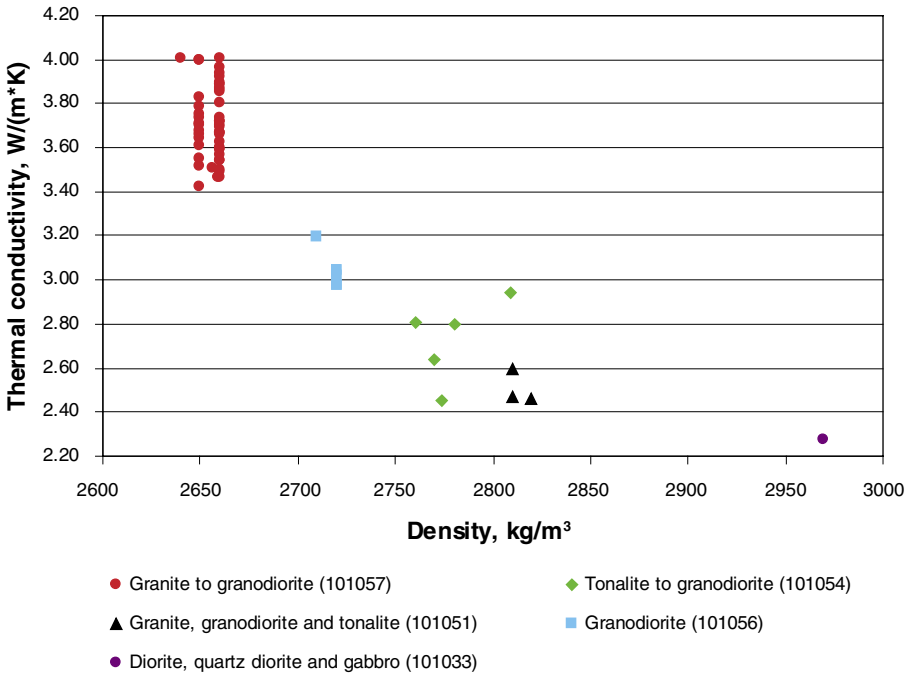

Figure 4-8. *Based on available data of rock types present at the Forsmark site investigation area, a trend between density and thermal conductivity is obvious between different rock types. However, a useful relationship within a certain rock type has not been found.*

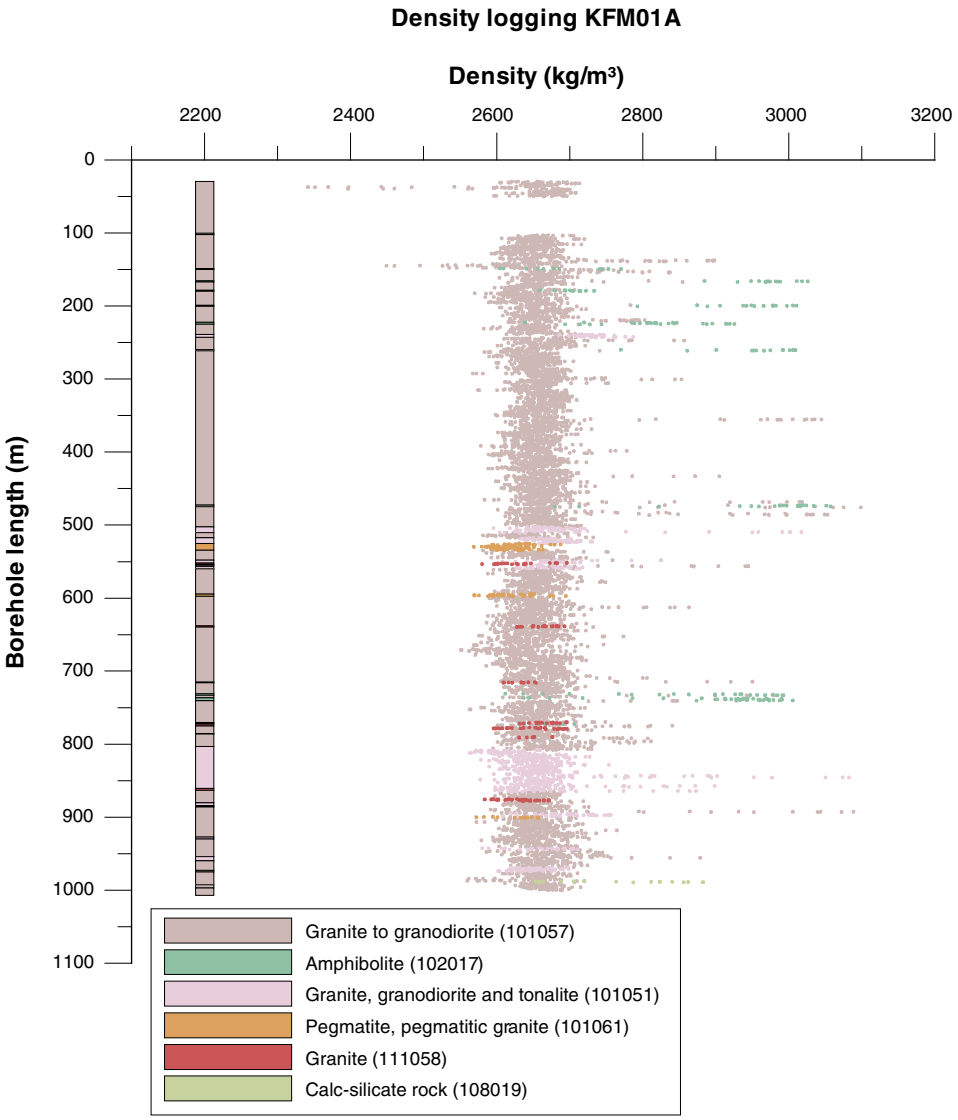

Figure 4-9. *Density logging of KFM01A with rock types marked in different colours.*

4.6 Rock type models (PDF) of thermal conductivity

4.6.1 Method

There are different data sets of thermal conductivity for the dominating rock types. The most reliable data comes from TPS measurements but these samples are probably not representative of the rock type due to the limited number of samples and the sample selection. Therefore, SCA calculations from the mineral distribution have to be included in the rock type model since they have a larger spatial distribution in the rock mass.

Rock type models of thermal conductivity have been produced by adding the data from TPS measurements and SCA calculations. In cases where only SCA data is available the models are based on these. The SCA calculations of rock type 101057 are not corrected since the evaluation of primary data does not show this type of correction to be relevant, see section 4.4.3. For other rock types there are not enough data to support a correction.

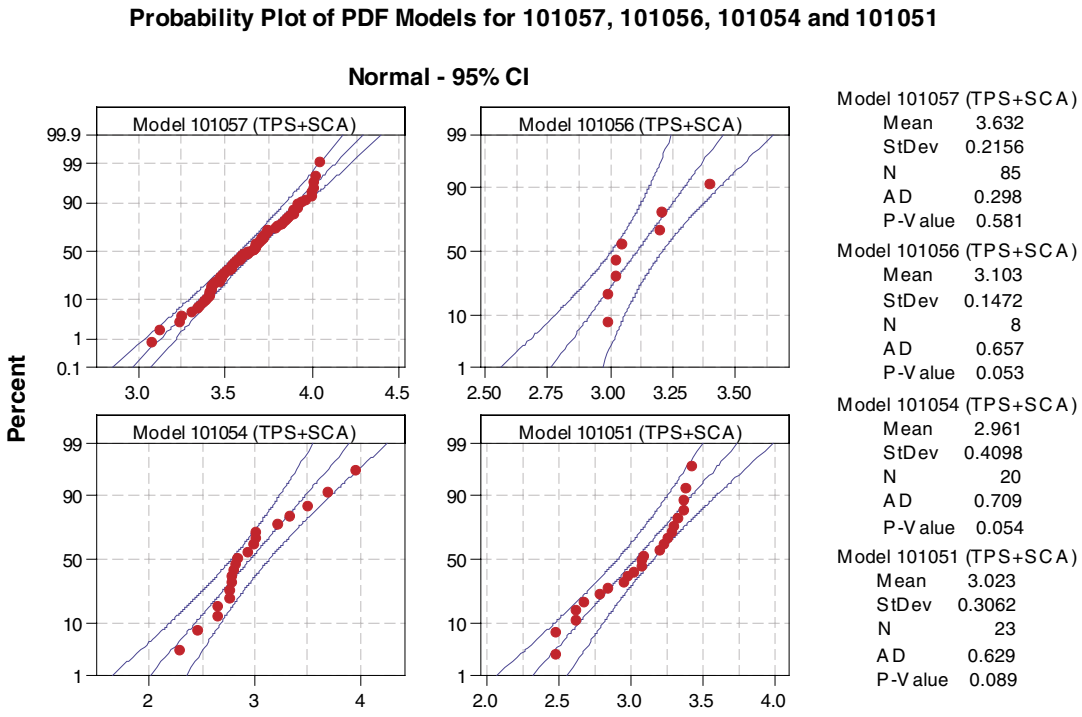

Figure 4-10. *Probability plots (normal distributions) of thermal conductivity separated on the rock types granite to granodiorite (101057), granodiorite (101056), tonalite to granodiorite (101054) and granite, granodiorite and tonalite (101051).*

All rock type models (Probability Density Functions, PDF:s) are assumed as normal (Gaussian) PDF:s. Probability plots, assuming normal distribution of thermal conductivities, are illustrated in Figure 4-10 and lognormal distributions in Appendix A.

4.6.2 Granite to granodiorite, metamorphic, medium-grained (101057)

For rock type 101057 there are two sources to thermal conductivity data, SCA calculations from mineral composition and TPS measurements. Data from the two methods are summarised in Table 4-17. Distribution models (PDF:s) based on data from the different methods are presented in Figure 4-11 and model properties of all rock types are presented in Table 4-21. In Figure 4-12 empirical cumulative distribution functions with fitted models (normal distributions) of rock type 101057 is presented. For some of the samples there are results from both SCA calculation and TPS measurements. In these cases the SCA-values are excluded and only the TPS-values are used in the model.

Table 4-17. Two different distributions of thermal conductivity (λ) based on different methods together with the model.

	λ – measured TPS measurements	**λ – modal Calculations from mineral composition**
Arithmetic mean (W/(m·K))	3.71	3.56
St. dev. (W/(m·K))	0.16	0.24
Number of samples	49	56
Comment		
Mean of model (W/(m·K))	3.63	
St. dev. of model (W/(m·K))	0.22	

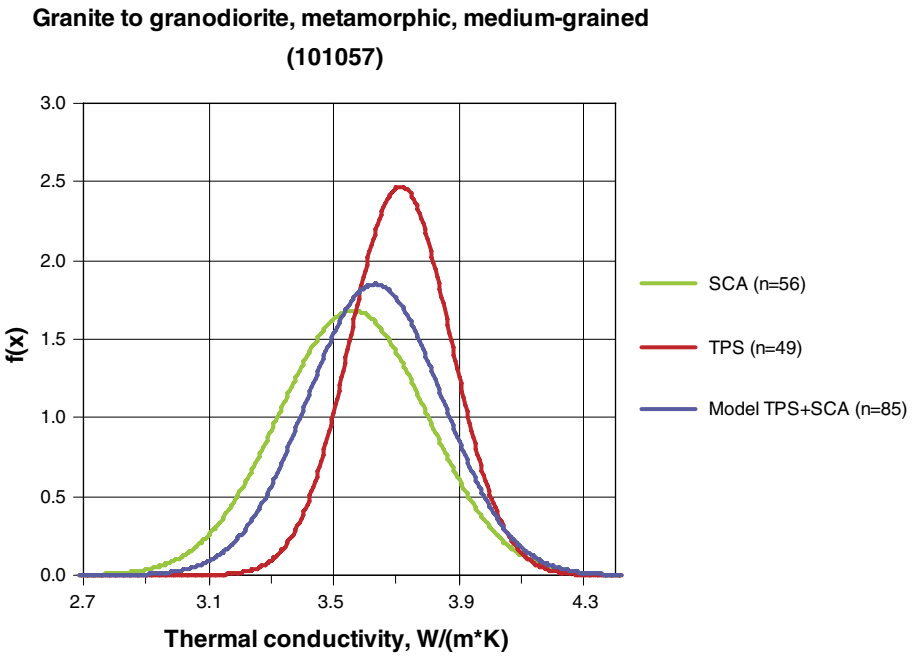

Figure 4-11. *Rock type models (PDF) for calculated values from mineral composition (SCA) and measured values (TPS) based on rock type 101057, granite to granodiorite.*

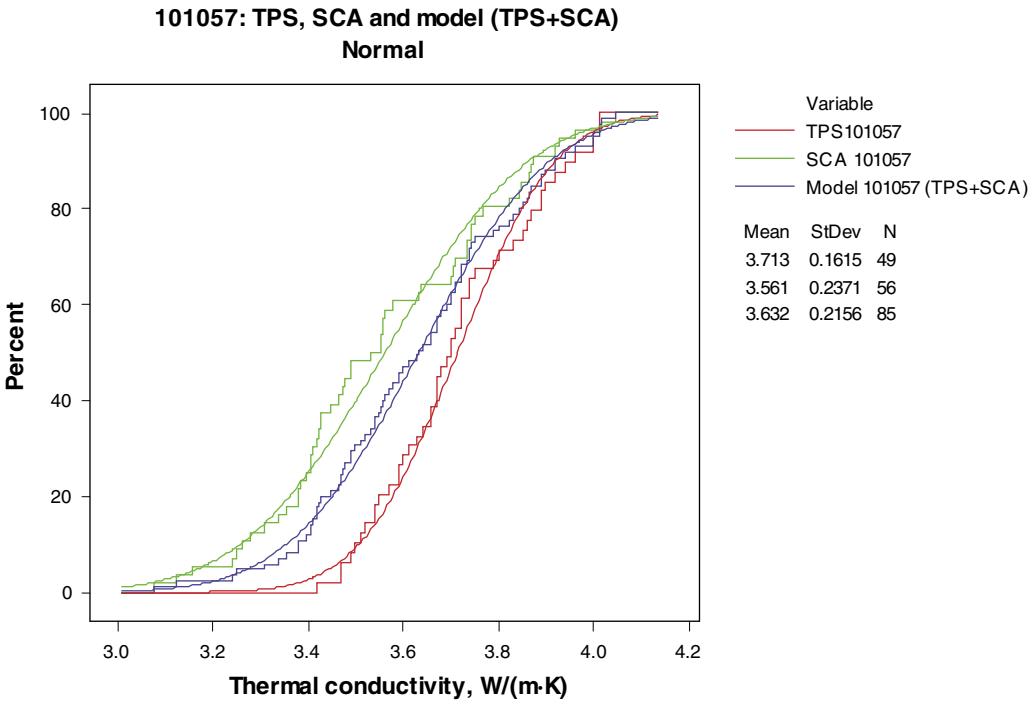

Figure 4-12. *Cumulative histogram of granite to granodiorite (101057) with data from two different methods and a model where TPS and SCA data has been put together.*

SCA calculations used in the comparison with TPS measurements have been excluded since both methods give a thermal conductivity of the same sample (20 samples excluded). Data from the two different methods has in probability plots shown to be lognormal distributed rather than normal distributed, see Appendix B. Although, data has been set as normal distributed since the probability plots show the distribution still good to use.

A model used in the domain modelling of rock type 101057 is calculated as a composition of both TPS measurements and SCA calculations. The model of TPS measurements and SCA calculations has also, by probability plots, shown to be lognormal distributed rather than normal distributed but is still set to normal distributed, see Appendix B.

4.6.3 Granodiorite, metamorphic (101056)

Rock type models (PDF) based on data from two different methods are presented in Table 4-18 and Figure 4-13 and model properties of all rock types are presented in Table 4-21. Figure 4-14 presents empirical cumulative distribution functions with fitted models (normal distributions) of rock type granodiorite (101056).

Table 4-18. Thermal conductivity (λ) based on different methods together with the model.

	λ – measured TPS measurements	λ – modal Calculations from mineral composition
Arithmetic mean (W/(m·K))	3.04	3.20
St. dev. (W/(m·K))	0.09	0.19
Number of samples	5	3
Comment		
Mean of model (W/(m·K))	3.10	
St. dev. of model (W/(m·K))	0.15	

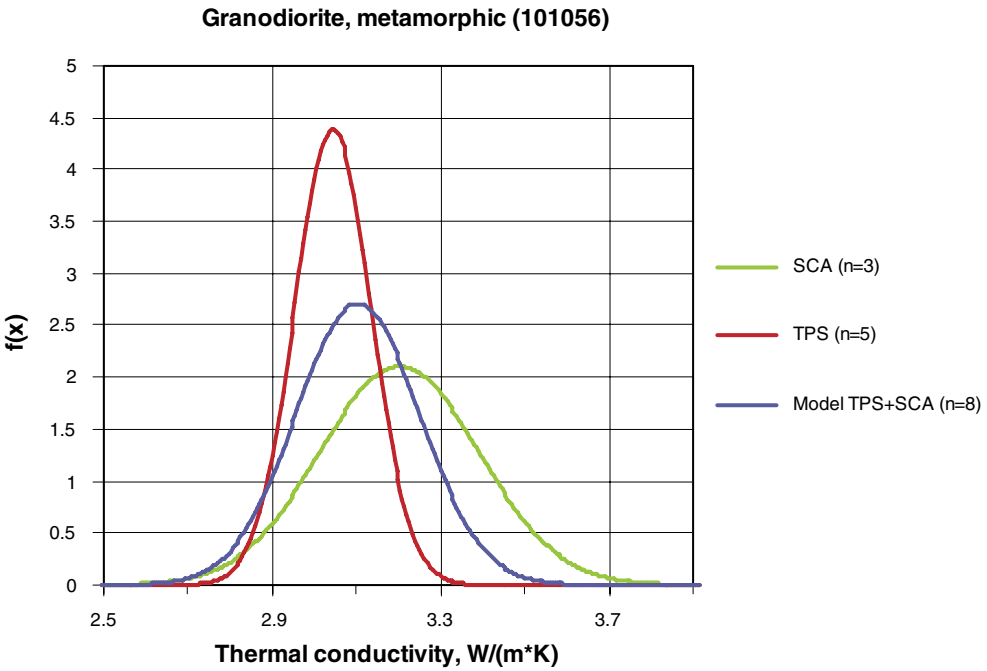

Figure 4-13. *Rock type models (PDF) for calculated values from mineral composition (SCA) and measured values (TPS) based on rock type granodiorite, 101056.*

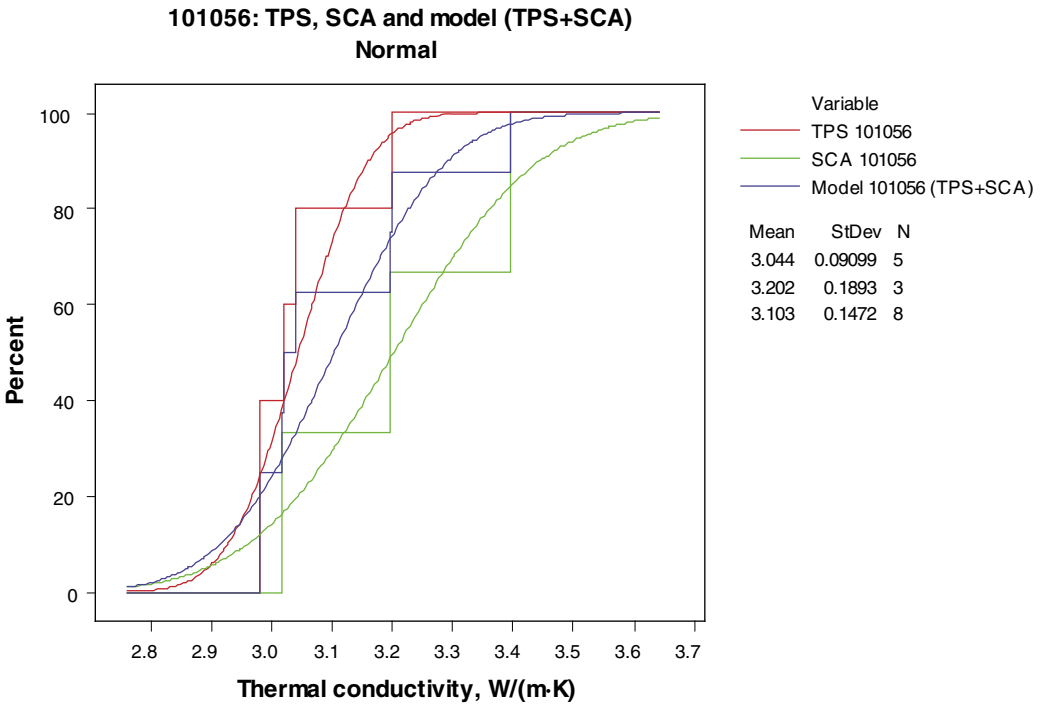

Figure 4-14. *Cumulative histogram of granodiorite (101056) with data from two different methods and a model where TPS and SCA data has been put together.*

For rock type granodiorite (101056) there are two sources to thermal conductivity data, SCA calculations based on mineral composition and TPS measurements. There are no SCA calculations which coincidence with TPS measurements and no samples have therefore been excluded. Data from the two different methods has in probability plots shown to be lognormal distributed rather than normal distributed, see Appendix B. Although, data has been set as normal distributed since the probability plots show the distribution still good to use.

A model used in the domain modelling of rock type granodiorite (101056) is calculated as a composition of both TPS measurements and SCA calculations. The model of TPS measurements and SCA calculations has also, by probability plots, shown to be lognormal distributed rather than normal distributed but is still set to normal distributed, see Appendix B.

4.6.4 Tonalite to granodiorite, metamorphic (101054)

Rock type models based on data from two different methods are presented in Table 4-19 and Figure 4-15 and model properties of all rock types are presented in Table 4-21. Figure 4-16 presents empirical cumulative distribution functions with fitted models (normal distributions) of rock type tonalite to granodiorite (101054). For two of the samples there are results from both SCA calculation and TPS measurements. In these cases the SCA-values are excluded and only the TPS-values are used in the model.

For rock type tonalite to granodiorite (101054) there are two sources to thermal conductivity data, SCA calculations and TPS measurements. SCA calculations used in the comparison with TPS measurements have been excluded since both methods give a thermal conductivity of the same sample (2 samples excluded). Data from the TPS method

has in probability plots shown to be normal distributed but data from the SCA method are lognormal distributed rather than normal distributed, see Appendix B. Although, data has been set as normal distributed since the probability plots show the distribution still good to use.

A model used in the domain modelling of rock type tonalite to granodiorite (101054) is calculated as a composition of both TPS measurements and SCA calculations. The model of TPS measurements and SCA calculations has also, by probability plots, shown to be lognormal distributed rather than normal distributed but is still set to normal distributed, see Appendix B.

Table 4-19. Thermal conductivity (λ) based on different methods together with the model.

	λ – measured TPS measurements	λ – modal Calculations from mineral composition
Arithmetic mean (W/(m·K))	2.73	3.03
St. dev. (W/(m·K))	0.19	0.42
Number of samples	5	17
Comment		
Mean of model (W/(m·K))	2.96	
St. dev. of model (W/(m·K))	0.41	

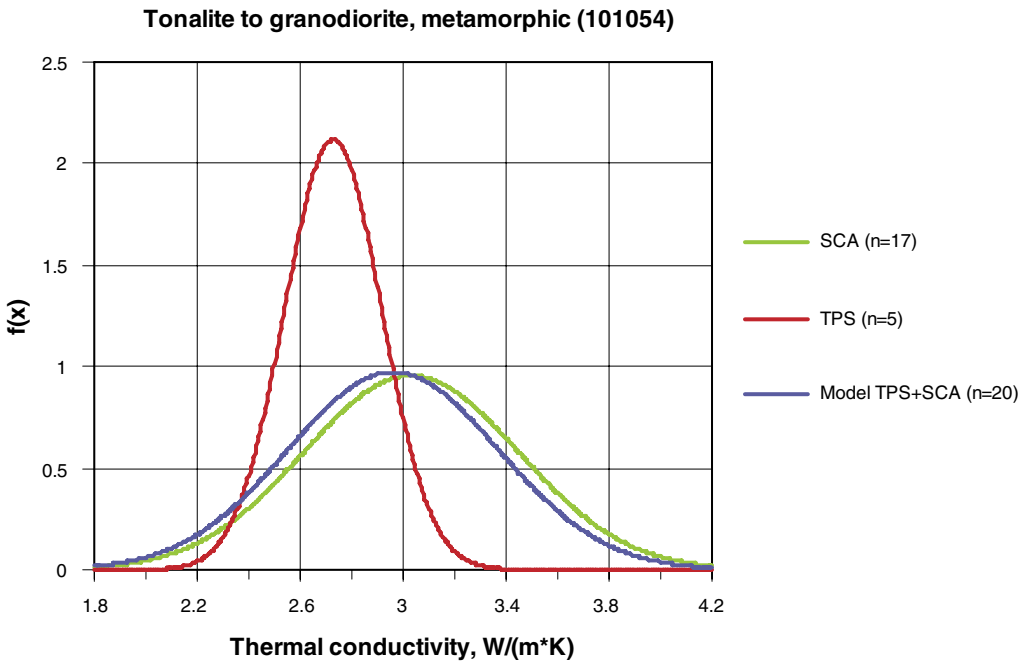

Figure 4-15. *Rock type models (PDF) of calculated values from mineral composition (SCA) and measured values (TPS) based on rock type 101054, tonalite to granodiorite.*

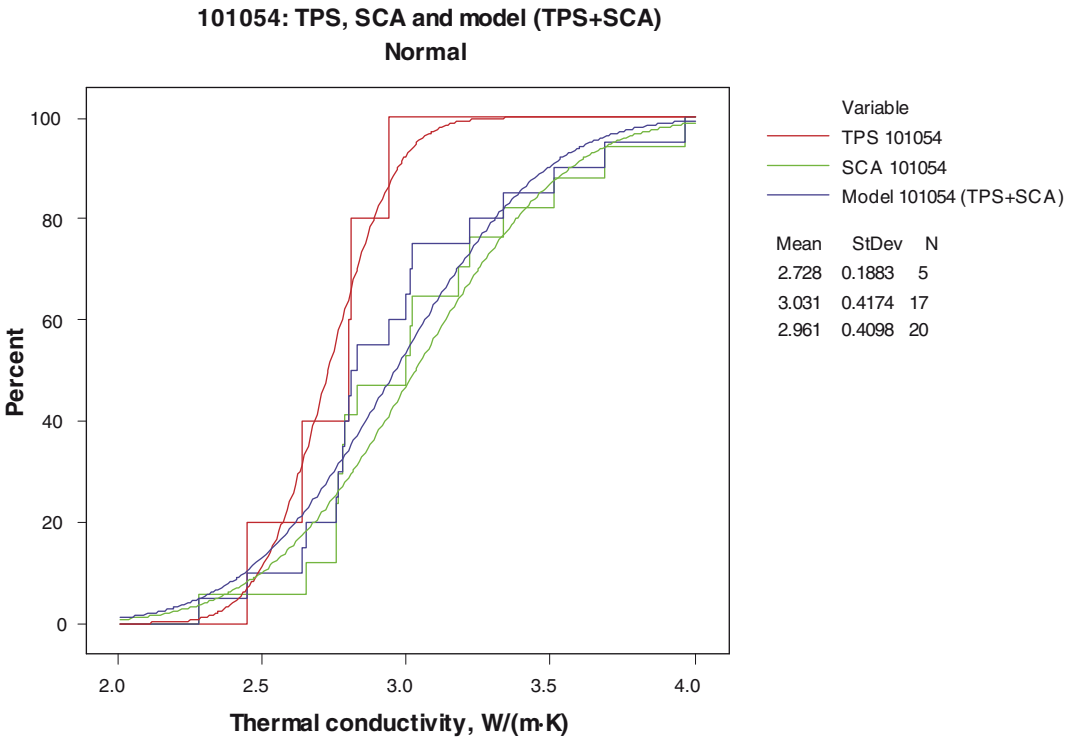

Figure 4-16. *Cumulative histogram of tonalite to granodiorite (101054) with data from two different methods and a model where TPS and SCA data has been put together.*

4.6.5 Granite, granodiorite and tonalite, metamorphic, fine- to medium-grained (101051)

Rock type models based on data from two different methods are presented in Table 4-20 and Figure 4-17 and model properties of all rock types are presented in Table 4-21. Figure 4-18 presents empirical cumulative distribution functions with fitted models (normal distributions) of rock type granite, granodiorite and tonalite (101051). For one of the samples there are results from both SCA calculation and TPS measurements. In this case the SCA-value is excluded and only the TPS-value is used in the model.

Table 4-20. Thermal conductivity (λ) based on different methods together with the model.

	λ – measured TPS measurements	**λ – modal Calculations from mineral composition**
Arithmetic mean (W/(m·K))	2.51	3.10
St. dev. (W/(m·K))	0.08	0.24
Number of samples	3	21
Comment		
Mean of model (W/(m·K))	3.02	
St. dev. of model (W/(m·K))	0.31	

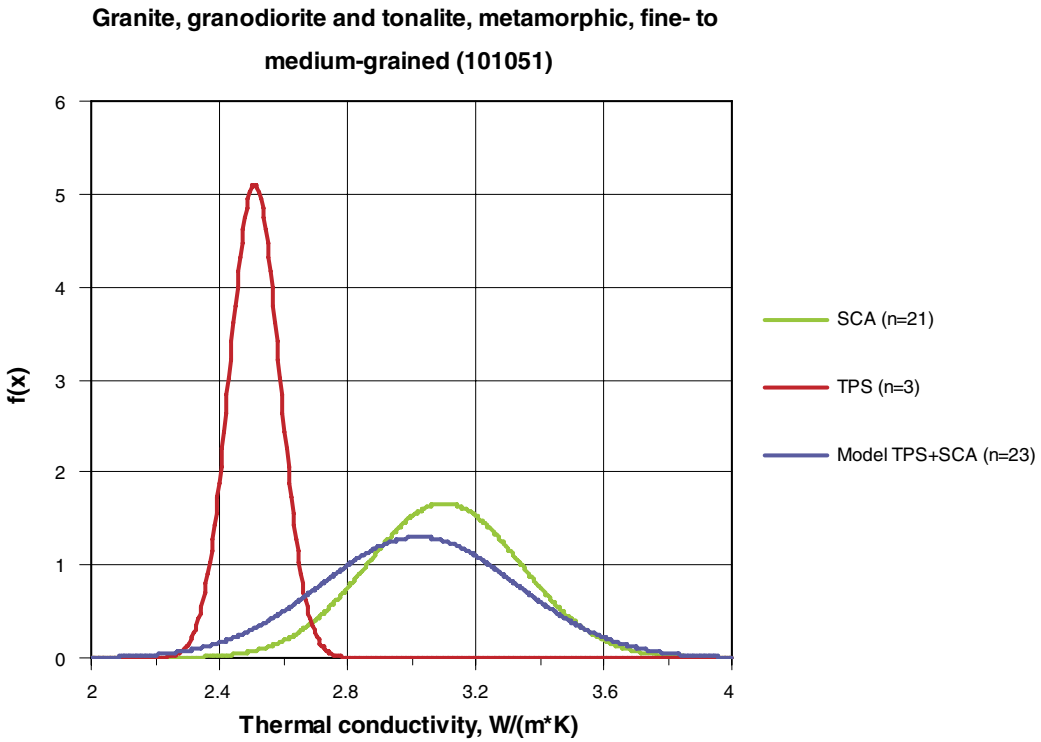

Figure 4-17. *Rock type models (PDF) of calculated values from mineral composition (SCA) and measured values (TPS) based on rock type 101051, granite, granodiorite and tonalite.*

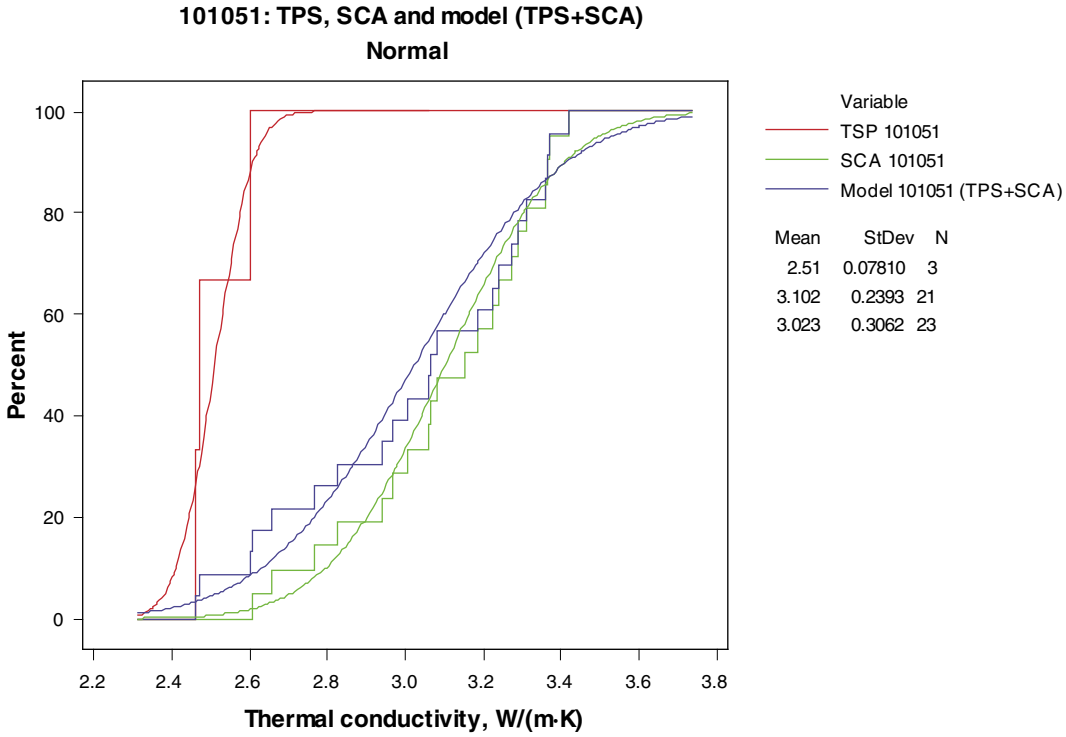

Figure 4-18. Cumulative histogram of granite, granodiorite and tonalite (101051) with data from two different methods and a model where TPS and SCA data has been put together.

For rock type granite, granodiorite and tonalite (101051) there are two sources to thermal conductivity data, SCA calculations and TPS measurements. SCA calculations used in the comparison with TPS measurements have been excluded since both methods give a thermal conductivity of the same sample (1 sample excluded). Data from the TPS method has in probability plots shown to be lognormal distributed and data from the SCA method are normal distributed rather than lognormal distributed, see Appendix B. Although, data has been set as normal distributed since the probability plots show the distribution still good to use.

A model used in the domain modelling of granite, granodiorite and tonalite (101051) is calculated as a composition of both TPS measurements and SCA calculations. The model of TPS measurements and SCA calculations has, by probability plots, shown to be normal distributed, see Appendix B.

4.6.6 Other rock types

For other rock types except granite to granodiorite (101057), granodiorite (101056), tonalite to granodiorite (101054) and granite, granodiorite to tonalite (101051) the extent of data is rather limited and in most cases only SCA calculations were available when modelling the different rock types. In Figure 4-19 empirical cumulative distribution functions of pegmatite, pegmatitic granite (101061), felsic to intermediate volcanic rock (103076), granite (101058), granite (111058) and diorite, quartz diorite and gabbro (101033) is presented together with fitted models (normal distributions). Model properties of all rock types are presented in Table 4-21.

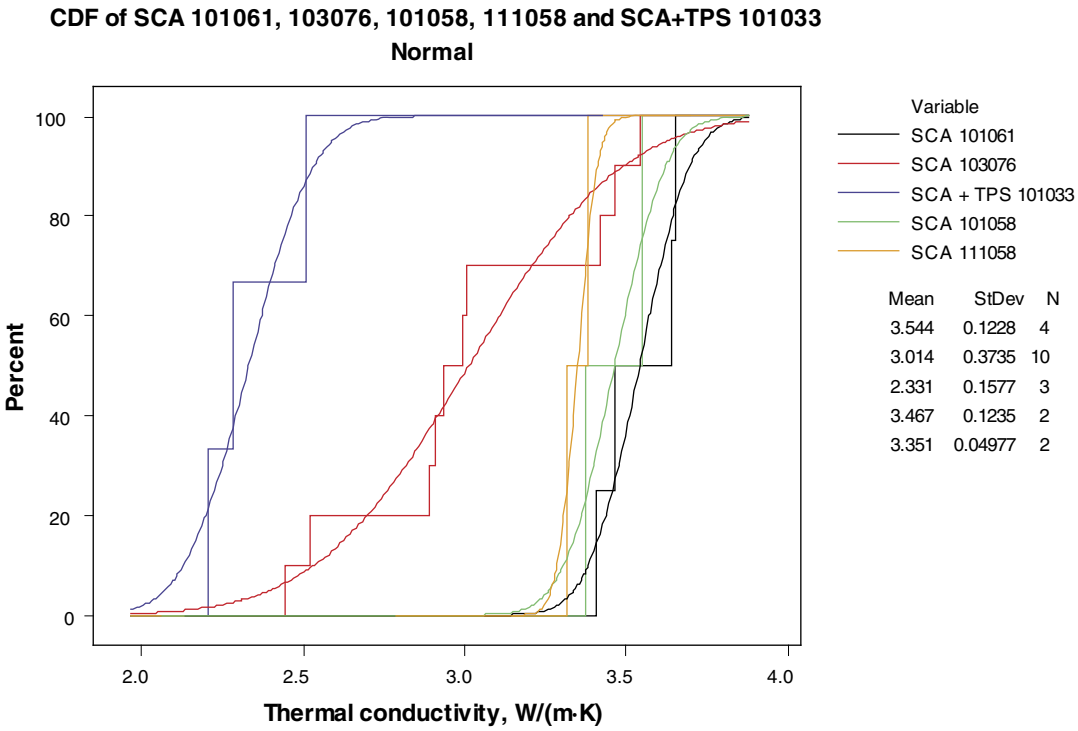

Figure 4-19. *Cumulative histogram of pegmatite, pegmatitic granite (101061), felsic to intermediate volcanic rock (103076), granite, metamorophic, aplitic (101058), granite, fine- to medium-grained (111058) and diorite, quartz diorite and gabbro (101033). For 101033 data are from two different methods and a model TPS and SCA data put together is illustrated. For 101061, 103076, 101058 and 111058 only SCA data was available.*

Table 4-21. Model properties (normal distributed) of thermal conductivity (W/(m·K)) from different methods and combinations divided on rock type.

Rock code (name) and samples	Arithmetic mean	St. dev.	Number of samples
101057 (granite to granodiorite)			
TPS	3.71	0.16	49
SCA	3.56	0.24	56
TPS+SCA	3.63	0.22	85
101056 (granodiorite)			
TPS	3.04	0.09	5
SCA	3.20	0.19	3
TPS+SCA	3.10	0.15	8
101054 (tonalite to granodiorite)			
TPS	2.73	0.19	5
SCA	3.03	0.42	17
TPS+SCA	2.96	0.41	20
101051 (granite, granodiorite and tonalite)			
TPS	2.51	0.08	3
SCA	3.10	0.24	21
TPS+SCA	3.02	0.31	23
101061 (pegmatite, pegmatitic granite)			
SCA	3.54	0.12	4
103076 (felsic to intermediate volcanic rock)			
SCA	3.01	0.37	10
101033 (diorite, quartz diorite and gabbro)			
TPS	2.28		1
SCA	2.36	0.21	2
TPS+SCA	2.33	0.16	3
101058 (granite, metamorohic, aplitic)			
SCA	3.47	0.12	2
111058 (granite, fine- to medium-grained)			
SCA	3.35	0.05	2

4.7 Spatial variability

A variogram based on TPS-measurement for granite to granodiorite (101057) is showed in Figure 4-20. The variogram indicates strong correlation up to about 0.5–1 m. Such small scale variability is probably evened out over a larger scale.

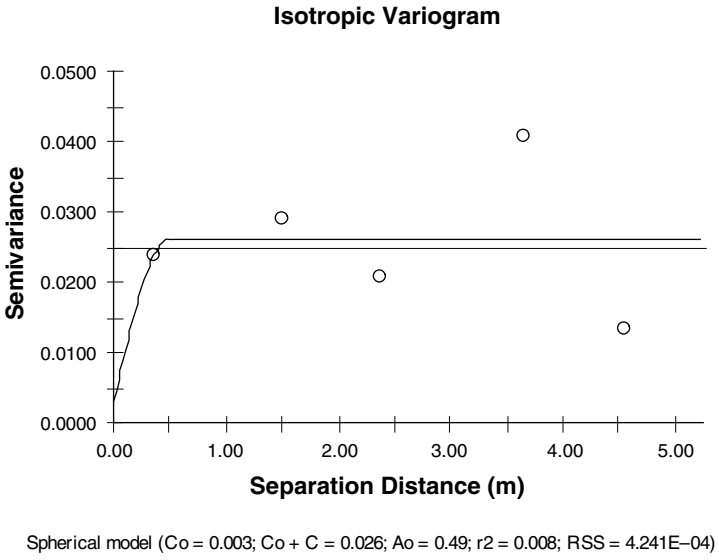

Figure 4-20. *Variogram of the thermal conductivity for granite to granodiorite (101057) with a separation distance of 5 m. Data is based on TPS measurements and the straight line indicates the sample variance. The variogram is highly uncertain due to the limited amount of data and therefore it is not used in the subsequent chapters.*

4.8 Heat capacity

4.8.1 Measurement method

Heat capacity has been measured with the TPS (Transient Plane Source) method.
For method description see section 4.3.1.

4.8.2 Measurement result

In Table 4-22 the results from all conducted measurements of heat capacity is summarised /Adl-Zarrabi, 2003; 2004a,b,c,d/. Observe that samples from rock types tonalite to granodiorite (101054), granite, granodiorite and tonalite (101051) and granodiorite (101056) all arise from short distances of 0.2–1 m in the boreholes KFM03 and KFM04. The representativeness of the values can therefore be discussed.

Table 4-22. Measured heat capacity (MJ/(m³·K)) of samples (all TPS measurements) with different rock types, using the TPS method. Samples are from boreholes KFM01A, KFM02A, KFM03A and KFM04A together with 5 surface samples.

Rock code	Rock name	Sample location	Arithmetic mean	St. dev.	Max	Min	Number of samples
101057	Granite to granodiorite	Borehole KFM01A, KFM02A, KFM03A and sample PFM001159 and PFM001164	2.17	0.17	2.54	1.76	49
101054	Tonalite to granodiorite	Borehole KFM03A, PFM001157 and PFM001162	2.12	0.20	2.39	1.93	5
101051	Granite, granodiorite and tonalite	Borehole KFM03A	2.17	0.05	2.22	2.13	3
101056	Granodiorite	Borehole KFM04A	2.25	0.07	2.34	2.16	5
101033	Diorite, quartz diorite and gabbro	PFM001158	2.33		2.33	2.33	1

4.8.3 Temperature dependence

The temperature dependence of heat capacity has been investigated by measurements, for rock type granite to granodiorite (101057), at three different temperatures (20, 50 and 80°C) /Adl-Zarrabi, 2003; 2004a,b,c,d/. The temperature dependence of each sample is illustrated in Figure 4-21 and summarised for granite to granodiorite (101057) in Table 4-23. With increasing temperature the heat capacity for the rock type also increases by 27.5%/100°C temperature increase, calculated mean value of 18 samples. However, the increase varies from 15.9% to 54.8% for the individual samples.

Table 4-23. Measured temperature dependence of heat capacity (per 100°C temperature increase) on samples with different rock types from boreholes KFM01A, KFM02A and KFM03A.

Rock code	Rock name	Sample location	Mean	St. dev.	Number of samples
101057	Granite to granodiorite	**B**oreholes KFM01A, KFM02A and KFM03A	27.5%	8.6%	18

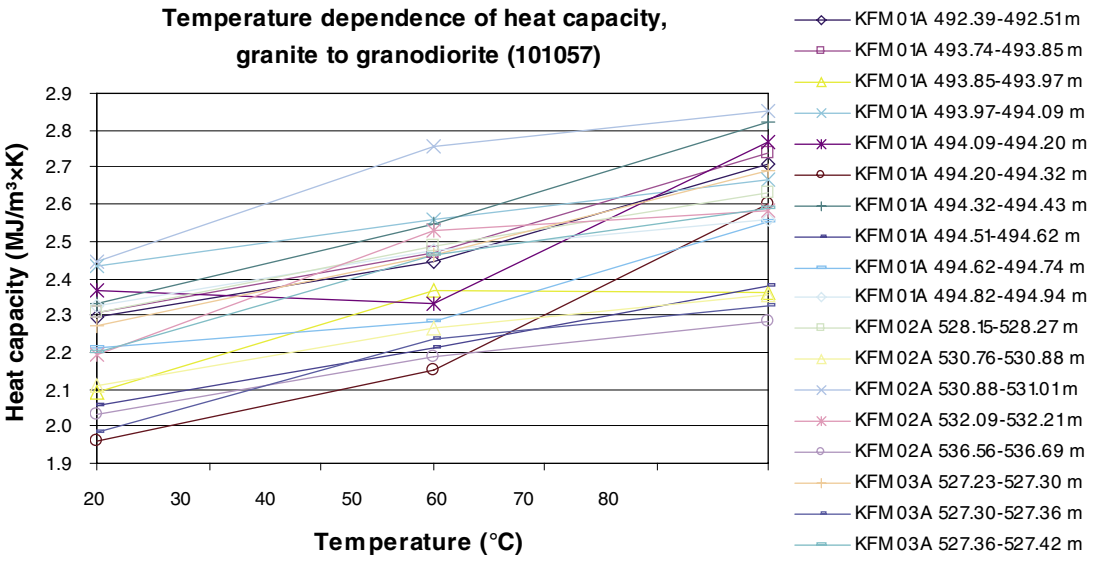

Figure 4-21. *Temperature dependence of heat capacity, rock type granite to granodiorite (101057).*

4.8.4 Rock type models

Rock type models of heat capacity have been produced from the results of the TPS measurements. For heat capacity the normal distribution of data is presented in Figure 4-22.

Models of heat capacity for different rock types are presented in Table 4-24. Data is normal distributed which is illustrated in Figure 4-22.

Table 4-24. Rock type models of heat capacity for rock types 101057,101054, 101051 and 101056.

Rock code	Rock name	Mean	St. dev.	Number of samples	Distribution
101057	Granite to granodiorite	2.17	0.172	49	normal
101054	Tonalite to granodiorite	2.12	0.201	5	normal
101051	Granite, granodiorite and tonalite	2.17	0.045	3	normal
101056	Granodiorite	2.25	0.066	5	normal

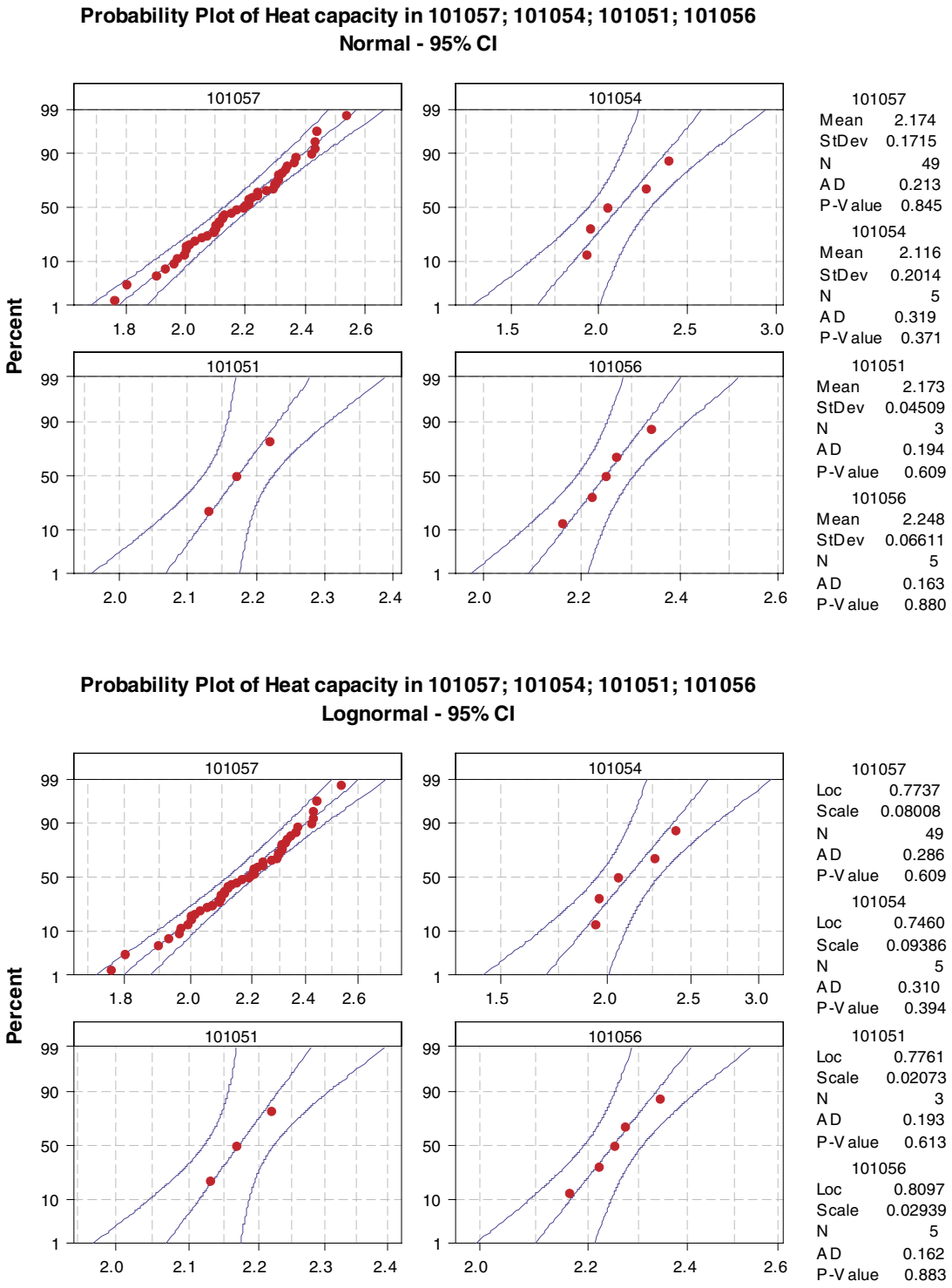

Figure 4-22. *Probability plots (normal and lognormal distributions) of heat capacity separated on rock types granite to granodiorite (101057), tonalite to granodiorite (101054), granite, granodiorite and tonalite (101051) and granodiorite (101056). There are no major differences in fit between the normal and lognormal models.*

4.9 Coefficient of thermal expansion

The coefficient of thermal expansion has been measured on samples from the Forsmark area and they are presented in Table 4-25, distributed on rock types. Samples from three different boreholes (KFM01A, KFM02A and KFM03A) have been investigated. The mean value of measured thermal expansion varies for the different rock types between $7.2 \cdot 10^{-6}$ and $8.0 \cdot 10^{-6}$ m/(m·K).

Table 4-25. Measured thermal expansion (m/(m·K)) on samples with different rock types from boreholes KFM01A, KFM02A and KFM03A (interval of temperature: 20–80°C).

Rock code	Rock name	Sample location	Arithmetic mean	St. dev.	Min	Max	Number of samples
101057	Granite to granodiorite	Borehole KFM01A, KFM02A, KFM03A	7.7E–06	2.2E–06	2.1E–06	1.5E–05	44
101054	Tonalite to granodiorite	Borehole KFM03A	7.2E–06	1.6E–06	5.3E–06	8.2E–06	3
101051	Granite, granodiorite and tonalite	Borehole KFM03A	8.0E–06	1.8E–06	6.5E–06	1.0E–05	3

For the dominating rock type, 101057, in domain RFM029 a mean value of the thermal expansion coefficient is suggested as $7.7 \cdot 10^{-6}$ m/(m·K).

4.10 In situ temperature

4.10.1 Method

The temperature and gradient profiles has been investigated for the boreholes KFM01A, KFM01B, KFM02A, KFM03A and KFM04A. The temperature for the boreholes were measured by fluid temperature loggings.

To all series with temperature measurements, an equation was fitted. Both linear, second degree and third degree equations where evaluated. The linear equations where estimated to be good enough, and higher degree equations did not give a larger correspondence.

The thermal gradients were calculated for the midpoint of a 9 m interval and for the midpoint of a 50 m interval. This means that 91 and 501 temperature values, respectively, were used for each gradient value. The gradients were calculated according to Equation 4-1.

$$Gradient = \frac{1000(n\Sigma zT - \Sigma z\Sigma T)\sin\varphi}{n\Sigma z^2 - (\Sigma z)^2} \qquad \text{Equation 4-1}$$

Parameter z is the depth co-ordinate (m), T is the measured temperature (K), φ is the angle (°) between the borehole and a horizontal line and n is the number of temperature measurements in an interval of 9 or 50 m, respectively.

Data from the bore holes have earlier been investigated and reported to the Sicada database /Mattsson and Keisu, 2004; Mattsson et al. 2004; Thunehed, 2004/. The main purpose if these investigations were to provide information to the geological core mapping and to the single-hole interpretation. Gradients, calculated within these investigations, have been used for comparison in this work. When calculating the gradient, /Mattsson and Keisu, 2004; Mattsson et al. 2004; Thunehed, 2004/ have used filtered data for the temperature. In this work, filtered temperature data have been used for three boreholes (KFM01B, KFM02A and KFM03A), while data that are not filtered have been used for the two other boreholes (KFM01A and KFM04A). For data from borehole KFM01B a 3 poin average filter was used, while for KFM02A and KFM03A a 17 point average filter was used.

4.10.2 Results

The results from the temperature loggings, the equations for the temperature and the calculated gradients are presented in Figure 4-23 to Figure 4-28. Figure 4-23 illustrates a summary of all investigated boreholes while Figure 4-24 to Figure 4-28 the boreholes separately. The y-axis in the figures illustrates depth below sea level (not the borehole length). In Table 4-26 the elevation at the start point for each borehole is presented. The differences depend on the ground level above sealevel.

The temperature at 500 m depth is calculated to be in the interval 11.2–12.0°C for the boreholes KFM01A, KFM02A, KFM03A and KFM04A from the Forsmark site, see Figure 4-23. The temperature for KFM01B is anomalous compared to the other boreholes. The reason for this is not known. KFM01B does not reach 500 m and is therefore not included in the calculation of mean temperature at 500 and 600 m depth in Table 4-27. At 470 m the temperature in this borehole is 10.0°C. In Table 4-27 the temperature for the boreholes are presented at the depths 400 m, 500 m and 600 m. The inclinations for the boreholes are given as mean values. KFM01A, KFM02A and KFM03A are almost perpendicular to the ground, while the angle for KFM01B is a bit smaller and KFM04A has an inclination of about 54°.

The reason for the deviant temperature in borehole KFM01B is unknown. The borehole is excluded from the calculation of the mean in Table 4-27.

Close to the surface (ca 0–100 m) there are large variations in the temperature and some temperature measurement have failed, the value –999° is showed , these data have been excluded. Deeper, the temperature seems to be almost linear with depth. In the loggings, the temperature was measured every 10 cm.

Table 4-26. Elevation (metres above sealevel) for the start point for each investigated borehole at the Forsmark site.

Bore hole	Elevation (metres above sealevel)
KFM01A	3.1
KFM01B	3.1
KFM02A	7.4
KFM03A	8.3
KFM04A	8.7

Table 4-27. Temperature (°C) for the five investigated boreholes at the Forsmark site, at different levels. Borehole inclinations are also included for the boreholes, given as a mean value for each borehole.

Borehole	Temperature at the depth 400 m	Temperature at the depth 500 m	Temperature at the depth 600 m	Inclination (°)
KFM01A	10.6	11.7	12.9	80
KFM01B	9.2	–	–	75
KFM02A	10.8	11.8	12.9	84
KFM03A	10.8	12.0	13.1	85
KFM04A	10.2	11.2	12.3	54
Arithmetic mean (KFM01B excluded)	10.6	11.7	12.8	

Times for core drillings and fluid temperature loggings for four of the boreholes are given in Table 4-28. The times between core drilling and temperature logging are about 12 weeks for KFM01A, 21 weeks for KFM02A, 6 weeks for KFM03A and 4 days for KFM04A. The relatively short period between the drilling activity and temperature logging might result in a disturbance of the logging results due to the borehole not being stabilised. The drilling activity increases the temperature in the borehole but a temperature decrease probably occurs due to the added drilling fluid. Also a temperature equalisation occurs in the borehole when the drilling fluid is transported in the borehole. However, the difference in temperature is relatively small for a specified depth but the influence on the design of a repository may be significant.

The calculated angle between the borehole and a horizontal line for KFM01A decreases from about 84° at a depth of 100 m to about 75° at –950 m. The gradient has earlier been calculated by /Mattsson et al. 2004/. The difference between the gradients is small, even though filtered data were used in that investigation and data used here were not filtered. From the top of the borehole to about 300 m, the gradient decreases. Then it increases up to 13°C/km at –950 m above sealevel. There are only small oscillations for the gradient (calculated for 9 m intervals) in the upper part of the borehole. In the intervals 700–800 and 850–930 m depth the oscillations are somewhat greater. This might be because of water bearing fractures in this part of the borehole or it might be noise related, which is indicated by the repeatedly occurring wavelength /Mattsson et al. 2004/.

Table 4-28. Occasions for core drilling and fluid temperature and resistivity loggings for the boreholes KSH01A, KSH02 and KSH03A.

Borehole	Core drilling Start time	Core drilling Stop time	Fluid temperature and resistivity logging
KFM01A	2002-06-25	2002-10-28	2003-04-25
KFM02A	2003-01-08	2003-03-12	2003-08-05
KFM03A	2003-04-16	2003-06-23	2003-08-08
KFM04A	2003-05-20	2003-11-19	2003-11-23

For KFM01B the angle for the borehole decreases from about 77.5° at –100 m to about 71.5° at –450 m. Calculated gradient for comparison was received from Sicada /Mattsson et al. 2004/. The difference between the two calculations is small, not more than 0.5%. The gradient from Sicada seems to be slightly smaller, than the one calculated here The gradient grows by depth, at 100 m depth it is approximately 7°C/km and at 400 m depth it is approximately 11°C/km. Two anomalies can be seen, one at 150–250 m and one at 420–460 m.

The angle for KFM02A decreases from about 86° at 100 m depth to about 81° at 950 m depth. From the database, Sicada, a gradient for comparison, was received /Thunehed, 2004/. In two small sections, 515–520 m depth and at the bottom of the borehole (982 m), there were great differences between the two gradients. For the rest of the borehole the difference was less than 10%. There are oscillations for the calculated gradient, especially from the top down to 500 m depth and below 800 m. This might be caused by water bearing fractures /Thunehed, 2004/. At –700 m the gradient is about 12°C/km.

For KFM03A the angle between the borehole and a horizontal line varies between 82.5° and 86°. The angle is decreasing with time. There are also values for the gradient calculated earlier and received from the database /Thunehed, 2004/. There are small oscillations for the gradient. Between –620 and –650 m, there is a section with greater oscillation. This might be caused by water bearing fractures /Thunehed, 2004/. The gradient is about 13°C/km at the depth 800 m. The gradient increases slightly by depth.

The angle for borehole KFM04A decreases from about 62° at 100 m depth to 44° at the end of the borehole (800 m depth). No earlier calculated gradient for comparison has been found. The variations and anomalies for the gradient is larger for KFM04A than for the other, here investigated boreholes, especially from the top of the borehole down to 600 m depth. Contrary to the other boreholes, the gradient for KFM04A seems to slightly decrease with depth. At 300 m depth the gradient is about 7.5°C/km, while it is about 6°C/km at 700 m depth.

The small differences, mentioned above, between the gradients calculated here and the ones received from Sicada /Mattsson et al. 2004; Thunehed, 2004/, might have different reasons. Here, temperature data received from Sicada are used. They are rounded, which causes a small error in the results. The data used by /Mattson et al. 2004/ and /Thunehed, 2004/ were filtered, while the data used here are not for two of the boreholes.

The measured temperature and the calculated gradient are presented both in one figure for all investigated boreholes and in one figure per borehole.

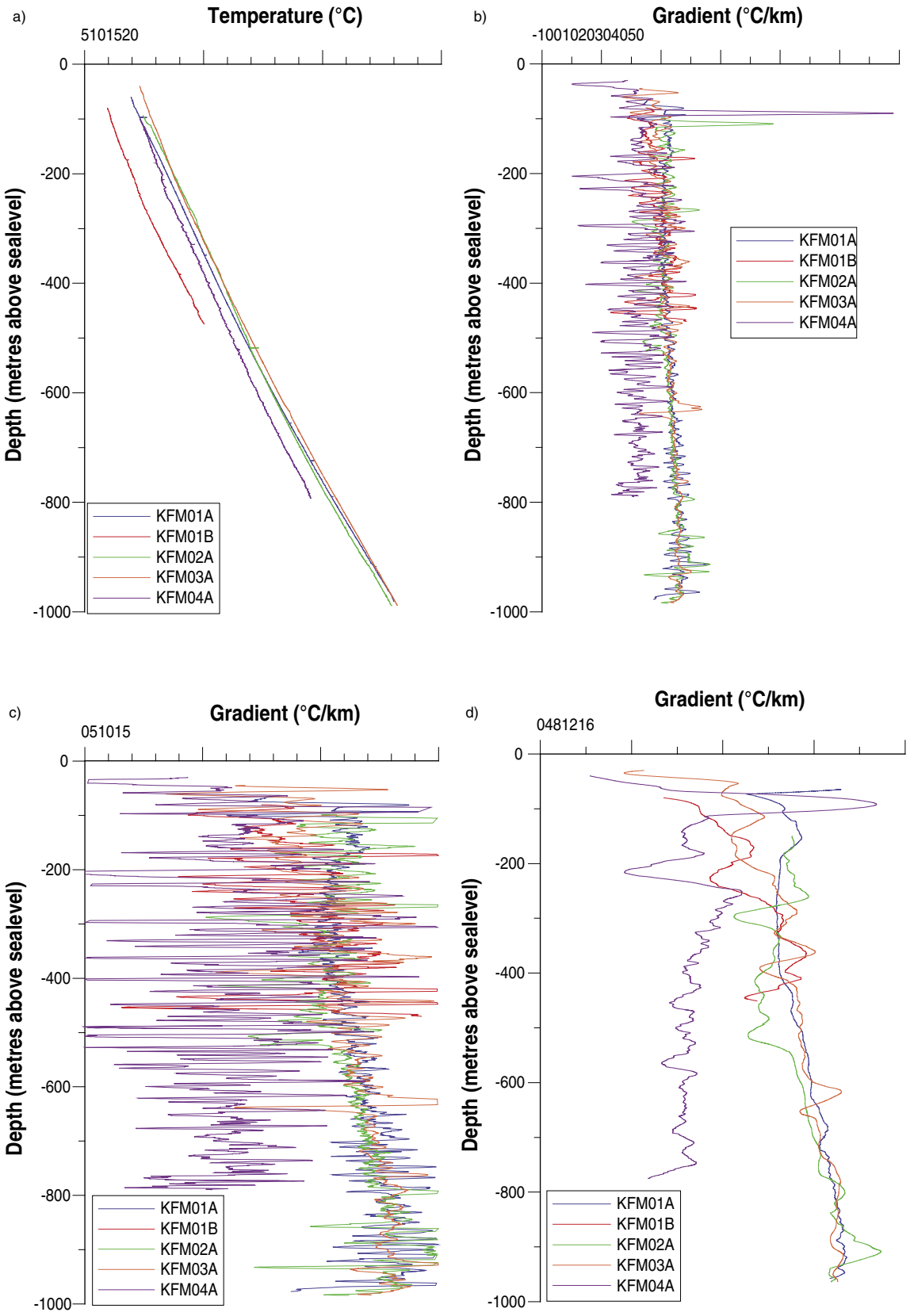

Figure 4-23. *Temperature (a) and gradient (b–d) for five boreholes at Forsmark. Figure b and c shows the temperature gradient calculated for nine metre intervals, while figure d shows the gradient calculated for 50 m intervals.*

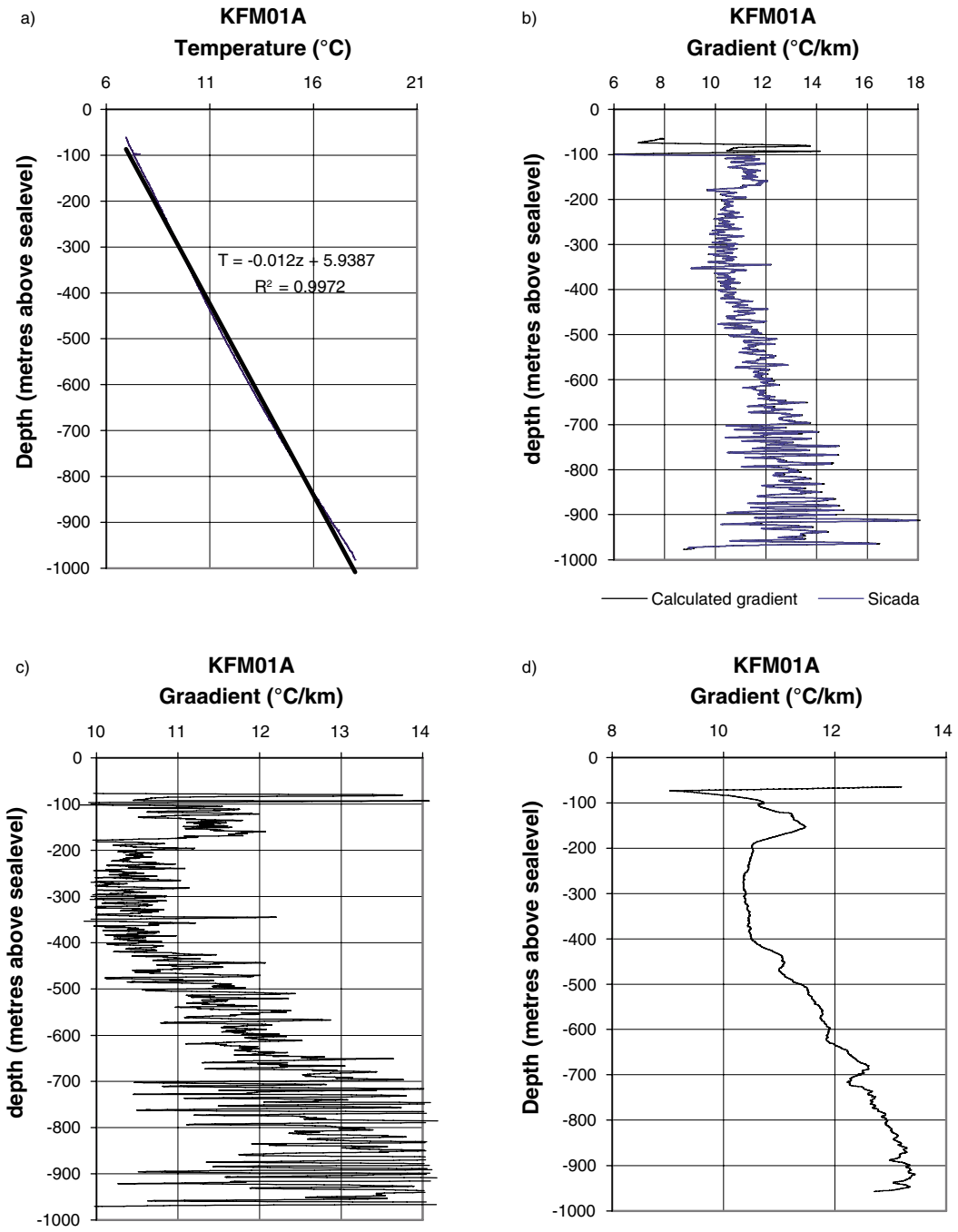

Figure 4-24. *Temperature (a) and gradient (b–d) for KFM01A. Figure b and c shows the gradient calculated for nine metre intervals, while figure d shows the gradient calculated for 50 m intervals.*

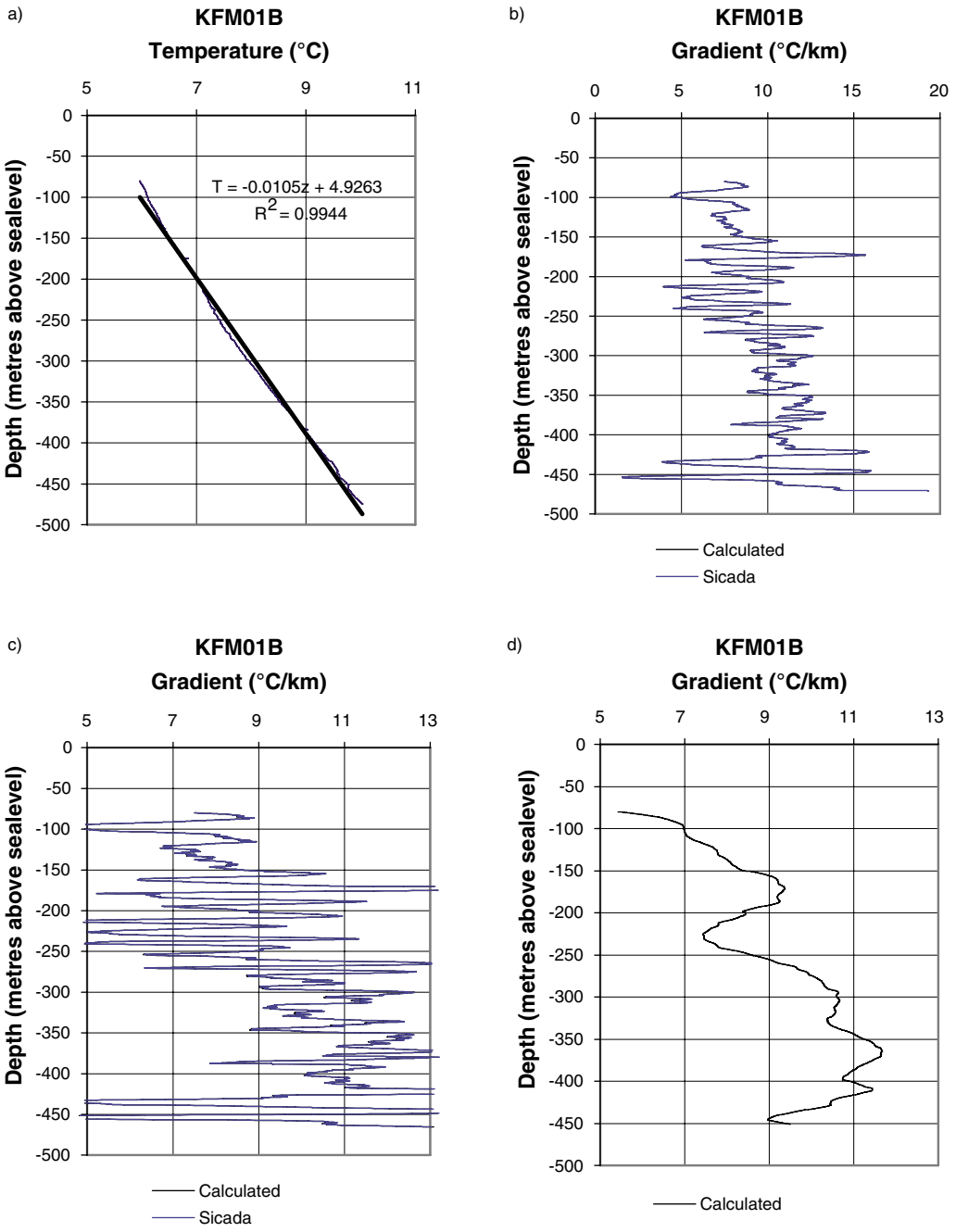

Figure 4-25. *Temperature (a) and gradient (b–d) for KFM01B. Figure b and c shows the gradient calculated for nine metre intervals, while figure d shows the gradient calculated for 50 m intervals.*

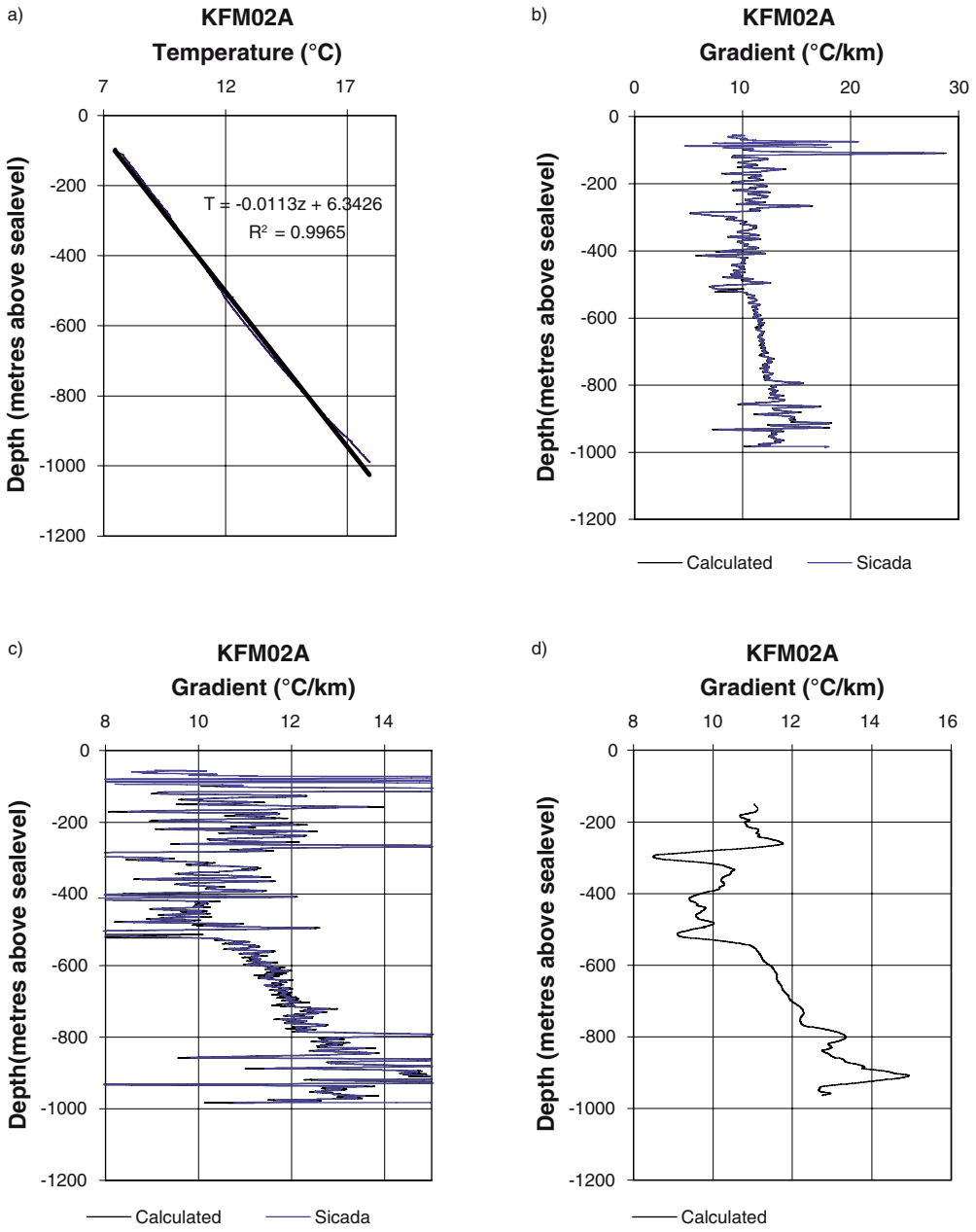

Figure 4-26. *Temperature (a) and gradient (b–d) for KFM02A. Figure b and c shows the gradient calculated for nine metre intervals, while figure d shows the gradient calculated for 50 m intervals.*

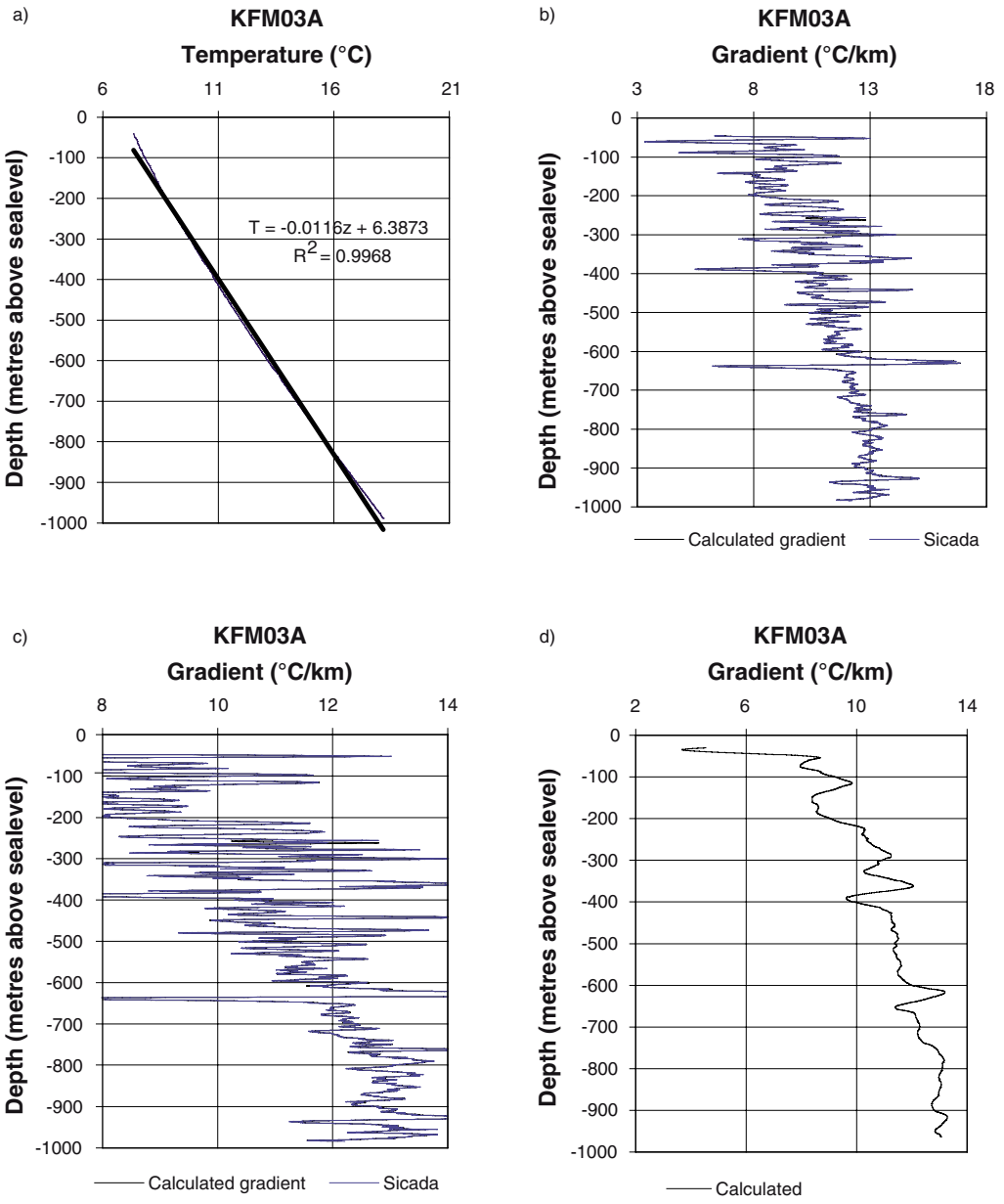

Figure 4-27. *Temperature (a) and gradient (b–d) for KFM03A. Figure b and c shows the gradient calculated for nine metre intervals, while figure d shows the gradient calculated for 50 m intervals.*

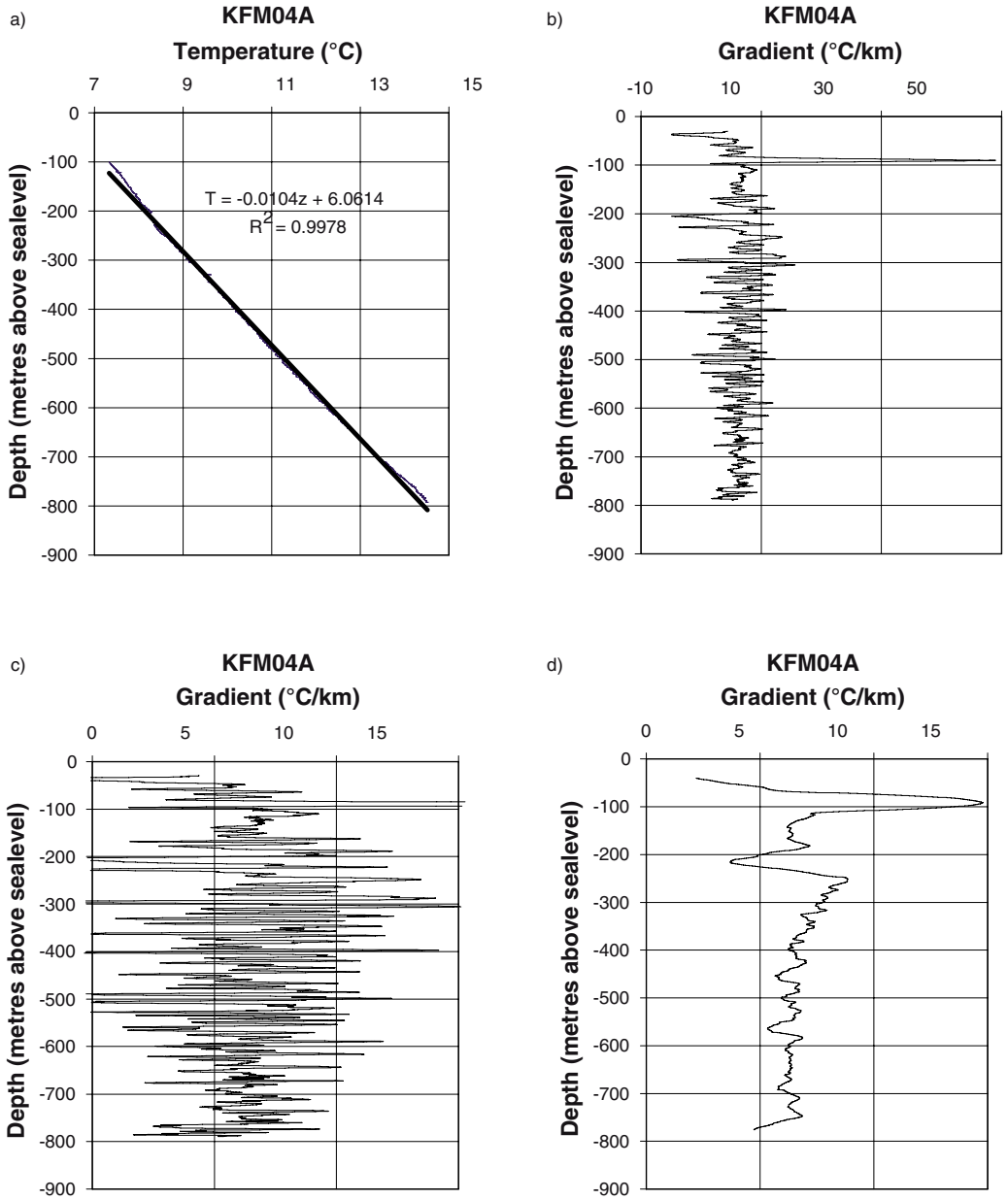

Figure 4-28. *Temperature (a) and gradient (b–d) for KFM04A. Figure b and c shows the gradient calculated for nine metre intervals, while figure d shows the gradient calculated for 50 m intervals.*

5 Thermal model

5.1 Modelling assumptions and input from other disciplines

5.1.1 Geological model

The lithological model from the Forsmark site descriptive model version 1.2 is the geometrical base for the thermal model and is described in section 4.2 and in /SKB, 2005/. The geological Boremap log of the boreholes, showing the distribution of dominant and subordinate rock types, has been used as input to the thermal modelling jointly with a lithological domain classification of borehole intervals (Table 5-2).

The geological model with rock type distributions of two rock domains RFM029 and RFM012 is illustrated in Table 5-1 where the dominating rock types are marked in red (preliminary version of geological model, July 2004). For other rock domains there is not enough data to make a quantitative estimate.

When modelling the domains, a calculation of the rock type composition including subordinate rock types is conducted, see Table 5-1. For rock type compositions divided on each borehole which constitute the lithological domain (calculated in the thermal domain modelling), see section 5.4.1. The calculation might differ from the composition presented in the geological model, mainly since the thermal domain modelling includes rock type sections with an occurrence less than 1m from the Boremap logging.

Table 5-1. Comparison between rock type proportions (%) used in domain modelling and in the geological model. Dominating rock types are marked in red.

Rock code	Rock name	Domain RFM029		Domain RFM012	
		Modelling	Geological model	Modelling	Geological model
101057	Granite to granodiorite	74.1	84	57.7	68
101051	Granite, granodiorite and tonalite	9.9	10	21.0	24
101061	Pegmatite, pegmatic granite	7.3	2	10.9	4
102017	Amphibolite	4.8	3	4.9	2
103076	Felsic to intermediate volcanic rock	0.1		3.1	2
111058	Granite	3.3	1	0.9	
101058	Granite	0.1		0.5	
Others		0.4		1.0	

Table 5-2. Boreholes classified by domain.

Domain	Borehole
RFM029	KFM01A KFM01B KFM02A KFM03A/3B, 6–220 m and 293–1,000 m KFM04A, 500–1,001.5 m KFM05A
RFM018	KFM04A 12–177 m
RFM017	KFM03A/03B 220–293 m
RFM012	KFM04A 177–500 m

5.1.2 Borehole data

All of the boreholes mentioned in Table 5-2, except KFM05A, have been used for the modelling of thermal properties on domain. KFM05A is not used in the current version of the geological model and therefore not used here either.

5.2 Conceptual model

There are three main causes for the spatial variability of thermal conductivity at the domain level; (1) small scale variability between minerals, (2) spatial variability within each rock type, and (3) variability between the different rock types making up the domain. The first type entails variability in small samples (TPS measurements and modal analysis). At this scale, the small scale variability can be substantial. However, the variability is reduced when the scale increases.

The second type of variability is caused by spatial variability in sample data within a rock type and cannot be explained by small scale variations. This variability has different importance due to rock type. The reason for the spatial variability within a rock type is the process of rock formation but also the system of classifying the rock types. The variability cannot be reduced, but the uncertainty of the variability may be reduced. This is achieved by collecting large number of samples at varying distances from each other, so that reliable variograms can be created.

A large number of samples are needed to study spatial variability within a rock type. For rock type granite to granodiorite (101057) a variogram is presented in Figure 4-20. The result indicates a short range of variability, but the variability is large because of limited number of TPS measurements. Variogram for larger scales has not been possible to produce due to too few samples.

The third type of variability is due to the presence of different rock types in the lithological domain. This variability is more pronounced where the difference in thermal conductivity is large between the most common rock types of the domain. Large such variability can also be expected in a domain of many different rock types. It is only reduced significantly when the scale becomes large compared to the spatial occurrence of the rock type.

Of importance at the domain level is the scale representative for the canister, i.e. at which the thermal conductivity is important for the heat transfer from the canister. At present knowledge, this scale is not known in detail but it is believed to be in the order of 1 to 10 m. Therefore, the approach in the domain modelling is to use different scales to study the scale effect, and to draw conclusions of representative thermal conductivity values from that.

5.3 Modelling approach for domain properties

5.3.1 Introduction

The methodology for domain modelling and the modelling of scale dependency were developed for the Prototype Repository at the Äspö HRL /Sundberg et al. 2005a/. In parallel, the domain modelling of Forsmark was performed. A number of different approaches are used in the modelling of the two domains RFM029 and RFM012. A modelling of domain RFM017 has not been possible to perform due to lack of representative borehole and sample data within the domain.

Modelling of the mean for the thermal conductivity at lithological domain level is performed according to the main approach (approach 1) described in Figure 5-1. This approach is applied to the two domains RFM029 and RFM012 (both dominated by the granite to granodiorite (101057)). However, in Forsmark the main approach does not take into account spatial variability within rock type and therefore the variance is underestimated. The two alternative/complementary approaches have been worked through in order to evaluate the results of the variance within the domain (approaches 2 and 3).

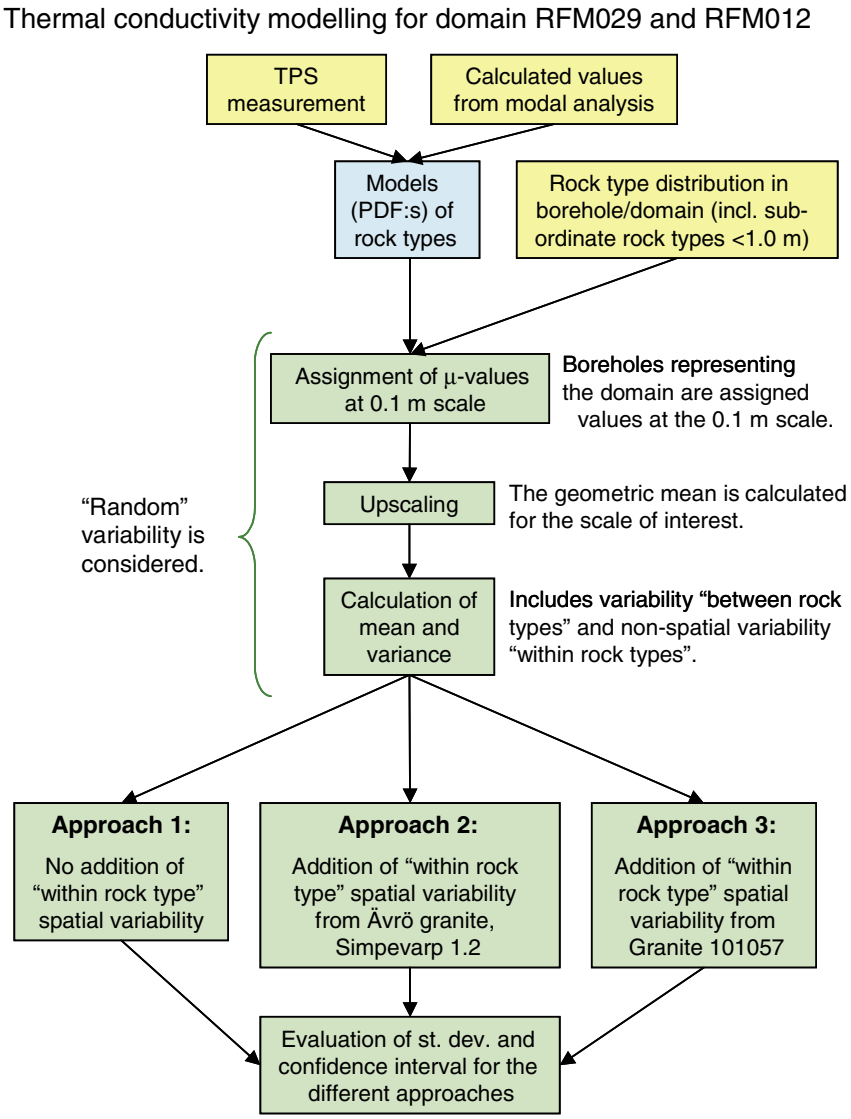

Figure 5-1. *Approach for estimation of thermal conductivity for domain RFM029 and RFM012. Yellow colour indicates the data level, blue the rock type level and green the domain level.*

5.3.2 Approach 1: Main approach

The domain modelling according to approach 1 is performed as follows:

Measured and calculated values from modal analysis are used to produce a PDF (Probability Density Function) model for rock types present in the domains, according to Table 4-21.

The summed up length of boreholes, or parts of boreholes, belonging to a domain is assumed to be a representative realisation of the domain. Each borehole belonging to the domain is divided into 0.1 m long sections and each section is assigned a thermal conductivity value according to the lithological classification of that section. Both dominating and subordinate rock types are considered in this context. The principle for the assignment of thermal properties is as follows:

- Thermal conductivity is randomly chosen according to the rock type model (PDF) based on measured (TPS) and calculated conductivities from mineral compositions (SCA).

For rock types where no rock type model (PDF) is available (due to lack of data), no value is assigned to that 0.1 m section (section ignored in the following upscaling). Such rock types, primary amphibolite (102017), have a low degree of occurrence in the domains and are therefore assumed not to influence the results significantly.

The next step is the upscaling from 0.1 m scale to larger scale. To study scale effect, upscaling is performed on of scales, from 0.1 m to 50 m. The upscaling is performed in the following way:

1. The boreholes representing the domain are divided into a number of sections with a length according to the desirable scale (0.1–50 m).
2. Thermal conductivity is calculated for each section by geometric mean calculations of the values at the 0.1 m scale.
3. Mean value and variance of all sections of the domain is calculated. For each scale, the calculations are repeated at least 10 times with different assignment of thermal conductivity values at the 0.1 m scale, according to 1 above. This produces representative mean and standard deviation values for the desired scale.
4. The calculations are repeated for the next scale.

The principle for upscaling of data for different rock types is illustrated both in Figure 5-2 and Figure 5-3. In Figure 5-2, 24 sections are indicated, each with a length of 0.1 m. For the scale 0.5 m, the thermal conductivity $\lambda_{0.5-1}$ is estimated as the geometric mean of the five 0.1 m sections, $\lambda_{0.5-2}$ as the geometric mean for the next five 0.1 m sections, and so on. The mean and variance is then computed for the 0.5 m scale. This sequence is repeated for the other scales of interest. In Figure 5-3 the effects of upscaling are shown. The geometric mean equation is simple to use and is often applied for mean estimation of transport properties /Dagan, 1981; Sundberg, 1988/. In 3D, the effective transport properties are influenced by the variance. However, in this thermal application the variance is low and therefore the geometric mean is sufficient. This is further discussed in /Sundberg et al. 2005a/.

Confidence intervals are calculated for each scale under the assumption of normal distributed data at the scale of interest.

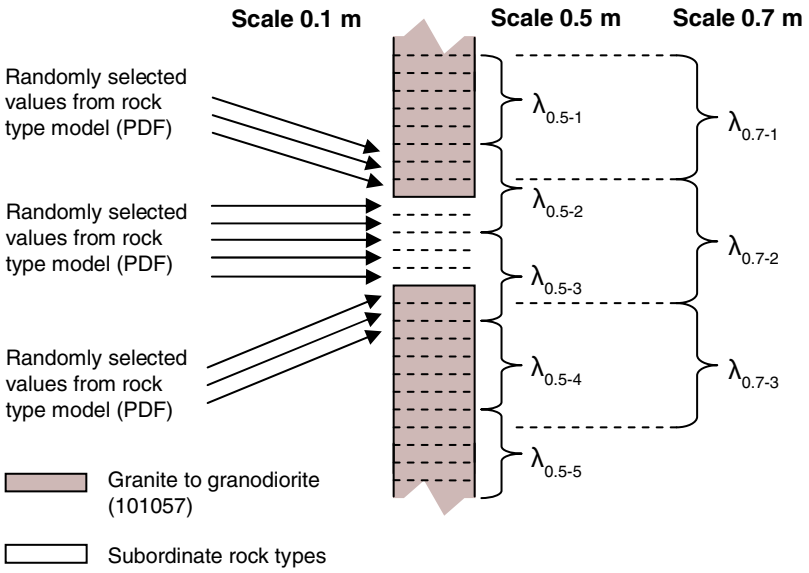

Figure 5-2. Thermal conductivity is assigned to 0.1 m sections by calculation from density loggings or randomly selected from the rock type models. Upscaling is done by calculating geometric means for different scales, for example 0.5 and 0.7 m.

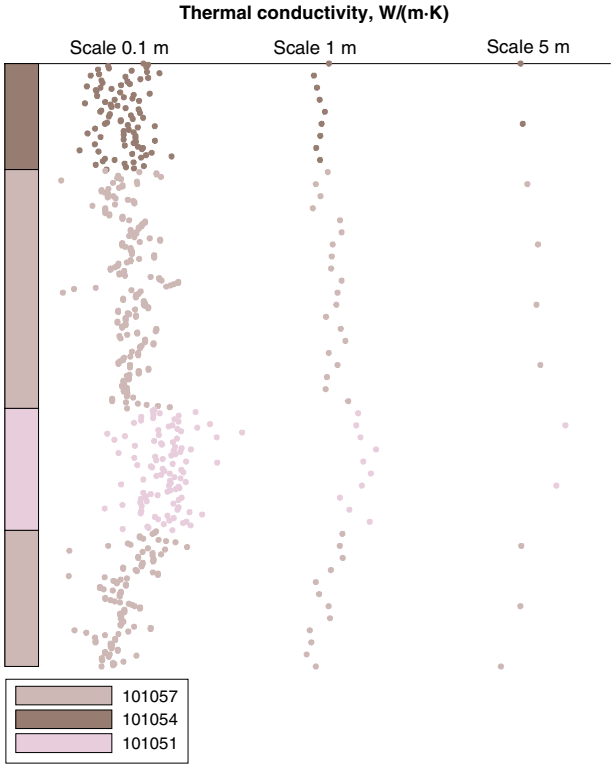

Figure 5-3. *Effects of applying the principle for upscaling of thermal conductivity, as given in Figure 5-2.As illustrated in the figure the spatial variability within rock type is levelled out due to the modelling concept. The figure illustrates the effects of upscaling in general and is not typical for the actual rock types or a specific borehole.*

5.3.3 Alternatives to main approach

The approach of randomly selecting thermal conductivity values from rock type models (PDF:s) without consideration of spatial variability "within rock types" was described above in the main approach. The reason for not considering the variation "within rock type" is that the density loggings are not possible to use since there is no relationship between density and thermal conductivity and therefore the spatial correlation within the dominating rock types is not considered. This modelling resulted in estimates of thermal conductivity at different scales, see Table 5-10. The variance from the main approach includes variability due to rock type changes in the boreholes ("between rock type" variability) but the variability within each rock type is effectively and rapidly reduced when the scale is increased because of the random assignment of thermal conductivity values. The resulting variance is therefore mainly a result of the presence of different rock types in the boreholes and for domain RFM029 and RFM012 the variance is underestimated.

One way of compensating for the variance reduction caused by ignoring spatial variability is to add the spatial variability within the dominating rock type in the domain. The spatial variability within the dominating rock type can be estimated in different ways which is presented here in two alternative/complementary approaches (2 and 3). For the two domains RFM029 and RFM012 the difference between approach 2 and 3 is in the way the "variability within rock type" is estimated. For approach 2 it is performed by looking at domain RSMA01 (Ävrö granite) from the Simpevarp area but in approach 3 it is achieved by studying TPS measurement within the dominating rock type of the considered domain.

The total variance for the domain can be estimated as the sum of variances due to different rock types /Sundberg et al. 2005b/ and the variance due to spatial variability within the dominating rock type: $V_{tot} = V_{between\ rock\ type} + V_{within\ rock\ type}$

The "between rock type" variability is qualitatively different from, and therefore likely to be independent of, the "within rock type" variability. Therefore, the addition of the variances is reasonable.

5.3.4 Approach 2: Addition of "within rock type" variance from the Simpevarp area

Variance caused by spatial variability (non-random) within rock type 501044 has been estimated for domain RSMA01 (dominated by Ävrö granite) at the Simpevarp area /Sundberg et al. 2005b/. In this approach the variance caused by spatial correlation within rock type 501044 (Ävrö granite) is assumed to be the same as for domain RFM029 and RFM012. Therefore, the spatial contribution of variance 0.037 W/(m·K) is added to the variance for domain RFM029 and RFM012 see Figure 5-16 and Table 5-10. The adding of variances is possible because the processes behind spatial variability due to correlation and random variability can be regarded as the effects of stochastic variables. It is reasonable to assume that these variables are fairly independent and addition of variances of stochastic variables is possible if they are independent.

However, the results are probably an overestimation of the variance since the spatial variation within rock type granite to granodiorite (101057) seems to be much smaller than in Ävrö granite (501044) in Simpevarp.

5.3.5 Approach 3: Addition of “between rock type” and “within rock type” variance from TPS measurements

For 101057 (granite to granodiorite), TPS measurements can provide a rough estimate of the spatial variability within the rock type. The variance as a function of scale was calculated with geometric mean for each scale. This type of variance is denoted “within rock type”. Although this approach only provides a rough estimate of the total variability, it encompasses all the major types of variability within the domain.

It is not easy to assess whether this approach under- or overestimates the total variance for the domain. There are several factors that may influence this, such as the spatial variability in subordinate rock types compared to dominating rock type. In addition, the variance “within rock type” is rather uncertain due to relatively few measurements and questions of representativeness for the samples. Still, it is believed that this approach gives a quite reasonable estimate of the variability compared to the other approaches.

5.3.6 Modelling appoach: Heat capacity

Domain models of heat capacity based on TPS measurements for domain RFM029 and RFM012 are calculated. A Monte Carlo simulation is performed by weighting the occurrence of different rock types in the domain together with the rock type models. The simulation calculates mean value together with confidence intervals regarding spatial distribution in data values for the heat capacity on domain level.

5.4 Domain modelling results

5.4.1 Approach 1: Main approach

When modelling domain RFM029 and RFM012, a calculation of the rock type composition including subordinate rock types is conducted. The calculation might in a smaller extent differ from the composition presented in the geological model depending on small differences in basic data. Figure 4-11, Figure 4-13, Figure 4-15 and Figure 4-17 illustrates the rock type models (PDF:s) for granite to granodiorite (101057), granodiorite (101056), tonalite to granodiorite (101054) and granite, granodiorite and tonalite (101051) used in the domain modelling. Results for the different approaches follows in separate sections and the concluding results for domain RFM029 and RFM012 is given in section 5.5.

For rock type other than granite to granodiorite (101057) the PDF:s are based on relatively few measurements and calculations. Problems with the representativeness of the rock mass might therefore occur, which can explain the difference between the two distributions.

In larger scale, the distributions get more skew. Even if data seems to be normal distributed in the scale 0.1 m, this might not be the case in a larger scale, like 10 m.

Domain RFM029

Table 5-3. Modelling results for the domain and per borehole with arithmetic mean and standard deviation of the thermal conductivity values at the 0.7 m scale, together with rock type distributions.

		Domain RFM029	KFM01A	KFM01B	KFM02A	KFM03A	KFM04A
Borehole interval			**29.5–1,007.2 m**	**15.6–498.4 m**	**12.0–1,006.0 m**	**102.2–219.9, 293–1,000.1 m**	**500.0–999.7 m**
Thermal conductivity at the 0.7 m scale (W/(m·K))	Arithmetic mean	3.55	3.54	3.58	3.52	3.55	3.58
	St. dev.	0.20	0.20	0.16	0.22	0.19	0.16
Granite to granodiorite (%)	101057	74.1	73.9	83.6	70.3	71.5	77.1
Granite, granodiorite and tonalite (%)	101051	9.9	10.1	5.5	14.6	9.2	5.2
Tonalite to granodiorite (%)	101054	0.0	0.0	0.0	0.0	0.1	0.0
Pegmatite, pegmatitic granite (%)	101061	7.3	5.9	6.7	5.8	9.7	9.3
Diorite, quartz diorite and gabbro (%)	101033	0.0	0.0	0.1	0.0	0.0	0.0
Granodiorite (%)	101056	0.0	0.0	0.0	0.0	0.1	0.0
Granite (%)	101058	0.1	0.0	0.4	0.0	0.0	0.4
Felsic to intermediate volcanic rock (%)	103076	0.0	0.0	0.0	0.0	0.0	0.4
Granite (%)	111058	3.3	4.8	0.3	3.2	4.5	1.7
Others (%)		5.3	5.3	3.4	6.0	5.0	5.8

Table 5-3 shows the rock type distribution in domain RFM029 and also per borehole in the domain. The modelling results of the mean value in different scales are illustrated in Figure 5-4. The mean value has a very small scale dependence. Figure 5-5 and Figure 5-6 shows clearly that the modelling results are not normal distributed. Instead two clusters are indicated with a thermal conductivity about 3.05 and 3.6 W/(m·K).

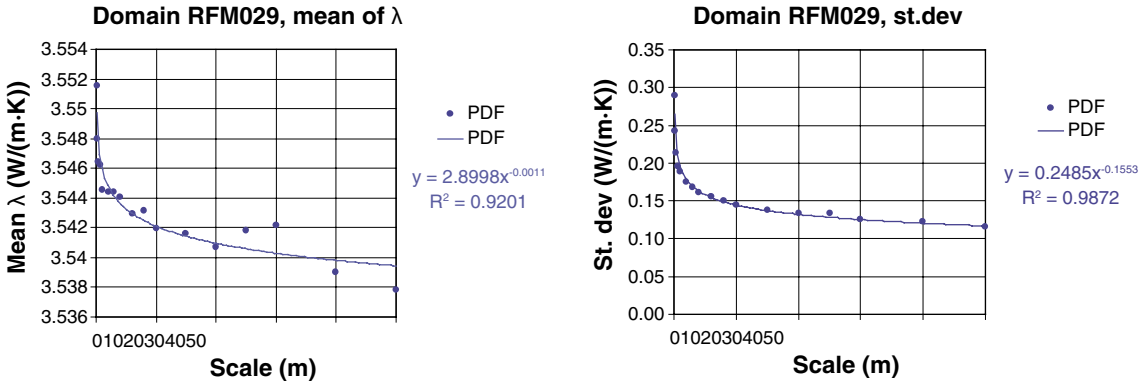

Figure 5-4. *Modelling results, mean and standard deviation for thermal conductivity, for domain RFM029 (granite to granodiorite). The small decrease in the mean when the scale increases could be an effect of using the geometric mean to estimate the effective thermal conductivity /Sundberg et al. 2005a/.*

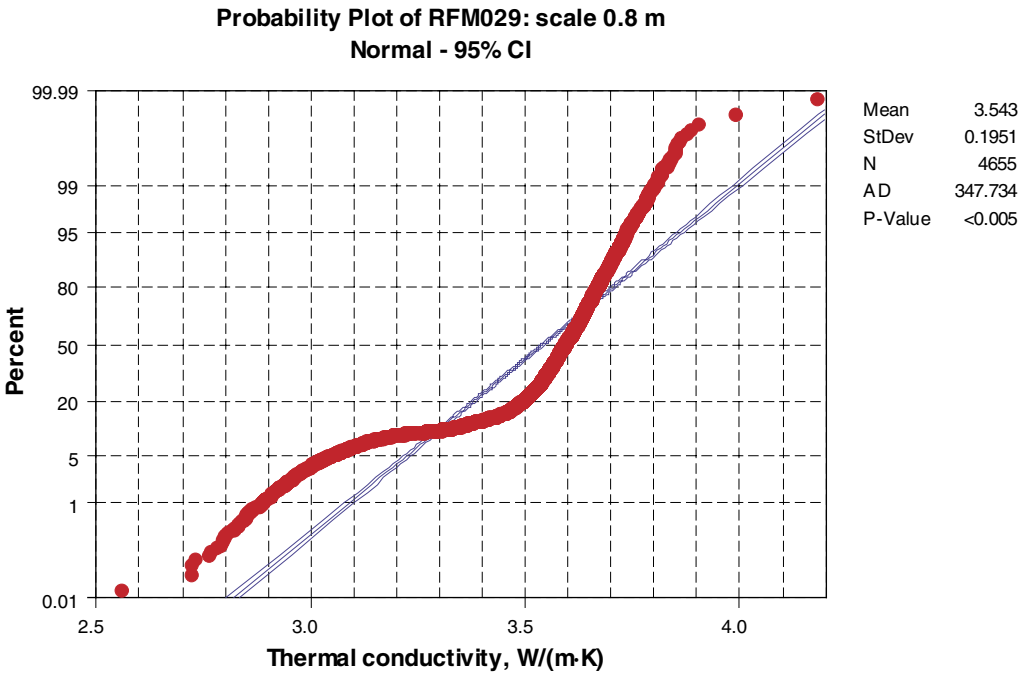

Figure 5-5. *Probability plot of modelling results for domain RFM029 at the 0.8 m scale. The results are clearly not normal distributed.*

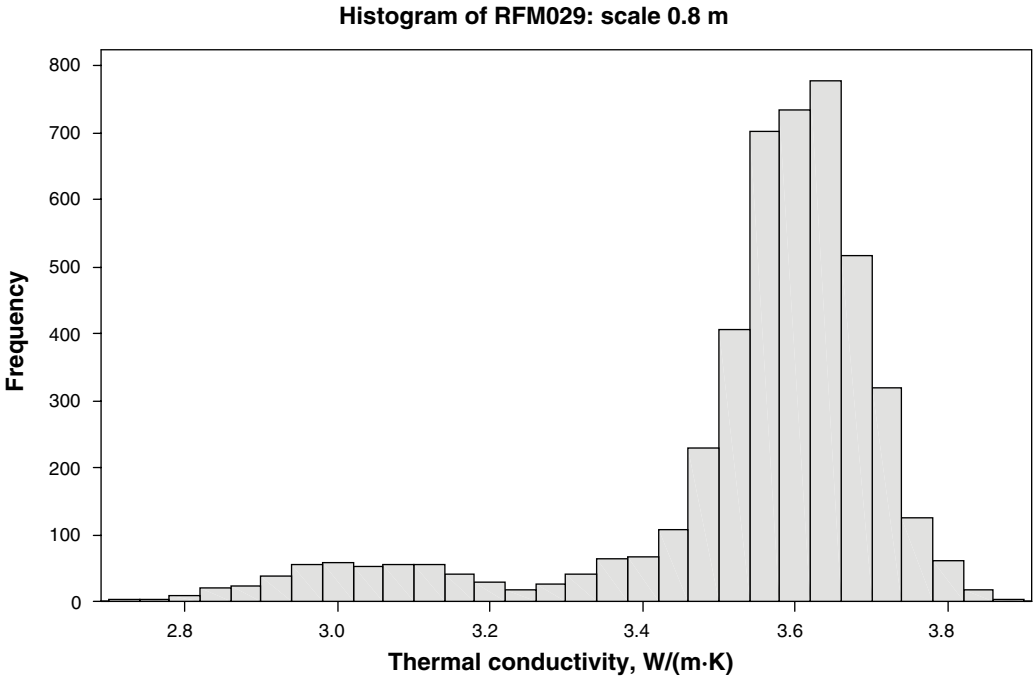

Figure 5-6. *Histogram of modelling results for domain RFM029 at the 0.8 m scale.*

In Table 5-4 the two-sided 95% interval is calculated from the modelling results.

Table 5-4. Modelling results for domain RFM029 of the thermal conductivity (W/(m·K)) in the 0.8 m scale. Two-sided 95% confidence interval with upper and lower confidence limits.

Lower confidence limit	Upper confidence limit
2.96	3.77

Domain RFM012

Table 5-5. Modelling results for the domain and per borehole with mean and standard deviation of the thermal conductivity at the 0.7 m scale and rock type distributions in percent.

		Domain RFM012	KFM04A
Borehole interval			**177.0–500.0 m**
Thermal conductivity at the 0.7 m scale (W/(m·K))	Arithmetic mean	3.46	3.46
	St. dev.	0.26	0.26
Granite to granodiorite (%)	101057	57.7	57.7
Granite, granodiorite and tonalite (%)	101051	21.0	21.0
Tonalite to granodiorite (%)	101054	0.0	0.0
Pegmatite, pegmatitic granite (%)	101061	10.9	10.9
Diorite, quartz diorite and gabbro (%)	101033	0.0	0.0
Granodiorite (%)	101056	0.0	0.0
Granite (%)	101058	0.5	0.5
Felsic to intermediate volcanic rock (%)	103076	3.1	3.1
Granite (%)	111058	0.9	0.9
Others (%)		5.9	5.9

Table 5-5 shows the rock type distribution in domain RFM012. The modelling results of the mean value in different scales are illustrated in Figure 5-7. The mean value has a very small scale dependence. Figure 5-8 and Figure 5-9 shows clearly that the modelling results are not normal distributed. Instead two clusters are indicated with a thermal conductivity about 3.05 and 3.6 W/(m·K).

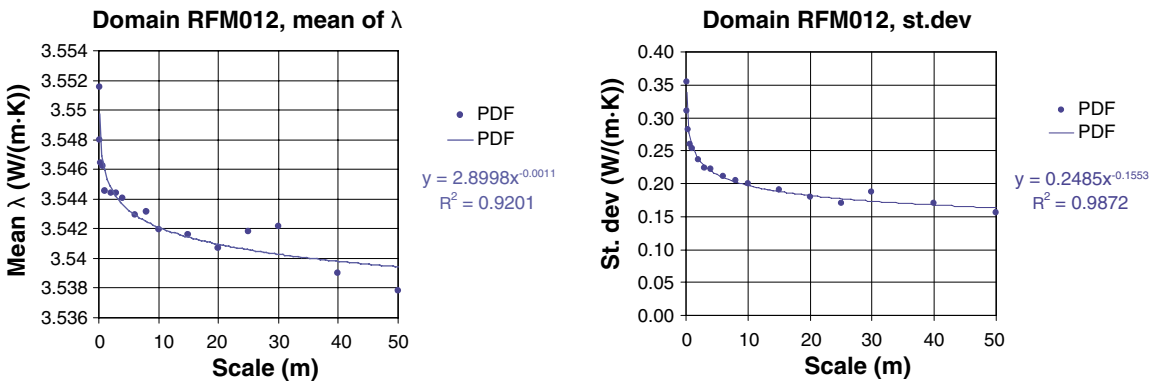

Figure 5-7. *Modelling results, mean and standard deviation for thermal conductivity, for domain RFM012 (granite to granodiorite).*

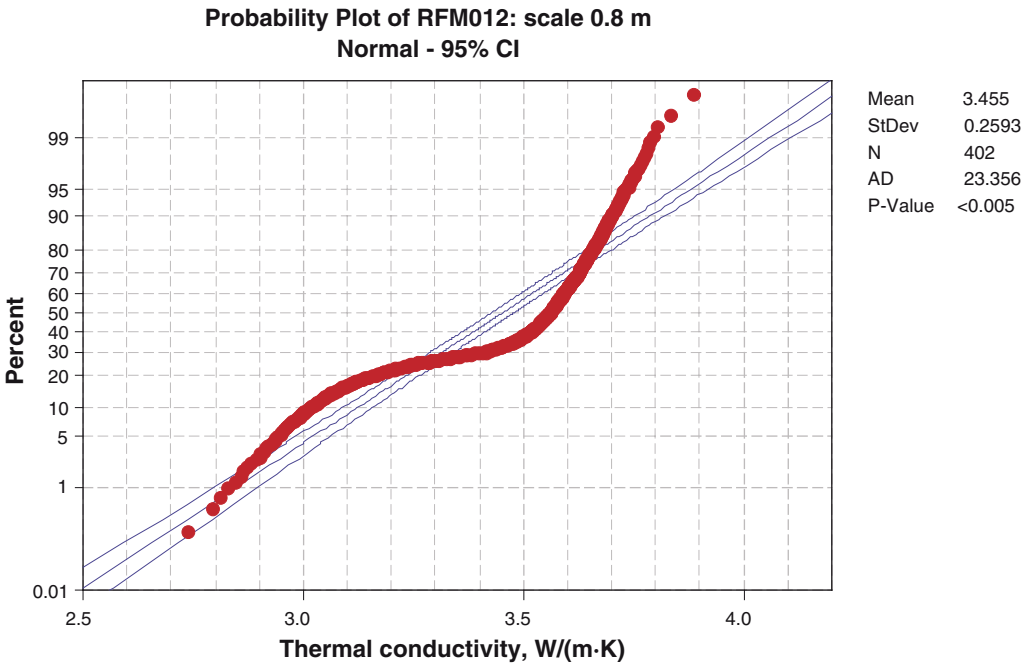

Figure 5-8. *Probability plot of modelling results for domain RFM012 at the 0.8 m scale. The results are clearly not normal distributed.*

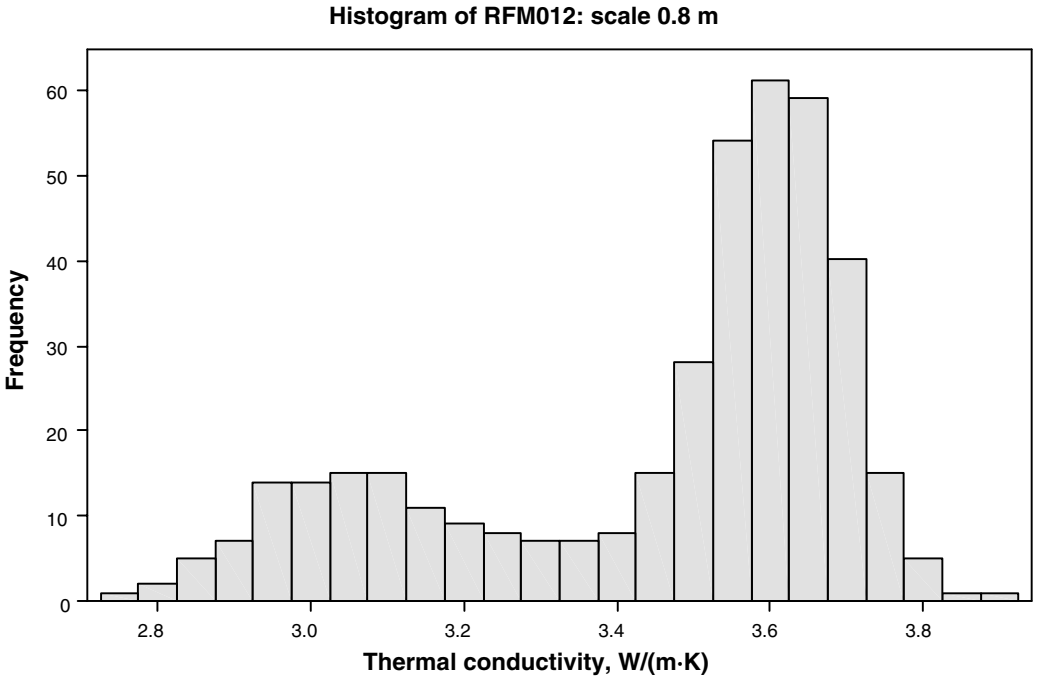

Figure 5-9. *Histogram of modelling results for domain RFM029 at the 0.8 m scale.*

In Table 5-6 the 2.5% and 97.5% percentile are calculated from the modelling results.

Table 5-6. Modelling results for domain RFM012 of the thermal conductivity (W/(m·K)) in the 0.8 m scale. Two-sided 95% confidence interval with upper and lower confidence limits.

Lower confidence limit (2.5% percentile)	Upper confidence limit (97.5% percentile)
2.90	3.76

Summary of results for RFM029 and RFM012

Table 5-7. Standard deviation and variance for thermal conductivity (W/(m·K)) on domain level in different scales. Numbers marked in red used in approach 2 or 3.

Scale	RFM029 Randomly from PDF		RFM012 Randomly from PDF	
	Standard deviation	Variance	Standard deviation	Variance
0.1	0.290	0.084	0.354	0.125
0.2	0.243	0.059	0.310	0.096
0.4	0.214	0.046	0.282	0.080
0.7	0.196	0.038	0.260	0.068
1	0.188	0.035	0.253	0.064
2	0.174	0.030	0.237	0.056
3	0.168	0.028	0.223	0.050
4	0.161	0.026	0.221	0.049
6	0.155	0.024	0.212	0.045
8	0.150	0.023	0.205	0.042
10	0.144	0.021	0.200	0.040
15	0.137	0.019	0.190	0.036
20	0.134	0.018	0.180	0.032
25	0.133	0.018	0.169	0.029
30	0.125	0.016	0.188	0.035
40	0.123	0.015	0.170	0.029
50	0.116	0.014	0.156	0.024

The thermal conductivity distributions for domain RFM029 and RFM012 are similar. In Figure 5-4 and Figure 5-7 the mean value of the thermal conductivity calculated according to the main approach is presented. Modelling results from both domains are shown in Figure 5-10.

Figure 5-11 and Figure 5-12 illustrates the modelled (according to the main approach) thermal conductivity plotted towards depth for the different boreholes which constitutes the two domains RFM029 and RFM012, both dominated by granite to granodiorite. The results are based on one simulation of the thermal conductivity. The plotted thermal conductivity values are calculated geometrical mean values over 50 me (moving average) and 2 m long sections, respectively. Figure 5-13 to Figure 5-15 shows the modelled thermal conductivity for each borehole. The influence of subordinate rock type sections is clearly visible as spikes in the figures, but the variability within rock types may be underestimated according to the modelling approach (1).

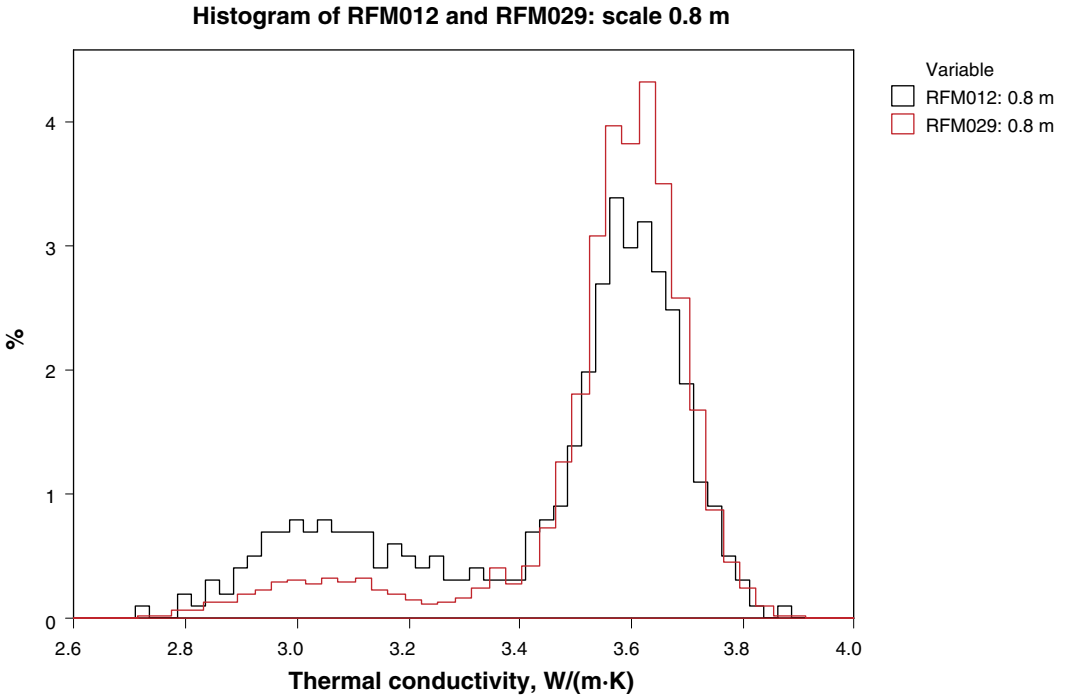

Figure 5-10. *Histogram (normalised) for comparison of modelling results between domain RFM012 and RFM029 at the 0.8 m scale.*

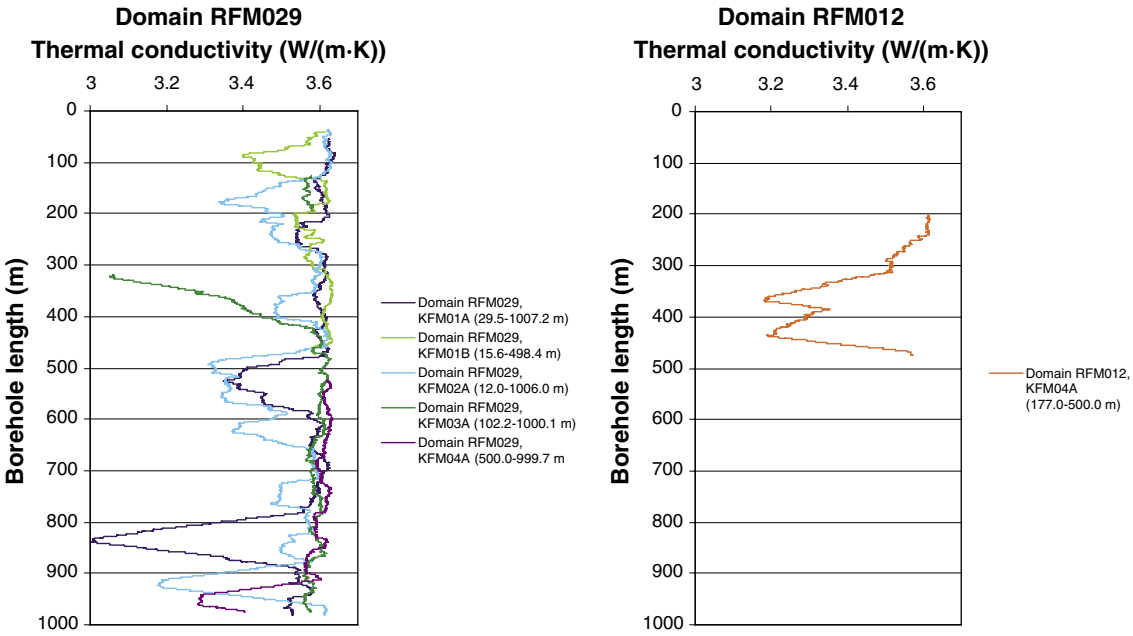

Figure 5-11. *Visualization of modelling results in the 50 m scale of the two domains (RFM029 and RFM012) separated on each borehole, which constitutes the domain. Thermal conductivity values are moving geometrical mean value calculations over 50 m long sections (50 m scale). The results origin from only one realisation.*

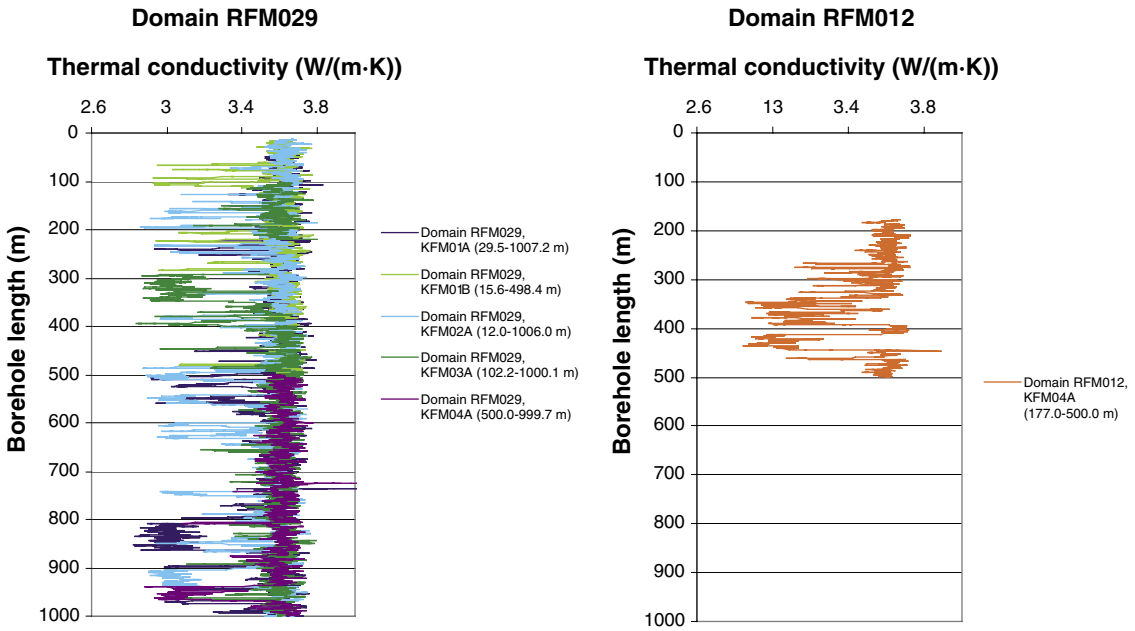

Figure 5-12. *Visualization of modelling results in the 2 m scale of the two domains (RFM029 and RFM012) separated on each borehole, which constitutes the domain. Thermal conductivity values are calculated as geometrical mean value over 2 m long sections (moving average). The results origin from only one realisation.*

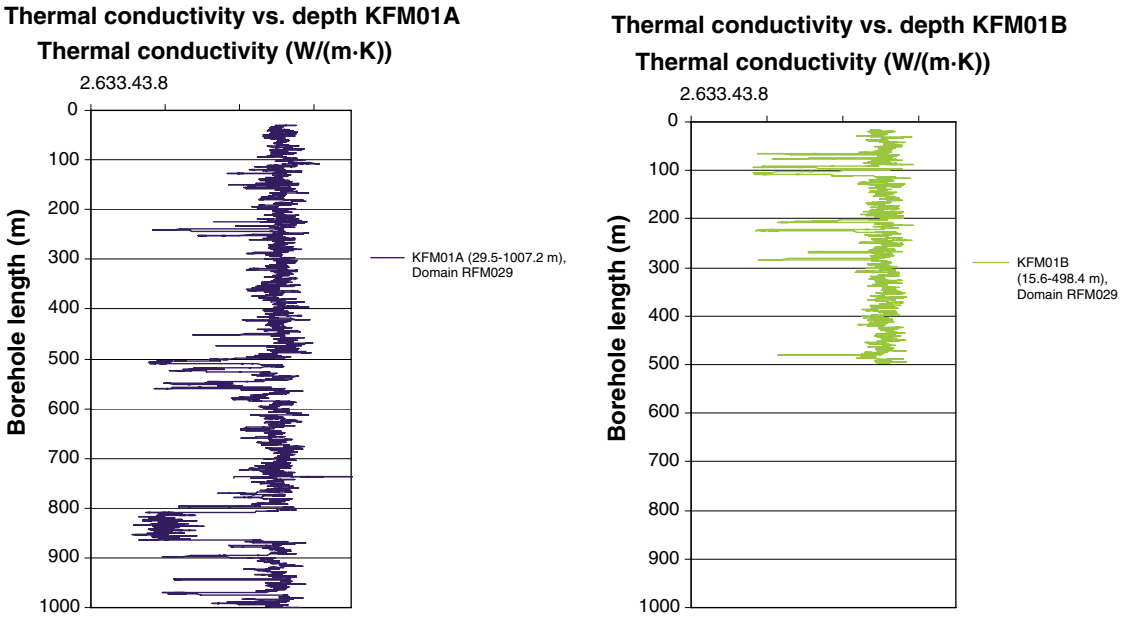

Figure 5-13. *Visualization of modelling results of borehole KFM01A and KFM01B. Thermal conductivity values are calculated as geometrical mean value over 2 m long sections (moving average). The results origin from only one realisation.*

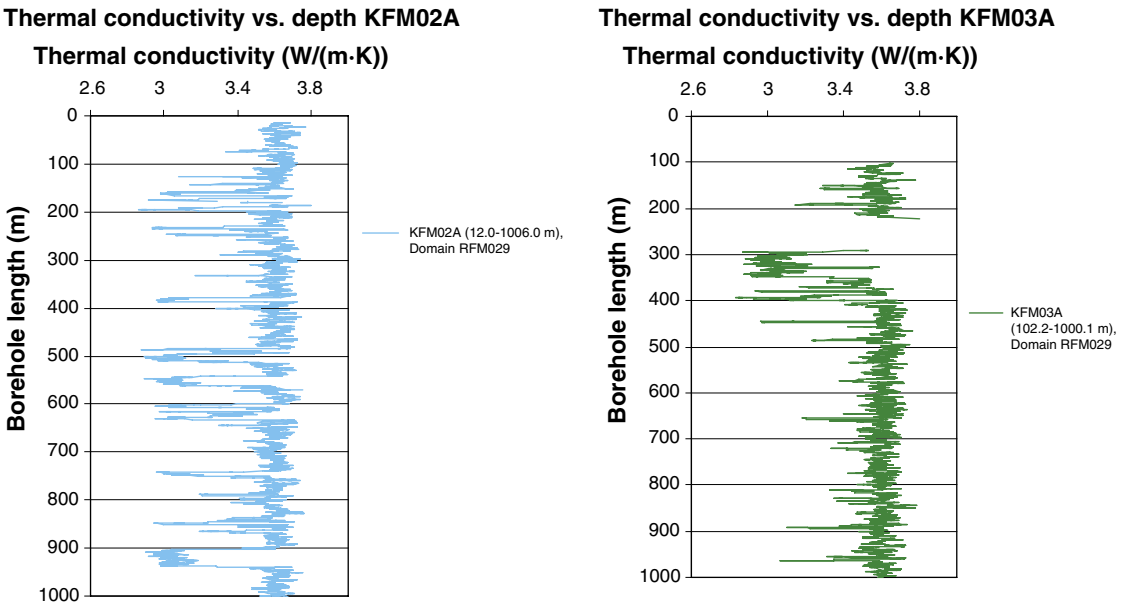

Figure 5-14. *Visualization of modelling results of borehole KFM02A and KFM03A. Thermal conductivity values are calculated as geometrical mean value over 2 m long sections (moving average). The results origin from only one realisation.*

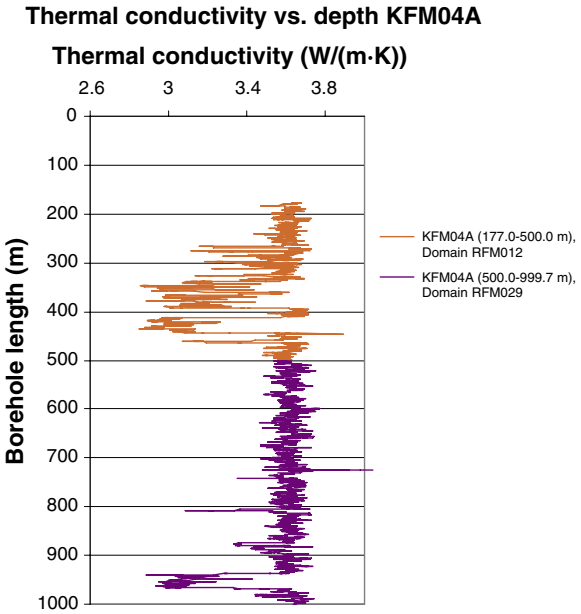

Figure 5-15. *Visualization of modelling results of borehole KFM04A separated on the two domains RFM029 and RFM012. Thermal conductivity values are calculated as geometrical mean value over 2 m long sections (moving average). The results origin from only one realisation.*

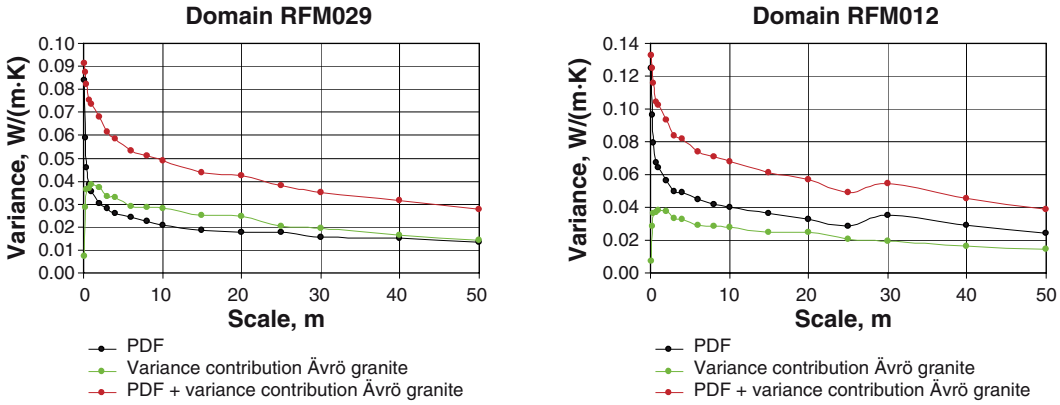

Figure 5-16. *Variance contribution from spatial distribution in the dominating rock type Ävrö granite (501044) of domain RSMA01 (Simpevarp area) added to domain RFM029 and RFM012. The shape of the curve for RFM012 at larger scale is a result of the distribution of rock types in the boreholes used for modelling.*

5.4.2 Approach 2: Addition of "within rock type" variance from the Simpevarp area

The variance in different scales, which is the result from approach 1, see Table 5-7, when only "random" variability is considered, has been added with the variance contribution from spatial distribution in rock type Ävrö granite from the Simpevarp area. The results are shown in Figure 5-16. However, the results are probably an overestimation of the variance since the spatial variation within rock type Ävrö granite cannot be assumed to be the same as for domain RFM029.

5.4.3 Approach 3: Addition of "between rock type" and "within rock type" variance from TPS measurements

The variance within rock type granite to granodiorite, 101057, is illustrated in Figure 5-17. This variance is based on only TPS-measurements, data from SCA-calculations have higher variance. The variance due to rock type changes in the boreholes ("between rock type" variability) is showed in Table 5-7 (V_1). In Table 5-8 this variance contribution from randomly assigned values (V_1) is added together with the variance within the rock type (V_2, see Figure 5-17). The total variance (V_{tot}) may then been viewed as a domain property where rock type granite to granodiorite (101057) represents domain RFM029 and RFM012.

Table 5-8. Variances (W/(m·K)) in two different scales for rock type granite to granodiorite (101057) – domain RFM029.

	Scale 0.4 m	Scale 0.7 m	Scale 2 m
Rock code	**101057 (RFM029)**	**101057 (RFM029)**	**101057 (RFM029)**
Variance (V_1), Table 5-7	0.046	0.038	0.030
Variance (V_2), Figure 5-17	0.013	0.011	0.0091
Variance (V_{tot})	0.059	0.049	0.040
St. dev_{tot}	0.24	0.22	0.20

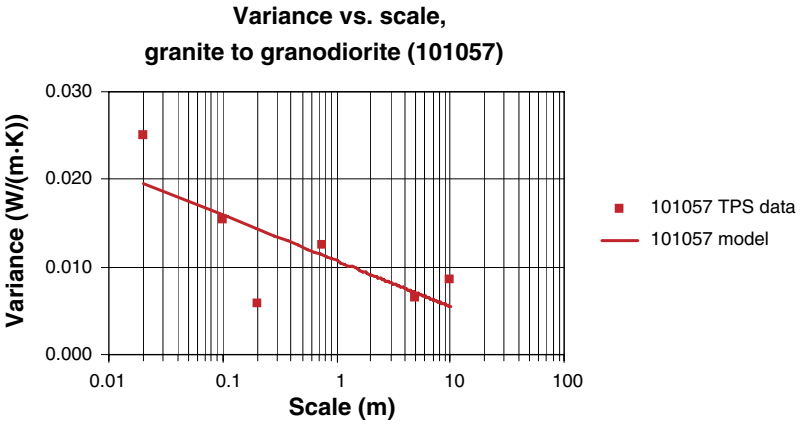

Figure 5-17. *Variability within rock type (V_2) for granite to granodiorite (101057). Note that data are sparse and based on 47 TPS measurements.*

It is not easy to assess whether this approach under- or overestimates the total variance. There are several factors that may influence if this approach under- or overestimates the total variance for the domain, such as the spatial variability in subordinate rock types compared to the dominating rock type. In addition, the variance V_2 in Figure 5-17 is rather uncertain due to relatively few measurements and questions of representativeness for the samples. Since Figure 5-17 is only based on TPS measurements, the variance at the 0.1 m scale is lower compared to if SCA data were also included.

5.4.4 Modelling results: Heat capacity

Calculations of mean value and confidence interval regarding distribution in data for the heat capacity have been done with a Monte Carlo simulation, see Figure 5-18, Figure 5-19 and Table 5-9. The measured values from rock type granite to granodiorite (101057), tonalite to granodiorite (101054), granite, granodiorite and tonalite (101051) and granodiorite (101056) have been assumed to be normal distributed, which also have been tested to be true. The models of the four different rock types are based on different numbers of measured values, for granite to granodiorite (101057) 49 samples, tonalite to granodiorite (101054), 5 samples, granite, granodiorite and tonalite (101051), 3 samples and granodiorite (101056), 5 samples. Other rock types have not been regarded since the number of samples were too few or did not exist at all.

Table 5-9. Heat capacity MJ/(m³·K) per domain with two-sided 95% confidence intervals under assumption of normal distribution. The data are valid at 20°C. At higher temperatures the heat capacity for rock type 101057 increase with about 25%/100°C, see 4.8.3.

Domain	Mean	St. dev.	Lower confidence limit	Upper confidence limit
RFM029	2.17	0.163	1.85	2.50
RFM012	2.17	0.149	1.86	2.49

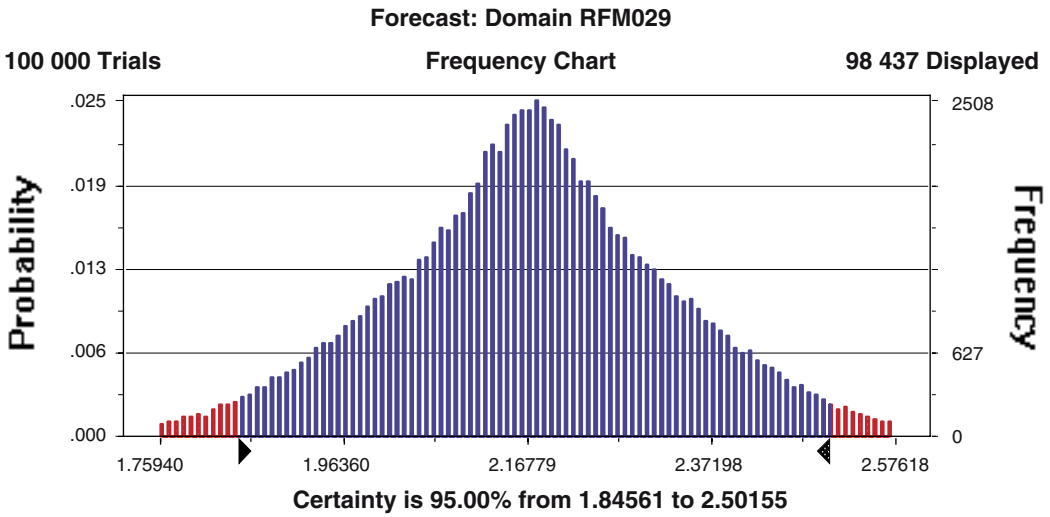

Figure 5-18. *Monte Carlo simulation results for the heat capacity of domain RFM029. Two-sided 95% confidence intervals are marked with arrows.*

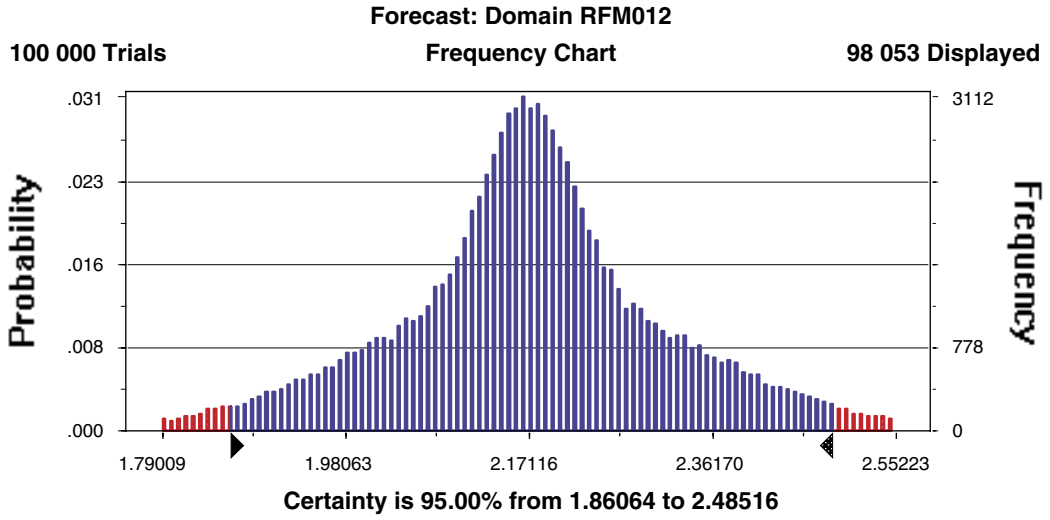

Figure 5-19. *Monte Carlo simulation results for the heat capacity of domain RFM012. Two-sided 95% confidence intervals are marked with arrows.*

5.5 Conclusion – modelling results

5.5.1 Thermal conductivity

Mean values representative for the thermal conductivity on domain level is presented in Table 5-11 based on modelling according to the main approach. Data for the 0.7 m scale are chosen, which are assumed to be representative for the canister scale. Table 5-10 also summarises the suggested standard deviation of thermal conductivity per domain in the canister scale.

The standard deviation has been estimated with three different approaches, where the results are summarised in Table 5-10. For approach 1, mean values and standard deviations are calculated for each scale. As described in the table, and also in previous sections, approach 1 probably underestimates the standard deviation and approach 2 overestimates it.

Table 5-10. Summary of standard deviations (W/(m·K)) from modelling results on domain level with the main approach (approach 1) compared to the two alternative approaches 2 and 3. Numbers within parenthesis are calculated variances with the resulting standard deviation in bold.

Approach	Scale (m)	RFM029	RFM012	Comment
1	0.7	**0.20** (random from PDF)	**0.26** (random from PDF)	Approach 1: possible underestimation of the standard deviation
	2	**0.17** (random from PDF)	**0.24** (random from PDF)	
2	0.7	**0.27** (0.038+0.037=0.075) (random+variance contr.)	**0.32** (0.068+0.037=0.105) (random+variance contr.)	Approach 2 gives an overestimation of the standard deviation.
	2	**0.26** (0.030+0.037=0.067) (random+variance contr.)	**0.30** (0.056+0.037=0.093) (random+variance contr.)	
3	0.4	**0.24** (0.046+0.013=0.059) (between+within rock type)	**0.30** (0.080+0.013=0.093) (between+within rock type)	Approach 3 is belived to underestimate the standard deviation for larger scales. The modelling in 0.7 m scale may give a reasonable estimation of the standard deviation for the domain in canister scale. The value is in between approach 1 and 2.
	0.7	**0.22** (0.038+0.011=0.049) (between+within rock type)	**0.28** (0.068+0.011=0.079) (between+within rock type)	
	2	**0.20** (0.030+0.0091=0.039) (between+within rock type)	**0.26** (0.056+0.0091=0.065) (between+within rock type)	

Approach 3 is believed to underestimate the standard deviation for domain RFM029 and RFM012 in larger scales, but modelling in the 0.7 m scale may give a reasonable estimation of the standard deviation in the canister scale, a value in between approach 1 and 2. Therefore, the standard deviation of the two domains is given the concluding value of 0.22 W/(m·K) and 0.28 W/(m·K), respectively, which is the result from approach 3 at the 0.7 m scale. The variance contribution due to spatial variability within rock types seems to be rather small and the total variability dominates of variability between different rock types within the domains. The modelling results for thermal conductivity from the three approaches are presented in Table 5-10 for up to three different scales.

It is not possible to fit any simple distribution model (eg. normal distribution) to the data for the two domains RFM012 and RFM029. Therefore, it is not possible to use the evaluated standard deviations from Table 5-10 to calculate confidence limits. However, it is easy to determine confidence limits for a specified scale based on the data set resulting from modelling approach 1. Approach 1 may result in underestimation of the variability in data, according to the discussion above, and the 0.7 m scale for approach 3 may give a better estimation. In Table 5-11 lower and upper confidence limits are indicated. They are based on modelling results according to approach 1 at the 0.7 m scale but are rounded off to two digits precision to compensate for the increased variability according to approach 3 (rounded off downwards for the lower confidence limit and upwards for the upper confidence limit). This results in the same confidence limits for the two domains.

The distribution in Table 5-11 is bimodal. In further modelling it is possible to use different distributions for different parts of the rock mass.

Table 5-11. Arithmetic mean and evaluated standard deviation of thermal conductivity (W/(m·K)) per domain in the possible canister scale. Two-sided 95% confidence intervals are indicated, see discussion in text. The values are valid at 20°C. At higher temperatures the thermal conductivity for the dominating rock type, granite to granodiorite (101057), decreases with about 10%/100°C.

Domain	Arithmetic mean	St. dev.	Indicated two-sided 95% confidence interval	
			Lower confidence limit	Upper confidence limit
RFM029	3.55	0.22	2.9	3.8
RFM012	3.46	0.28	2.9	3.8

Observe that the above table is valid at 20°C. The thermal conductivity decreases at higher temperatures with an arithmetic mean of 10.0% /100°C temperature increase (varies between 6.2–12.3%) for granite to granodiorite (101057) which dominates domain RFM029. For other rock types the temperature dependence has not been measured. In the modelling, domain RFM029 consists to 75% of 101057.

A comparison of the results on domain level presented in model version Forsmark 1.1 /SKB, 2004/ and the model version Forsmark 1.2 is given in Table 5-12.

Table 5-12. Comparison of modelling results (arithmetic mean and standard deviation) from Forsmark versions F1.1 and F1.2

Domain	Mean (W/(m·K))		Diff.	St. dev. (W/(m·K))	
	Version F1.1	Version F1.2	(F1.2–F1.1)/F1.1	VersionF1.1	Version F1.2
RFM029	3.41	3.55	4.1%	0.21	0.22
RFM012	*	3.46		*	0.28

* Data unavailable.

5.5.2 Heat capacity

Modelling of heat capacity on domain level is performed as a Monte Carlo simulation where the occurrence of different rock types in the domain is weighted together with the rock type models. Results are presented in Table 5-13 and rock type models with an extended methodology are presented in /Sundberg et al. 2005b/.

Observe that the above table is valid at 20°C. The heat capacity increases at higher temperatures with a mean value of 27.5% /100°C temperature increase (varies between 15.9% and 54.8%) for rock type granite to granodiorite (101057). For other rock types the temperature dependence has not been measured.

Table 5-13. Heat capacity MJ/(m³·K) per domain with two-sided 95% confidence intervals under assumption of normal distribution. The data are valid at 20°C. At higher temperatures the heat capacity for granite to granodiorite (101057) increase with about 25%/100°C.

Domain	Arithmetic mean	St. dev.	Lower confidence limit	Upper confidence limit
RFM029	2.17	0.163	1.85	2.50
RFM012	2.17	0.149	1.86	2.49

5.5.3 Coefficient of thermal expansion

No domain modelling is performed. For all domains a mean value for the coefficient of thermal expansion is suggested as $7–8 \cdot 10^{-6}$ m/(m·K), see section 4.9.

5.5.4 In situ temperature

No domain modelling is performed. For all domains a mean of the in situ temperature at 400, 500 and 600 m depth is estimated at 10.6, 11.7 and 12.8°C, respectively, see section 4.10.2.

Variations in the thermal gradient are under ideal conditions a result of the spatial variation of thermal conductivity. However, in available loggings the fluid temperature is disturbed and has also other uncertainties, see section 6.3. Because of these uncertainties the temperature gradient has not been used to evaluate the spatial variability in thermal conductivity.

6 Evaluation of uncertainties

A general description of uncertainties is provided in the strategy report for the thermal site descriptive modelling /Sundberg, 2003a/. The evaluation of uncertainties has been divided into sections depending on different thermal properties and also within the scales the uncertainties arise; data level, rock type level and domain level.

6.1 Thermal conductivity

6.1.1 Data level

TPS data

The accuracy of TPS measurements is better than 5% and the repetitiveness is better than 2% according to the manufacturer of the measurement equipment /Sundberg, 2002/. Note that this uncertainty refers to the measurement volume (approx. 10 cm^3) and not the volume of the sample, since only a subvolume of the sample is subject to measurement. If the TPS-measurement is supposed to represent the sample scale (approx. 0.1 dm^3) the uncertainty is larger and depends on the small-scale heterogeneity of the rock.

Comparison between different laboratories gives a slightly higher difference. The differences for measurement results from different laboratories, but according to the same method and made at the same sample are ± 5–6% for thermal conductivity and ± 10–12% for heat capacity for individual samples. Calculated as mean value for the investigated samples, the difference is small. The resulting differences are due to both the manual handling (eg. position the measurement device, preparation) of the samples and to the measurement itself. Comparison between different methods is discussed in /Sundberg et al. 2003/.

There is a potential bias (underestimation) in thermal conductivity data. The reason is that stress dependence has not been assessed. Measurements are made on stress released samples. However, the effect is assumed to be low since the samples are water saturated before measurement.

SCA data

The uncertainty associated with SCA data is significantly larger than for TPS data. For SCA data there are two main sources of uncertainty; (1) determination of the volume fraction of each mineral in the sample and (2) representative values of thermal conductivity of the different minerals.

When comparing TPS and SCA data, there is an uncertainty due to the fact that the modal analysis is not performed for the whole volume of the TPS sample, only a surface of the sample. In addition, the SCA calculation method presumes isotropic conditions. Because of anisotropy in Forsmark the orientation of the sample will effect the modal analysis and the calculated thermal conductivity.

6.1.2 Rock type level

Representativeness of data

The representativeness of samples selected for TPS measurements can be questioned since they are not taken with the purpose of statistically representing the rock mass. Similarly, the question of representativeness applies for the calculated values based on modal analyses (SCA method). For both measured and calculated data, non-probabilistic selection of samples has resulted in bias of unknown magnitude. The potential for bias, is largest for rock types with few thermal conductivity samples, such as granite, granodiorite and tonalite (101051), pegmatite, pegmatitic granite (101061), and granite (111058).

Rock type models

The rock type models were selected as normal distributions (PDF:s). There is a slight deviation between data and model and one contributing factor can be the question of representativeness for the samples. Generally, the rock type models slightly overestimate the occurrence of small thermal conductivity values and underestimate the number of large values. Rock type models are required in the domain modelling.

The data set is very small for several rock types, which implies that these rock type models are highly uncertain. This applies to tonalite to granodiorite (101054), granite, granodiorite and tonalite (101051), granodiorite (101056), and diorite, quartz diorite and gabbro (101033).

Anisotropy

The anisotropy on rock type level is depending on foliation or lineation. Measurements of samples have suggested anisotropic conditions in data but the interpretation is uncertain and the results might be overestimated in the small scale. The samples were taken in the dominating granite in domain RFM029, but quite close to the border of domain RFM012. This may imply that the samples have a higher degree of anisotropy compared to the rock in the central parts of domain RFM029.

There is an uncertainty in the anisotropy measurements since the used heat capacity values not have been measured separately.

Spatial variability within rock type

Models of the spatial variability within the occurring rock types of the Forsmark area have not been developed. The spatial variability is only considered in the domain modelling.

6.1.3 Domain level

Geological model

Uncertainty in the geological model results from uncertainty in the Boremap logging, interpretations of spatial occurrence of different rock types, and the extension of lithological domains both at the surface and at depth.

Influences from fractures, deformation zones, and water movements on thermal properties have not been considered. No thermal data are presently available from the deformation zones. This uncertainty may be of minor importance since such zones is not supposed to be situated in regions with high thermal flow caused by heat from canisters.

Representativeness of boreholes

It is not known how representative the boreholes are for the different domains. Since the number of boreholes in a domain is low, it is reasonable to believe that there is a bias present. This bias can only be reduced with additional boreholes, or a more complete understanding of the lithology.

Spatial variability within the domain

Spatial variability within the domain is handled in the domain modelling approaches but there are uncertainties in spatial variability within rock type.

Anisotropy

The anisotropy on domain level is depending on frequency and orientation of subordinate rock types occurring as dykes of significant extension and with different thermal characteristics. At the present stage no evaluation of the extent of such anisotropic occurrence has been made.

Significant scale for the canister

The significant scale is believed to be 1–10 m. A detailed investigation at which scale changes in thermal conductivity is significant for the heat transfer from the canister is performed for the prototype repository at Äspö HRL /Sundberg et al. 2005a/. This implies a source of uncertainty in the thermal modelling. It can be reduced by numerical simulation of heat flow. Here, the uncertainty is handled by selecting a sufficiently small scale not to underestimate the variability.

Upscaling methodology

For all rock types thermal conductivity values are randomly assigned at the 0.1 m scale based on the rock type models. These rock type models probably overestimate the variance at the 0.1 m scale. The reason is that TPS and SCA data represent a smaller scale. At the 0.1 m scale, some reduction of variance should already have taken place. Therefore, this approach overestimates the likelihood of small values.

In the main modelling approach, spatial variability within rock types is ignored. This results in a too large variance reduction when the scale increases. To compensate for this, the variance due to spatial variability within other rock types is assumed to be equal the spatial variability within the Ävrö granite present at the Simpevarp area (approach 2). This is probably an overestimation of the variance. In modelling approach 3 an addition of variance estimated from TPS data is conducted to compensate for spatial variability within rock types and this approach is assumed to give the most reasonable estimate of the variability compared to the other approaches.

Uncertainties in the modelling arise from lack of knowledge of spatial variability within the rock types present within the domains. The most straight-forward way of reducing this uncertainty is to collect considerable more data.

Statistical assumptions

The confidence intervals calculated for each domain are based on the assumption that domain data at the significant scale are normally distributed. This is an uncertain assumption. As long as knowledge of spatial variability is insufficient, it is not possible to check the validity of this assumption. However, data at other scales indicate that assumptions of normality are reasonable.

The rock type models have been considered as normal distributions although data is somewhat skewed. This results in a too small change of the mean value for the domain when the scale increases. The effect is however insignificant compared to the other uncertainties.

6.2 Heat capacity

There exists a problem with the representativeness for measured values (TPS data). The samples are relatively few and focused on certain parts of the rock volume.

When modelling the heat capacity, only the four most occurring rock types have been considered, 16–21% of the domains has not been taken into account. Calculations of the most occurring rock types are based on Boremap loggings including rock types with an occurrence less than 1 m.

No direct laboratory measurements of heat capacity have been performed. Instead, heat capacity has been determined through conductivity and diffusivity measurements performed with the TPS method.

6.3 In situ temperature

Temperature loggings from different boreholes show a variation in temperature at specified depth. The difference implies an uncertainty in temperature loggings and even small uncertainties may influence the design of the repository. Possible sources of uncertainty are timing of the logging after drilling (drilling adds to temperature disturbance), water movements along the boreholes, calibration error in the temperature logging or uncertainty in the measured inclination of the boreholes. The uncertainty imposed by water movements may be evaluated jointly with the hydrogeologists. However, this has not yet been done.

6.4 Thermal expansion

The representativeness of samples selected for thermal expansion measurements can be questioned. The samples are few and focused to certain parts of the rock volume.

There is a potential bias (underestimation) in thermal expansion data. The reason is that stress dependence has not been assessed. Measurements are made on stress released samples.

7 Feedback to other disciplines

In the thermal modelling, geological and geophysical information have been used. Cooperation with the geologists has been established. Mineralogical data and bore map data have been used and interpreted during the thermal modelling and comparative calculation of rock type models has been performed.

One important question for further modelling is the orientation and extension of subordinate rock types that may influence thermal anisotropic conditions at larger scales. A detailed description of the foliation/lineation in the rock is important for the layout of a repository (anisotropy in thermal properties at smaller scales). Also, a better understanding of the spatial distribution of subordinate rock types in the domains, would be useful.

Primary receiver of the result from the thermal modelling is Design. It is suggested that the design methodology is developed to take into account the variability in thermal conductivity. The end receiver of the thermal data is Safety Assessment.

8 Abbreviation list

SKB	Svensk Kärnbränslehantering AB
SP	Swedish National Testing and Research Institute
TPS	Transient Plane Source Method
SCA	Self Consistent Approximation
PDF	Probability Density Function
CDF	Cumulative Distribution Function
LCL	Lower Confidence Limit (of data)
UCL	Upper Confidence Limit (of data)
St. dev.	Standard Deviation
N	Number of data
AD	Anderson-Darling statistic
P-value	probability value
CI	Confidence Interval

References

Adl-Zarrabi B, 2003. Determination of thermal properties by the TPS-method. SKB P-03-08, Svensk Kärnbränslehantering AB.

Adl-Zarrabi B, 2004a. Drill hole KFM01A Thermal properties: heat conductivity and heat capacity determined using the TPS method and mineralogical composition by modal analysis. SKB P-04-159, Svensk Kärnbränslehantering AB.

Adl-Zarrabi B, 2004b. Drill hole KFM02A Thermal properties: heat conductivity and heat capacity determined using the TPS method and mineralogical composition by modal analysis. SKB P-04-161, Svensk Kärnbränslehantering AB.

Adl-Zarrabi B, 2004c. Drill hole KFM03A Thermal properties: heat conductivity and heat capacity determined using the TPS method and mineralogical composition by modal analysis. SKB P-04-162, Svensk Kärnbränslehantering AB.

Adl-Zarrabi B, 2004d. Drill hole KFM04A Thermal properties: heat conductivity and heat capacity determined using the TPS method and mineralogical composition by modal analysis. SKB P-04-199, Svensk Kärnbränslehantering AB.

Carlsson L, 2004. Drill hole KFM02A: Extensometer measurement of the coefficient of thermal expansion of rock. SKB P-04-164, Svensk Kärnbränslehantering AB.

Dagan G, 1981. Analysis of flow trough heterogeneous random aquifers by the method of embedding matrix, 1, Steady flow, Water resources res. 17 (1), 107–121.

Dinges C, 2004a. Forsmark site investigation, Drill hole KFM04A, Thermal properties: Anisotropic thermal conductivity and thermal diffusivity determined using the Hot Disk thermal constants analyser (the TPS technique). Svensk Kärnbränslehantering, Report in progress.

Dinges C, 2004b. Forsmark site investigation, Drill hole KFM01A, Thermal properties: thermal conductivity and specific heat capacity determined using the Hot Disk thermal constants analyser (the TPS technique) – Compared test, SKB P-04-186, Svensk Kärnbränslehantering.

Gustafsson S, 1991. Transient plane source techniques for thermal conductivity and thermal diffusivity measurements of solid materials. Rev. Sci. Instrum. 62, p 797–804. American Institute of Physics, USA.

Horai K, 1971. Thermal conductivity of rock-forming minerals. J. Geophys. Res. 76, p 1278–1308.

Horai K, Baldridge S, 1972. Thermal conductivity of nineteen igneous rocks, Application of the needle probe method to the measurement of the thermal conductivity of rock. Estimation of the thermal conductivity of rock from the mineral and chemical compositions. Phys. Earth Planet. Interiors 5, p 151.

Hot Disk, 2004. www.hotdisk.se, access 2004-09-22.

Liedberg L, 2004. Drill hole KFM03A: Extensometer measurement of the coefficient of thermal expansion of rock. SKB P-04-165, Svensk Kärnbränslehantering AB.

Mattsson H, Keisu M, 2004. Interpretation of borehole geophysical measurements in KFM04A, KFM06A (0–100 m), HFM10, HFM11, HFM12, HFM13, HFM16, HFM17 and HFM18. SKB P-04-143, Svensk Kärnbränslehantering AB.

Mattsson H, Thunehed H, Keisu M, 2004. Interpretation of borehole geophysical measurements in KFM01A, KFM01B, HFM01, HFM02 and HFM03. SKB P-04-80, Svensk Kärnbränslehantering AB.

Nielsen T, Ringgaard J, 2003. Geophysical borehole logging in borehole KFM01A, HFM01 and HFM02. SKB P-03-103, Svensk Kärnbränslehantering AB.

Nielsen T, Ringgaard J, 2004a. Geophysical borehole logging in borehole KFM02A, KFM03A and KFM03B. SKB P-04-97, Svensk Kärnbränslehantering AB.

Nielsen T, Ringgaard J, 2004b. Geophysical borehole logging in borehole KFM04A, KFM06A, HFM10, HFM11, HFM12 and HFM13. SKB P-04-144, Svensk Kärnbränslehantering AB.

Nielsen T, Ringgaard J, 2004c. Geophysical borehole logging in borehole KFM01B, HFM14, HFM15, HFM16, HFM17 and HFM18. SKB P-04-145, Svensk Kärnbränslehantering AB.

Petersson J, Berglund J, Danielsson P, Wängnerud A, Tullborg E-L, Mattsson H, Thunehed H, Isaksson H, Lindroos H, 2004. Petrography, geochemistry, petrophysics and fracture mineralogy of boreholes KFM01A, KFM02A and KFM03A+B. SKB P-04-103, Svensk Kärnbränslehantering AB.

SKB, 2004. Preliminary Site Description, Forsmark area – version 1.1. SKB R-04-15, Svensk Kärnbränslehantering AB.

SKB, 2005. Preliminary Site Description, Forsmark area – version 1.2. Svensk Kärnbränslehantering AB. Report in progress.

Stephens M B, Lundqvist S, Bergman T, Andersson J, Ekström M, 2003. Bedrock mapping. Rock types, their petrographics and geochemical characteristics, and a structural analysis of the bedrock based on Stage 1 (2002) surface data. SKB P-03-75, Svensk Kärnbränslehantering AB.

Stephens M B, 2004. SGU (Geological Survey of Sweden), Personal communication.

Sundberg J, 1988. Thermal properties of soils and rocks, Publ. A 57 Dissertation. Department of Geology, Chalmers University of Technology and university of Göteborg, Sweden.

Sundberg J, Gabrielsson A, 1999. Laboratory and field measurements of thermal properties of the rock in the prototype repository at Äspö HRL. SKB IPR-99-17, Svensk Kärnbränslehantering AB.

Sundberg J, 2002. Determination of thermal properties at Äspö HRL. Comparison and evaluation of methods and methodologies for borehole KA 2599 G01. SKB R-02-27, Svensk Kärnbränslehantering AB.

Sundberg J, 2003a. A strategy for the model development during site investigations version 1.0. SKB R-03-10, Svensk Kärnbränslehantering AB.

Sundberg J, 2003b. Thermal properties at Äspö HRL, Analysis of distribution and scale factors. SKB R-03-17, Svensk Kärnbränslehantering AB.

Sundberg J, Kukkonen I, Hälldahl L, 2003. Comparison of Termal Properties Measured by Different Methods. SKB R-03-18, Svensk Kärnbränslehantering AB.

Sundberg J, Back P, Hellström G, 2005a. Uncertainty analysis of thermal properties at Äspö HRL prototype repository, Development of methodology, (preliminary title), report in progress. Svensk Kärnbränslehantering AB.

Sundberg J, Back P, Bengtsson A, Ländell M, 2005b. Thermal modelling, Preliminary site description Simpevarp subarea – version 1.2. SKB R-05-24. Svensk Kärnbränslehantering AB.

Thunehed H, 2004. Interpretation of borehole geophysical measurements in KFM02A, KFM03A, KFM03B and HFM04 to HFM08. SKB P-04-98, Svensk Kärnbränslehantering AB.

Åkesson U, 2004. Drill hole KFM01A: Extensometer measurement of the coefficient of thermal expansion of rock. SKB P-04-163, Svensk Kärnbränslehantering AB.

Appendix A

Probability plots of thermal conductivity per rock type

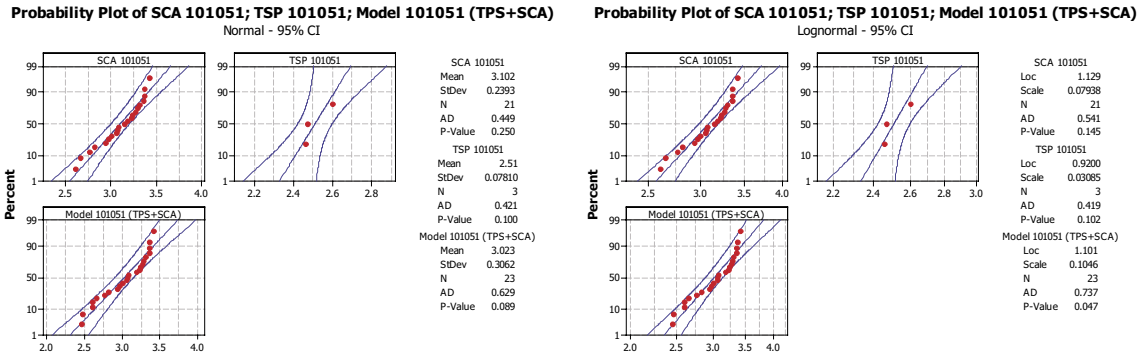

Figure A-1. *Probability plots of rock type granite, granodiorite and tonalite (101051), normal and lognormal distributions.*

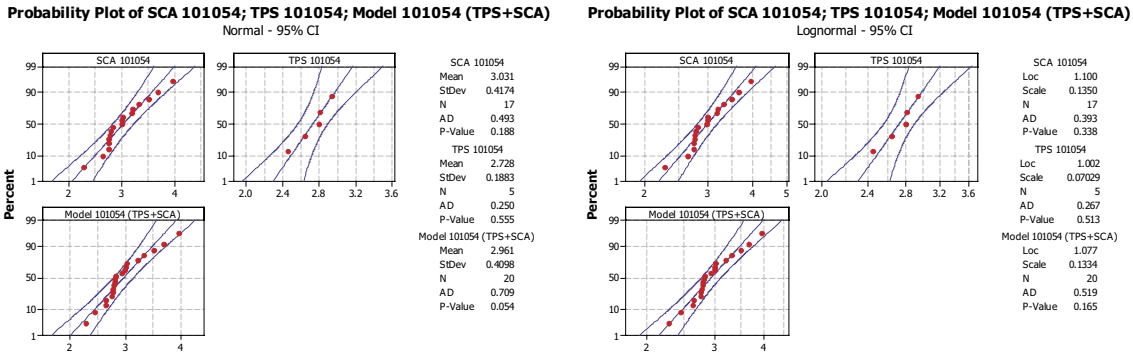

Figure A-2. *Probability plots of rock type tonalite to granodiorite (101054), normal and lognormal distributions.*

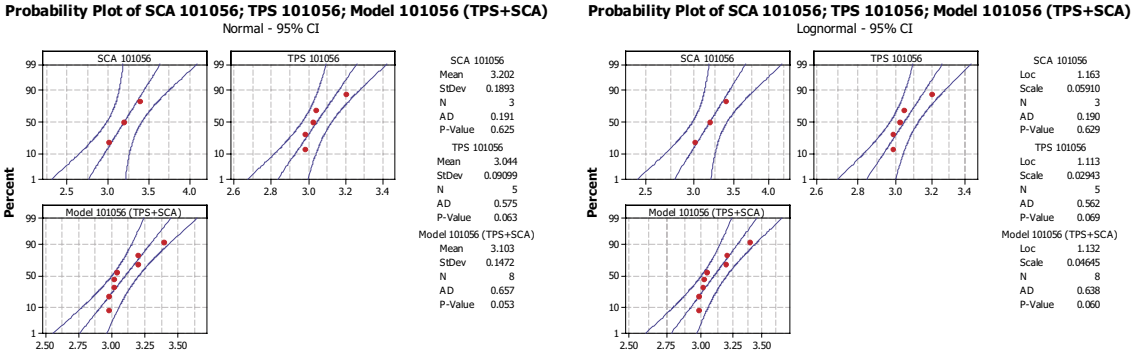

Figure A-3. *Probability plots of rock type granodiorite (101056), normal and lognormal distributions.*

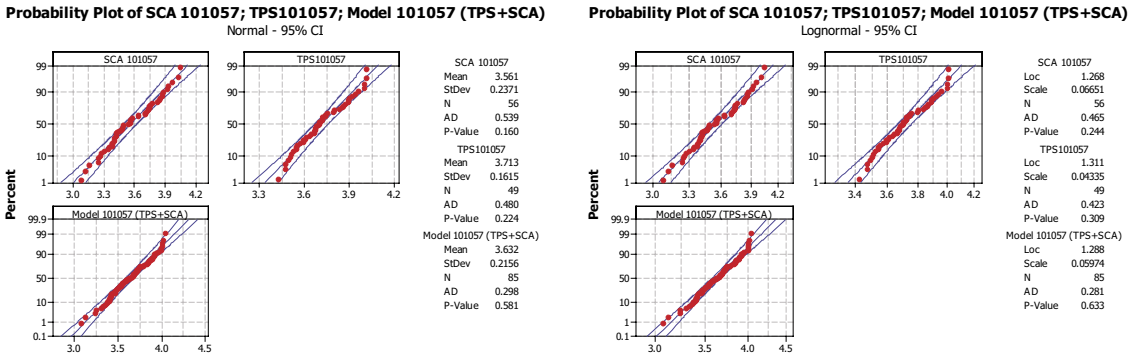

Figure A-4. *Probability plots of rock type granite to granodiorite (101057), normal and lognormal distributions.*

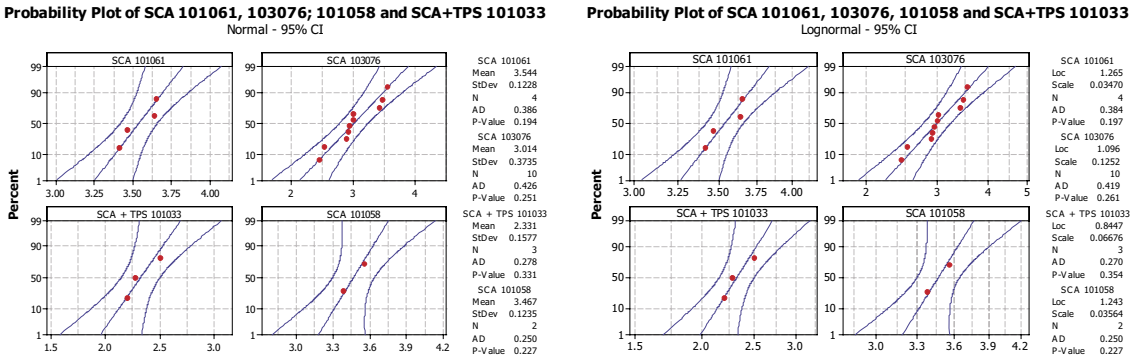

Figure A-5. *Probability plots of rock type pegmatite, pegmatitic granite (101061), felsic to intermediate volcanic rock (103076), granite (101058) and diorite, quartz diorite and gabbro (101033), normal and lognormal distributions.*

Appendix B

Probability plots of domain modelling results

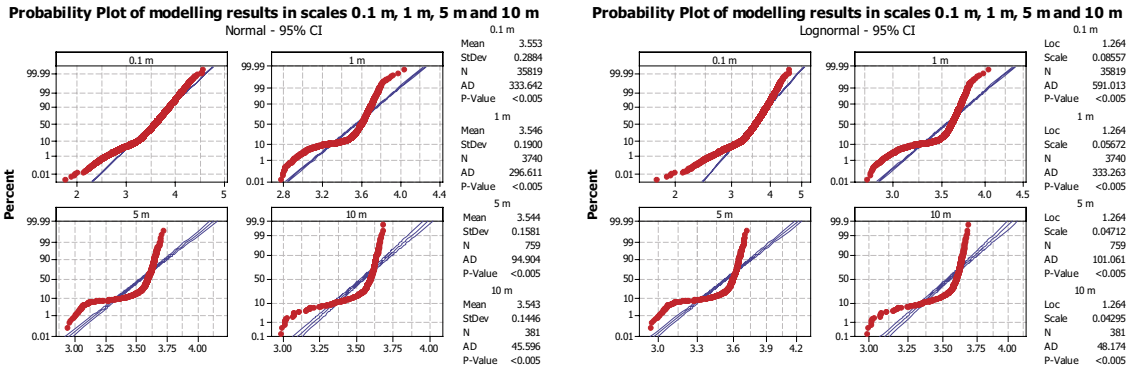

Figure B-1. *Probability plots of modelling results for four scales of domain RFM029 (dominated by granite to granodiorite), normal and lognormal distributions.*

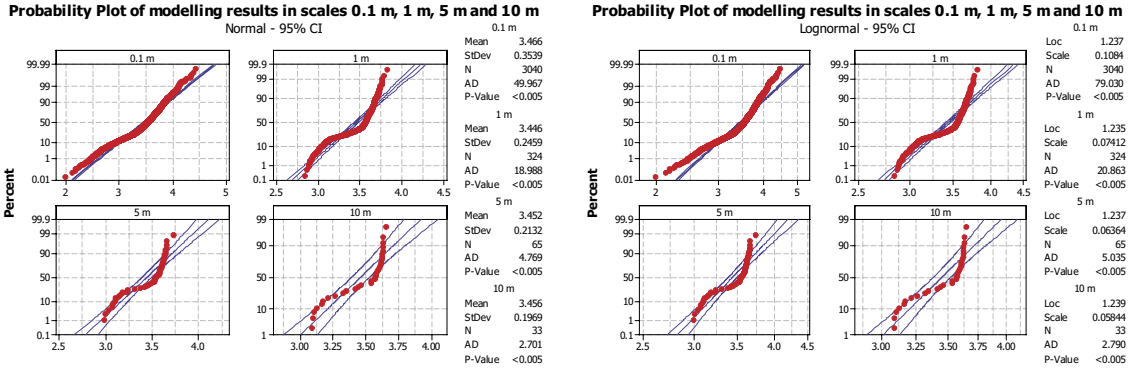

Figure B-2. *Probability plots of modelling results for four scales of domain RFM012 (dominated by granite to granodiorite), normal and lognormal distributions.*